

that line spacing and an electrode interval were of 40 m, which enabled to make a detailed pursuit of anomalies.

In search of gold, the dipole-dipole induced polarization method is often confronted with a difficulty to detect the high resistivity of quartz veins or zones of silicification. More difficulties are expected when the zone is not accompanied with sulphide minerals. In case of this, the principal object should be rather placed to seize a zone of low resistivity caused from clayey alteration zone which is accompanied with the zone of silicification. Yet, due to the facts that the resistivity values of the background in this area are low, ranging from 15 to 25 ohm-m, and there exist the zone of low resistivity less than 10 ohm-m in the eastern half of the area, delineation of clayey alteration zone was difficult to be conducted.

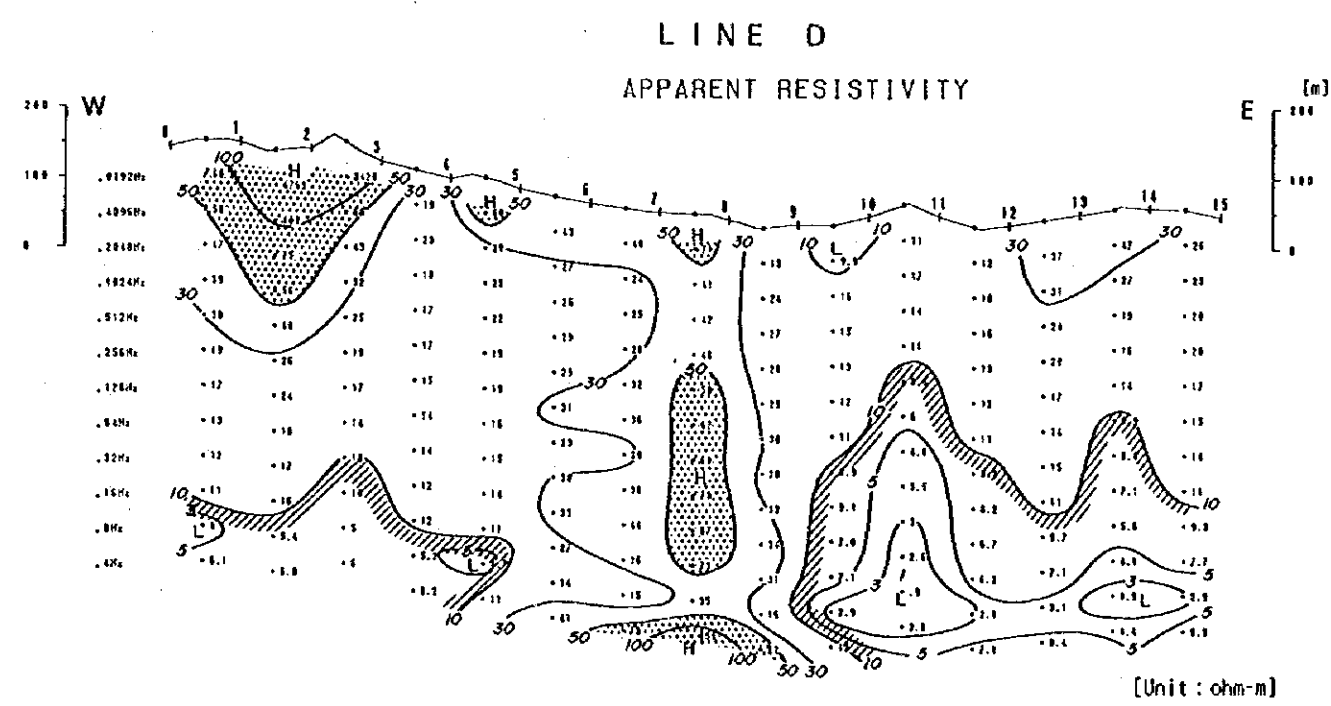
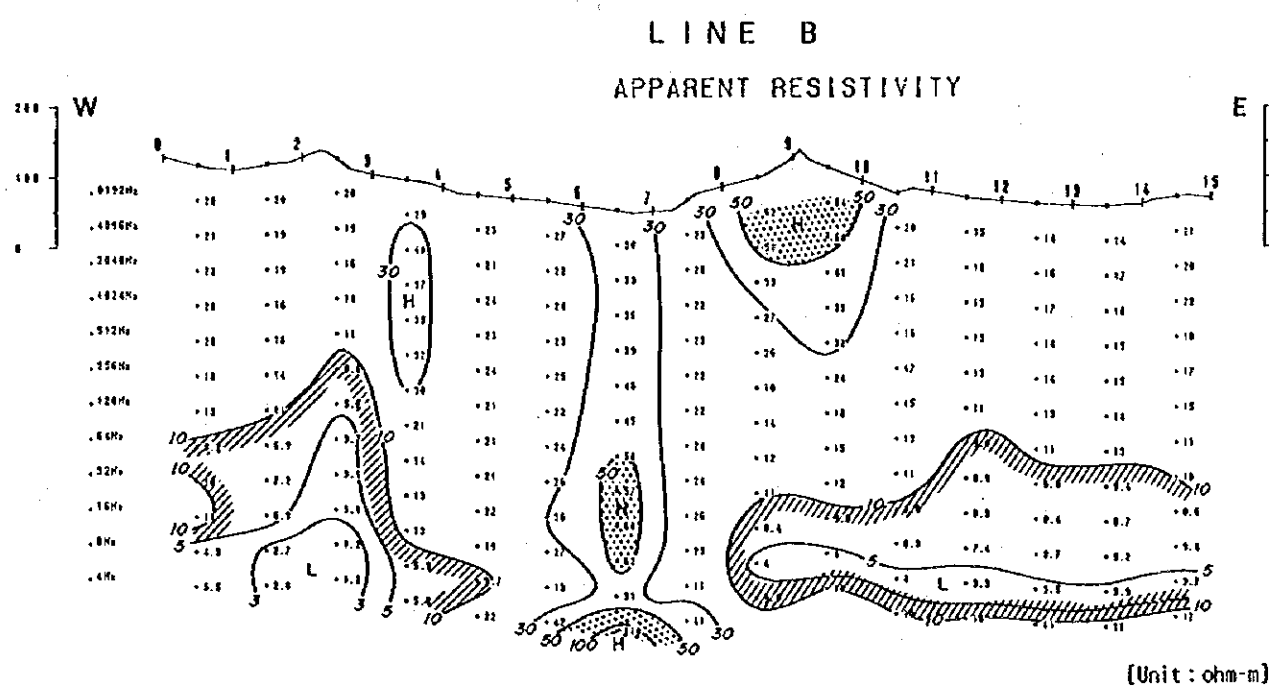
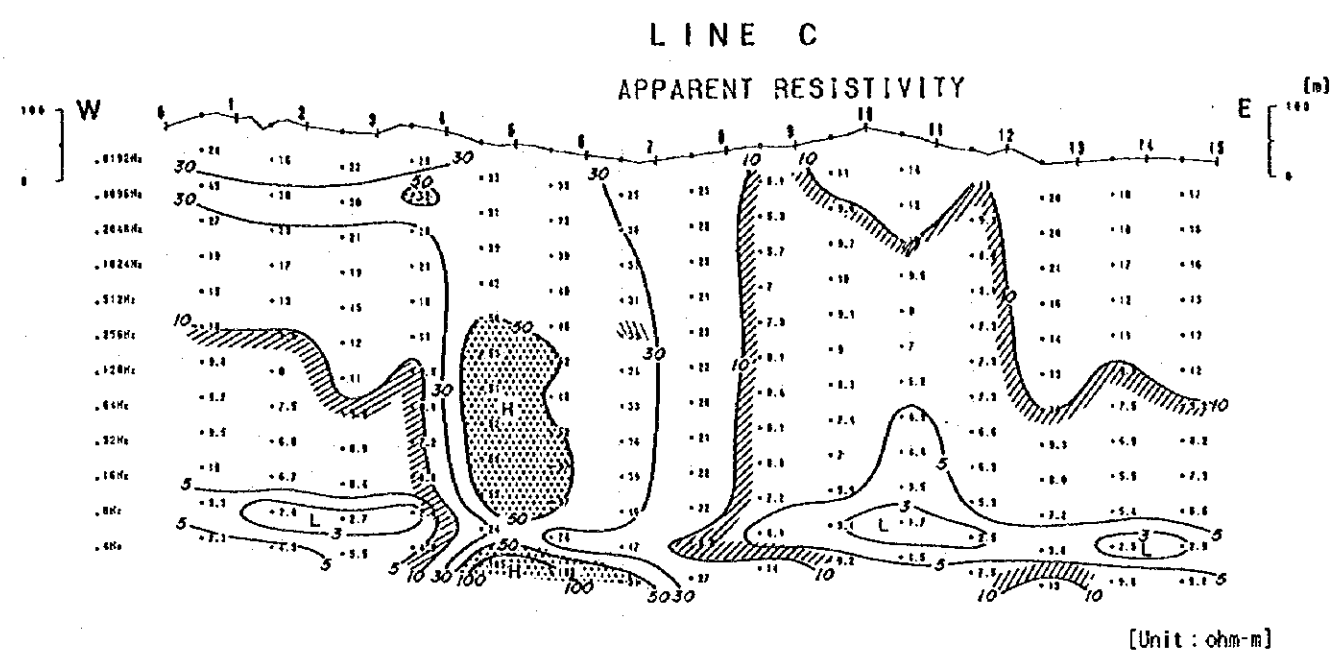
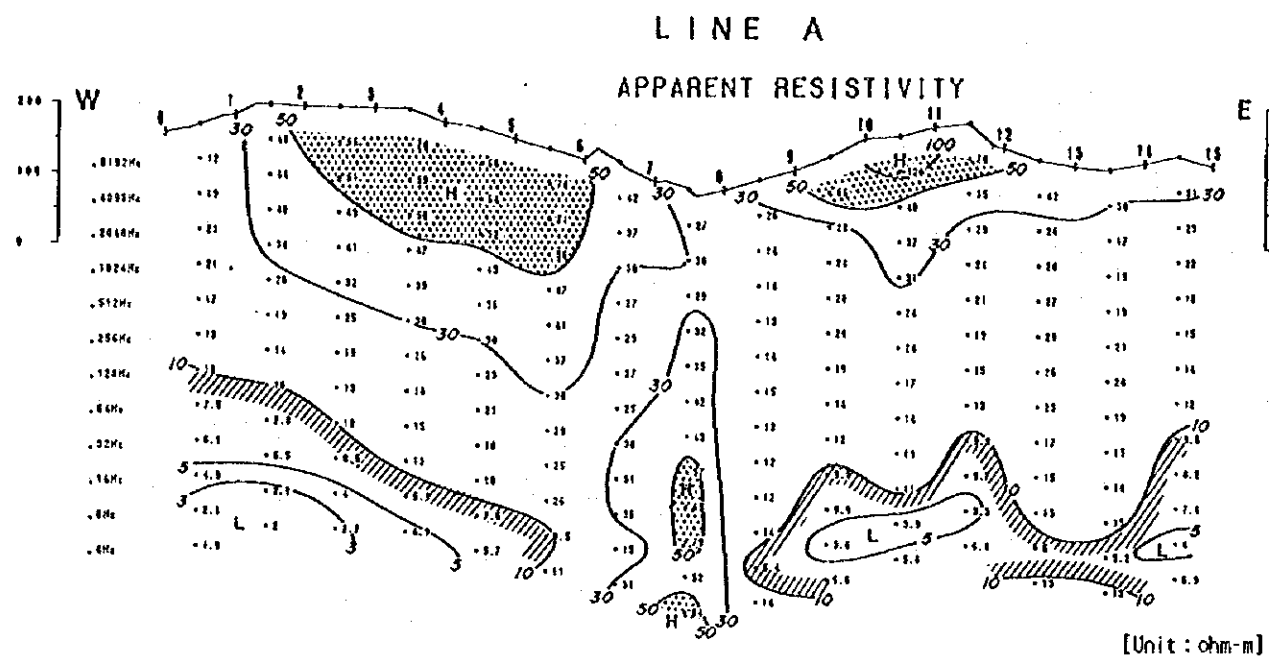
5-4-3 Laboratory investigation

The resistivity and chargeability of thirty rock samples including drill cores collected in the field are measured in the laboratory. The resistivity is highest in silicified rocks, and followed by basalt, andesite and volcanoclastic rocks in descending order. Values of resistivity range widely and rocks are difficult to be specified with values of their resistivities. The chargeability is of low values in a lump on the whole, and most samples are free from mineralization. The chargeability of rocks is highest in volcanoclastic rocks and followed by silicified rocks, andesite and basalt in descending order.

Discussion

As the number of samples are limited to be a total of thirty, a qualitative tendency only becomes obvious. Values of resistivity and chargeability vary in accordance with degree of mineralization alteration or of weathering. It is recommended that the degree of these is to be digitized to some extent, and data from many samples are to be treated statistically.

Analytical results on array type CSAMT and time domain IP methods are illustrated in Fig.2-5-21.



LEGEND

- H High Resistivity Zone
- L Low Resistivity Zone
- $50 \leq \rho_a$
- $\rho_a \leq 10$

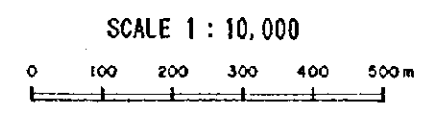
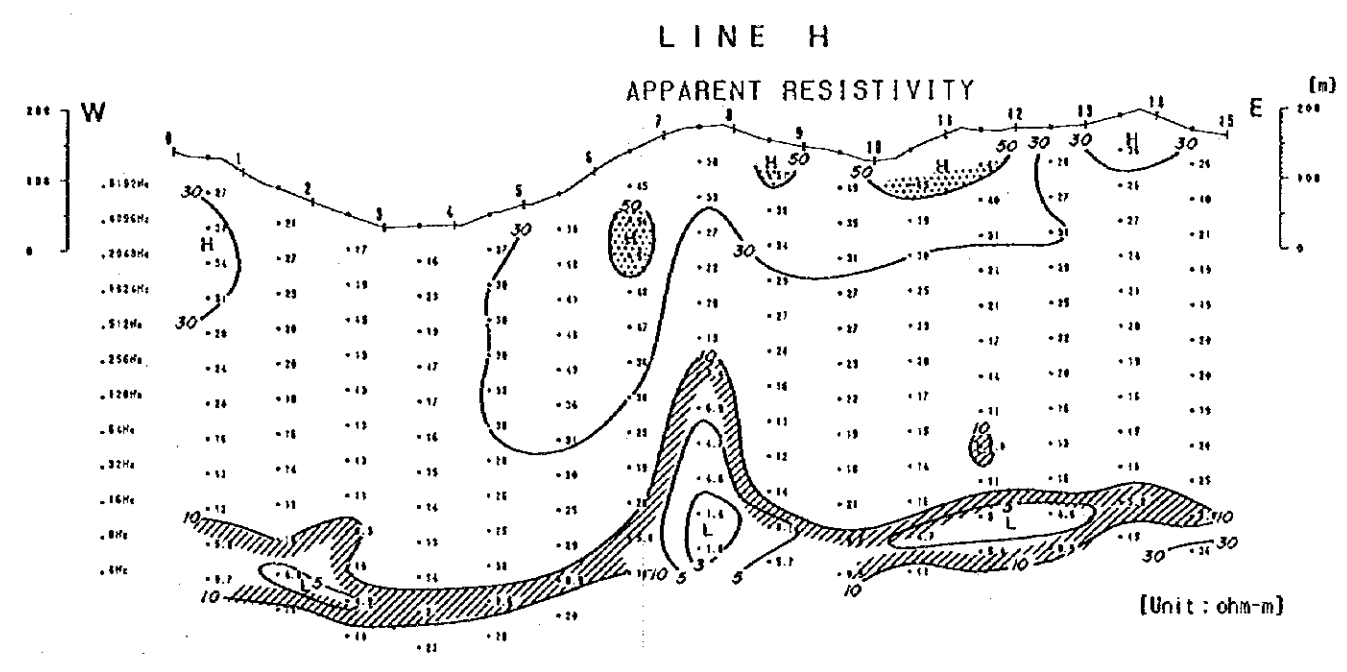
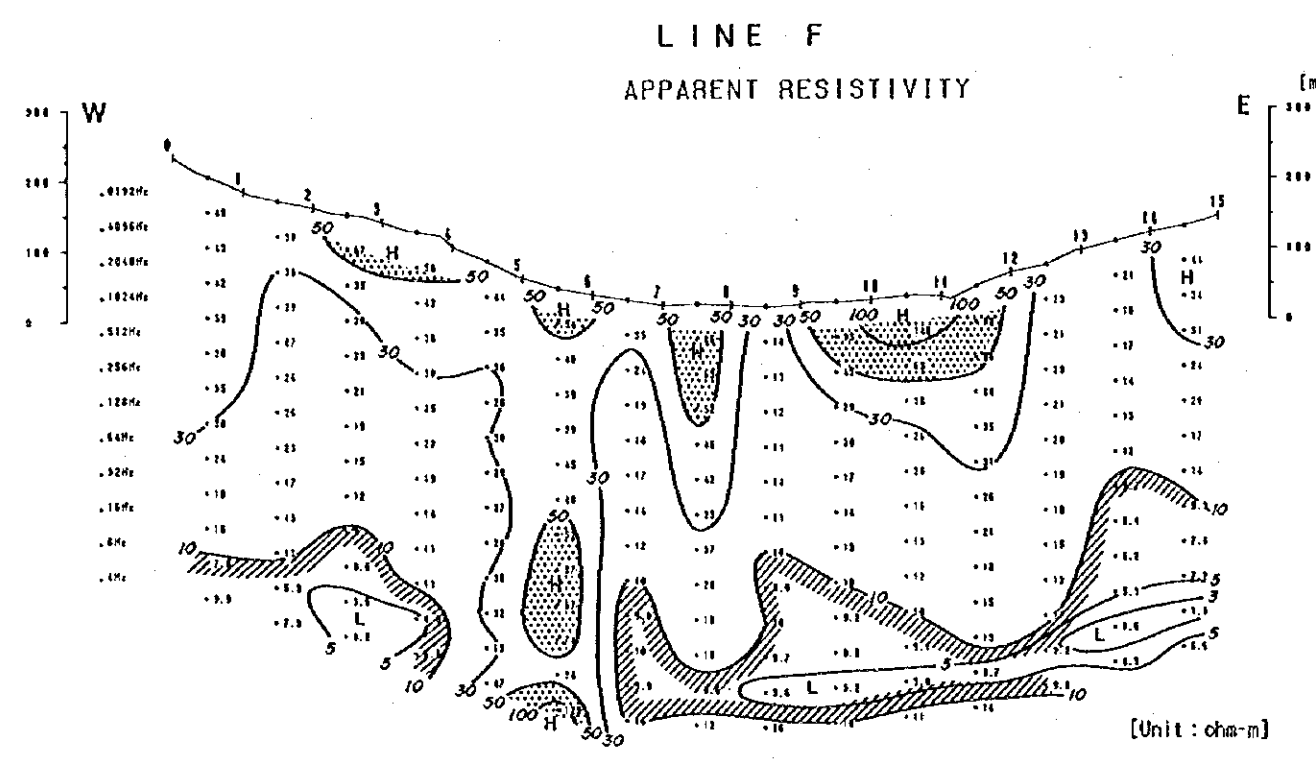
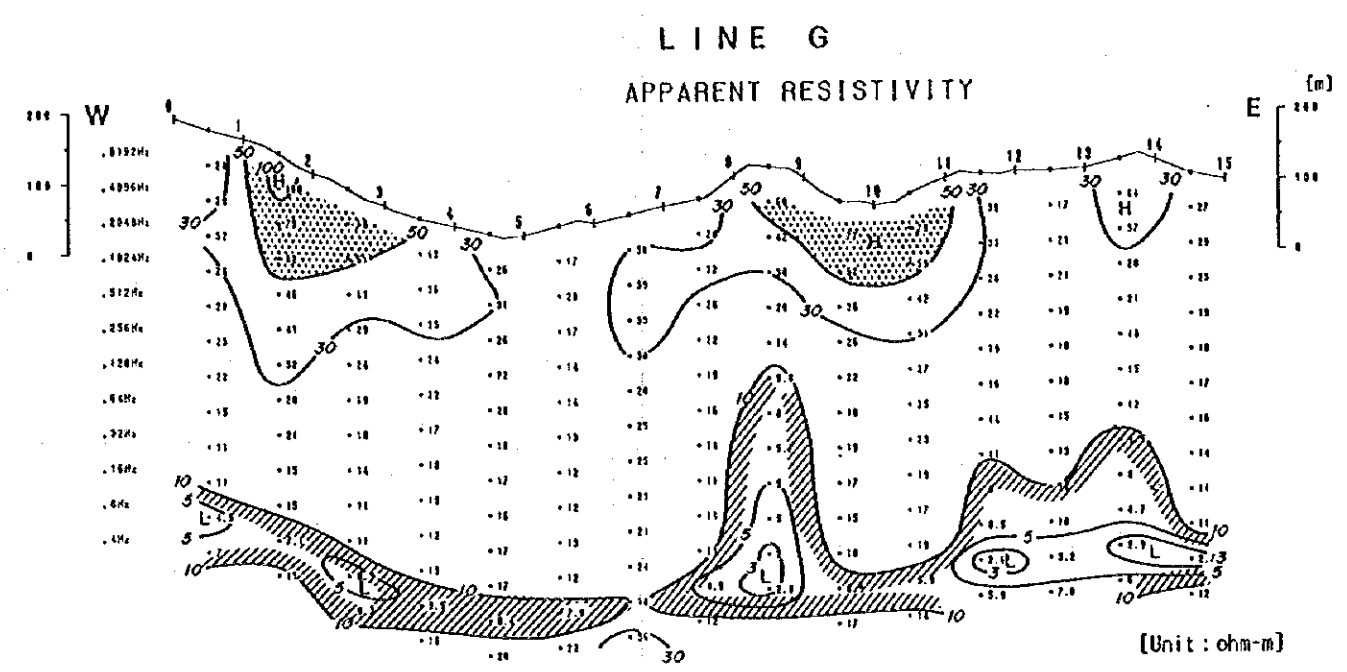
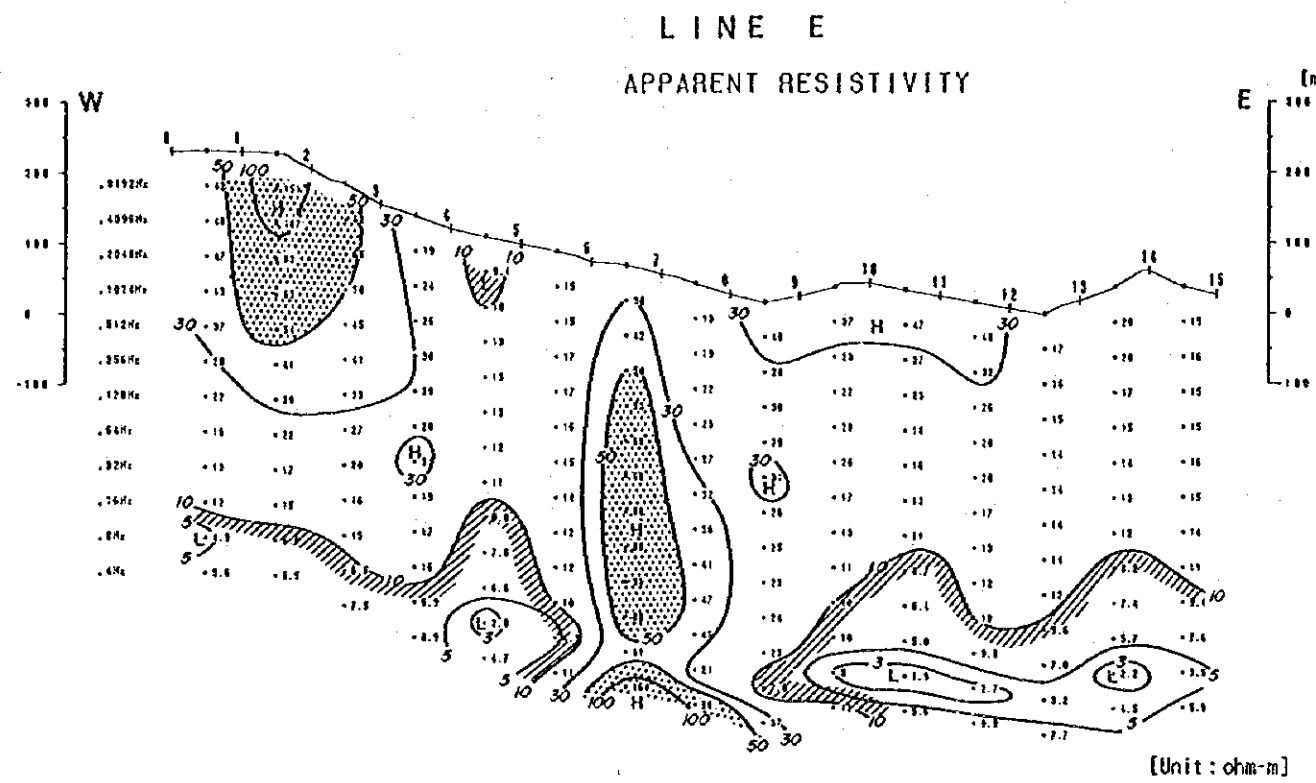


Fig. 2-5-6 (1) CSAMT Pseudosection of Apparent Resistivity [Line A-D]



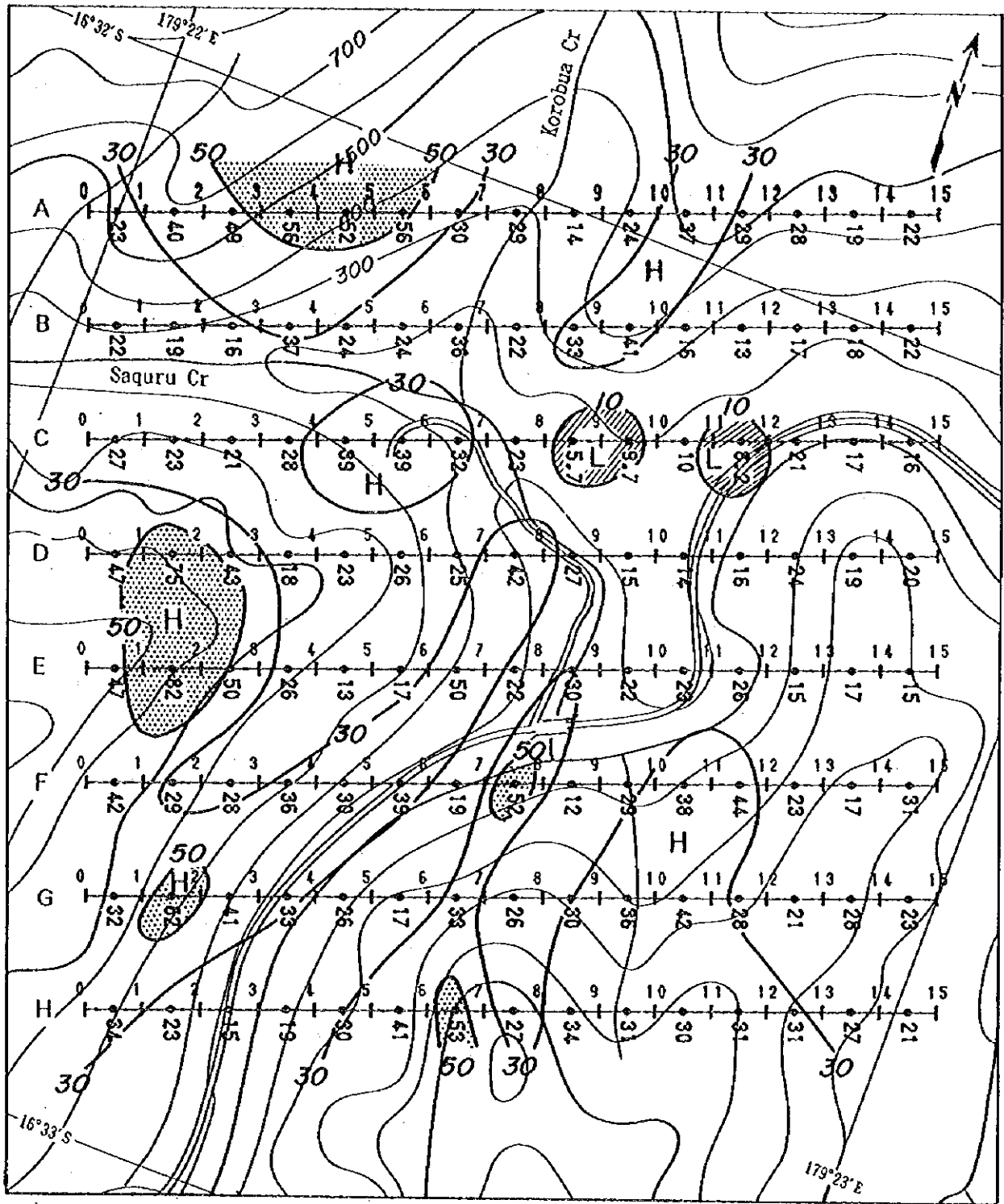
LEGEND

H High Resistivity Zone
L Low Resistivity Zone

$50 \leq \rho_a$
 $\rho_a \leq 10$

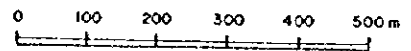
SCALE 1 : 10,000

Fig. 2-5-6 (2) CSAMT Pseudosection of Apparent Resistivity (Line E-H)



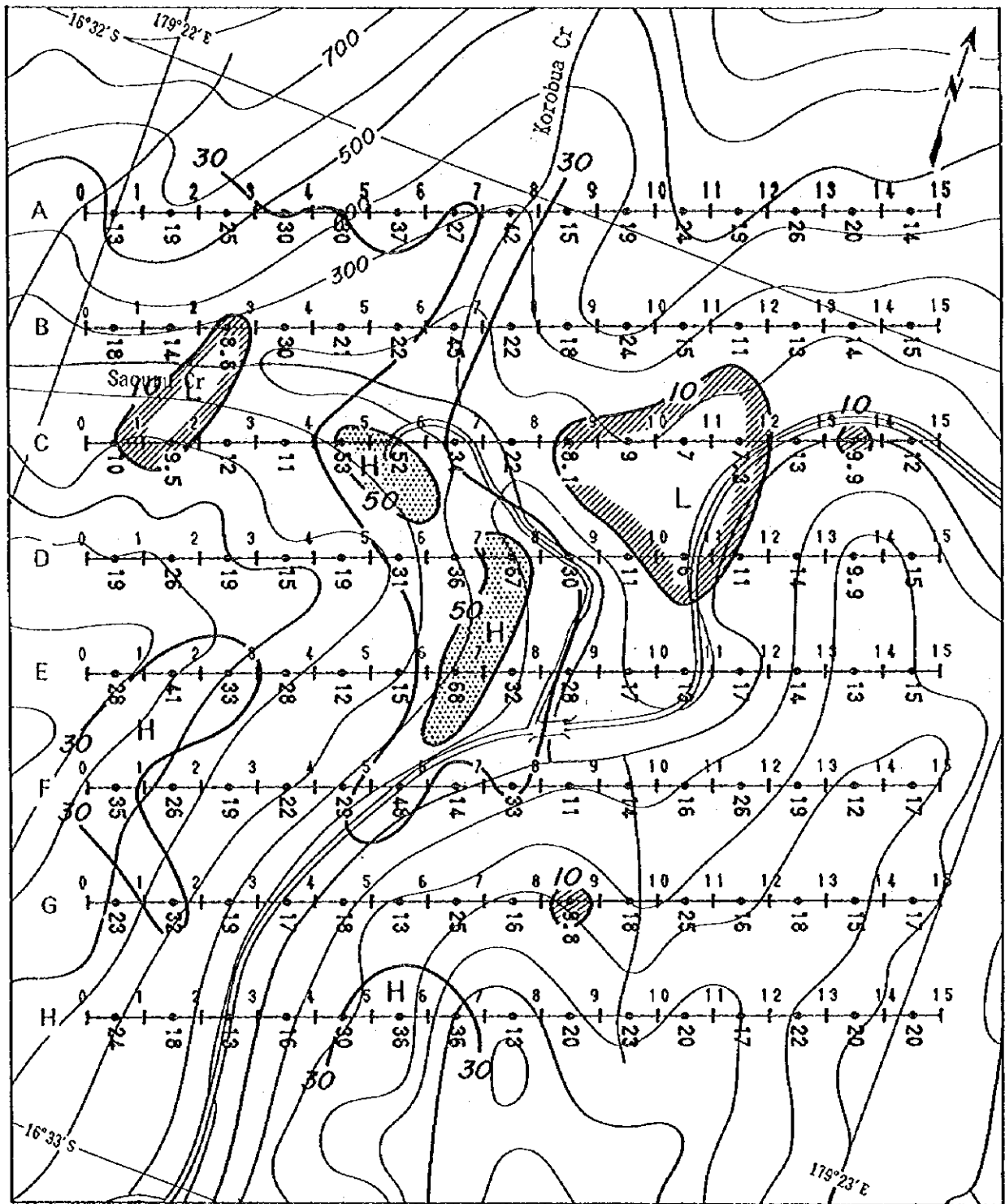
LEGEND

SCALE 1 : 10,000



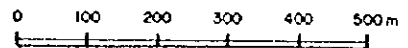
- | | | | | |
|---|----|--|---|-----------------------|
| 0 | 1 | Line Name & Station No. | H | High Resistivity Zone |
| A | 15 | Array CSAMT | L | Low Resistivity Zone |
| | | Resistivity (ohm-m) | | |
| | | | | 50 ≤ pa |
| | | | | pa ≤ 10 |
| | | Contour Line Value & Resistivity (ohm-m) | | |

Fig. 2-5-7 (1) CSAMT Plane Map of Apparent Resistivity [2,048Hz]



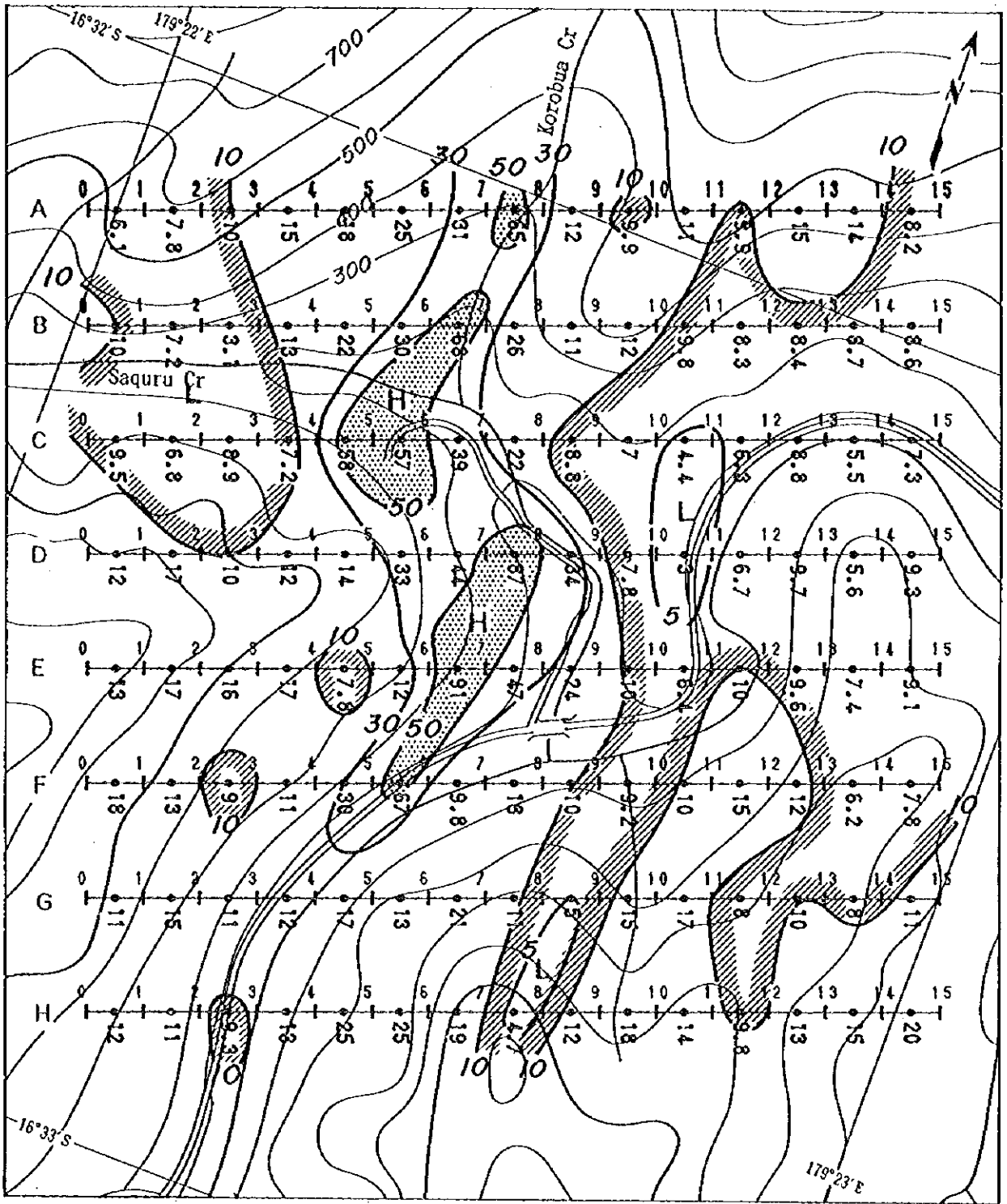
LEGEND

SCALE 1 : 10,000



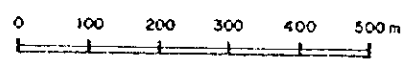
- | | | | | |
|---|-----|--|---|-----------------------|
| 0 | 1 | Line Name & Station No. | H | High Resistivity Zone |
| A | —●— | Array CSAMT | L | Low Resistivity Zone |
| | 15 | Resistivity (ohm-m) | | |
| | | | | $50 \leq p_a$ |
| | | | | $p_a \leq 10$ |
| | | Contour Line Value & Resistivity (ohm-m) | | |

Fig. 2-5-7 (2) CSAMT Plane Map of Apparent Resistivity [256Hz]



LEGEND

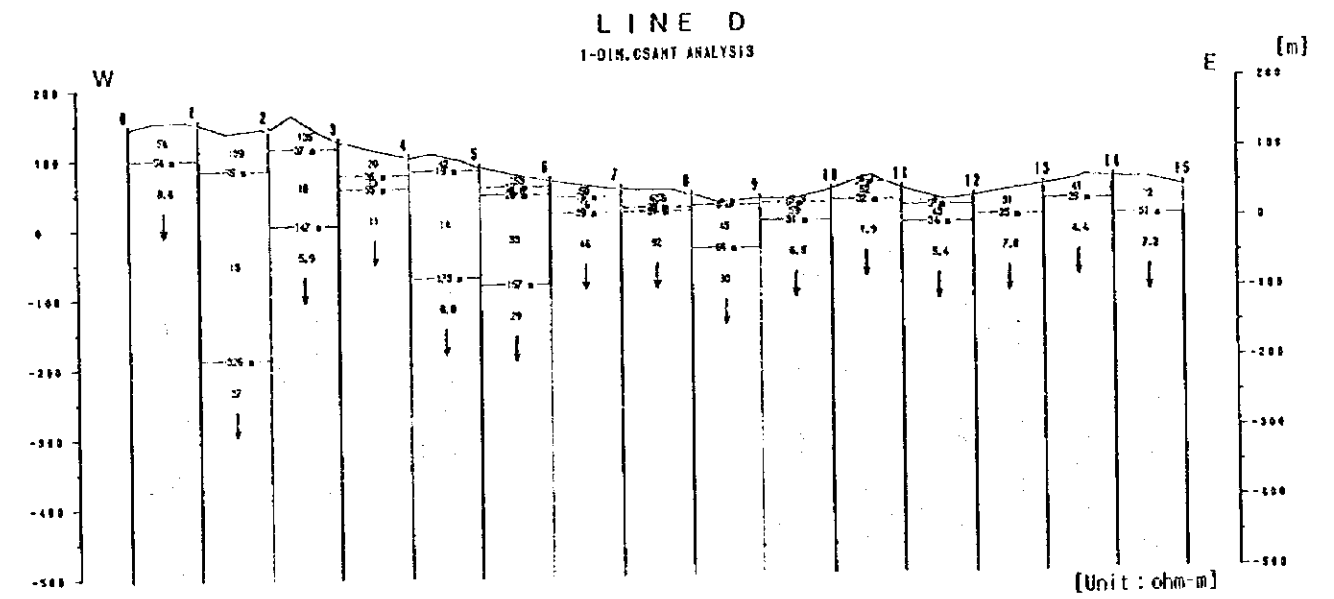
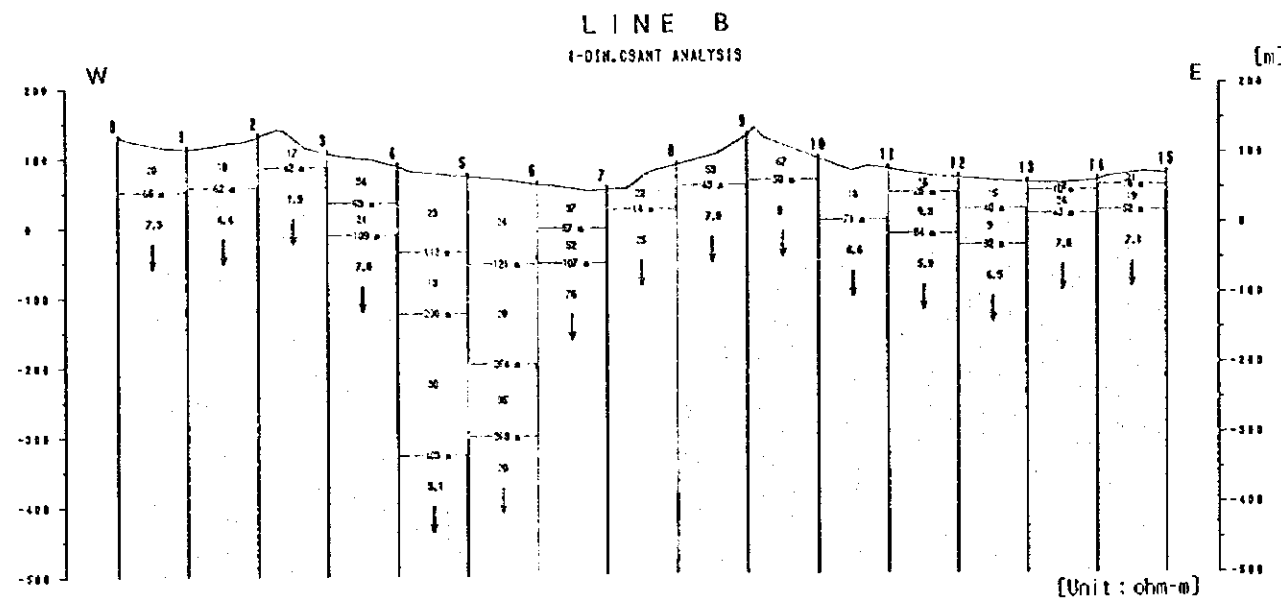
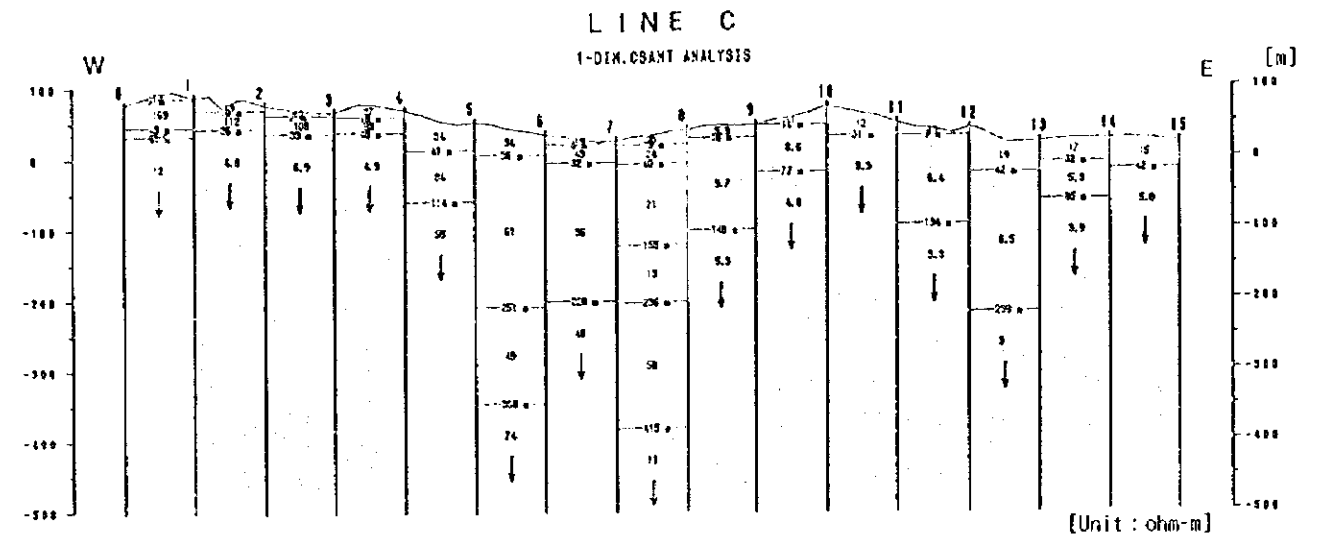
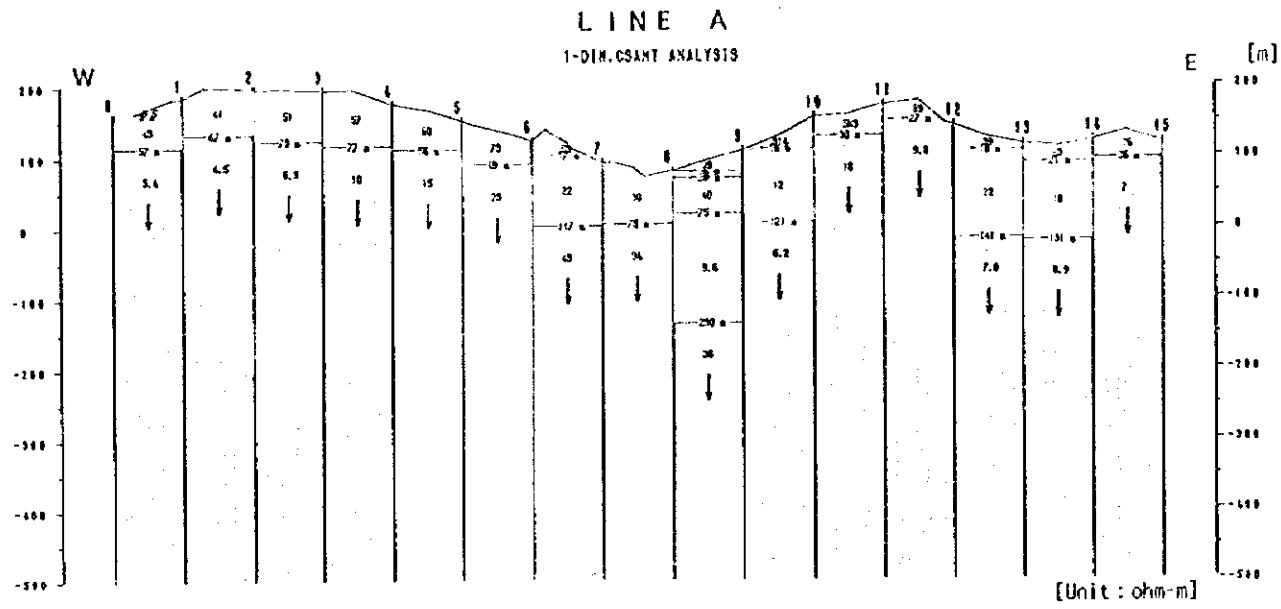
SCALE 1 : 10,000



- | | | | |
|---------------------------------------|--|---|--|
| <p>0 1
A —●—
15</p> <p>30</p> | <p>Line Name & Station No.
Array CSAMT
Resistivity (ohm-m)</p> <p>Contour Line Value &
Resistivity (ohm-m)</p> | <p>H</p> <p>L</p> <p> 50 ≤ pa</p> <p> pa ≤ 10</p> | <p>High Resistivity Zone</p> <p>Low Resistivity Zone</p> |
|---------------------------------------|--|---|--|

Fig. 2-5-7 (3) CSAMT Plane Map of Apparent Resistivity [32Hz]





LEGEND

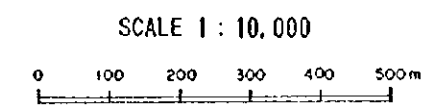
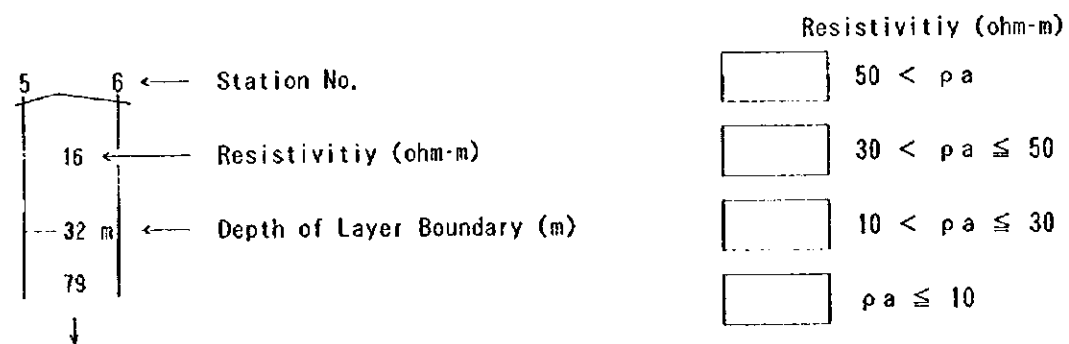
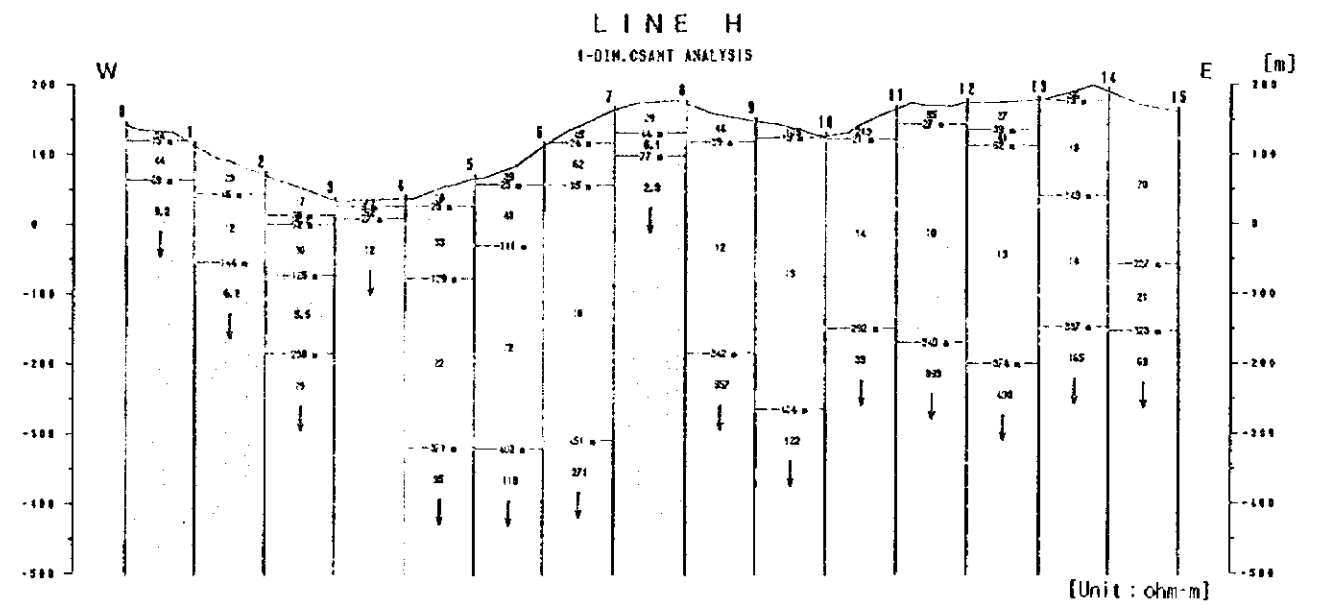
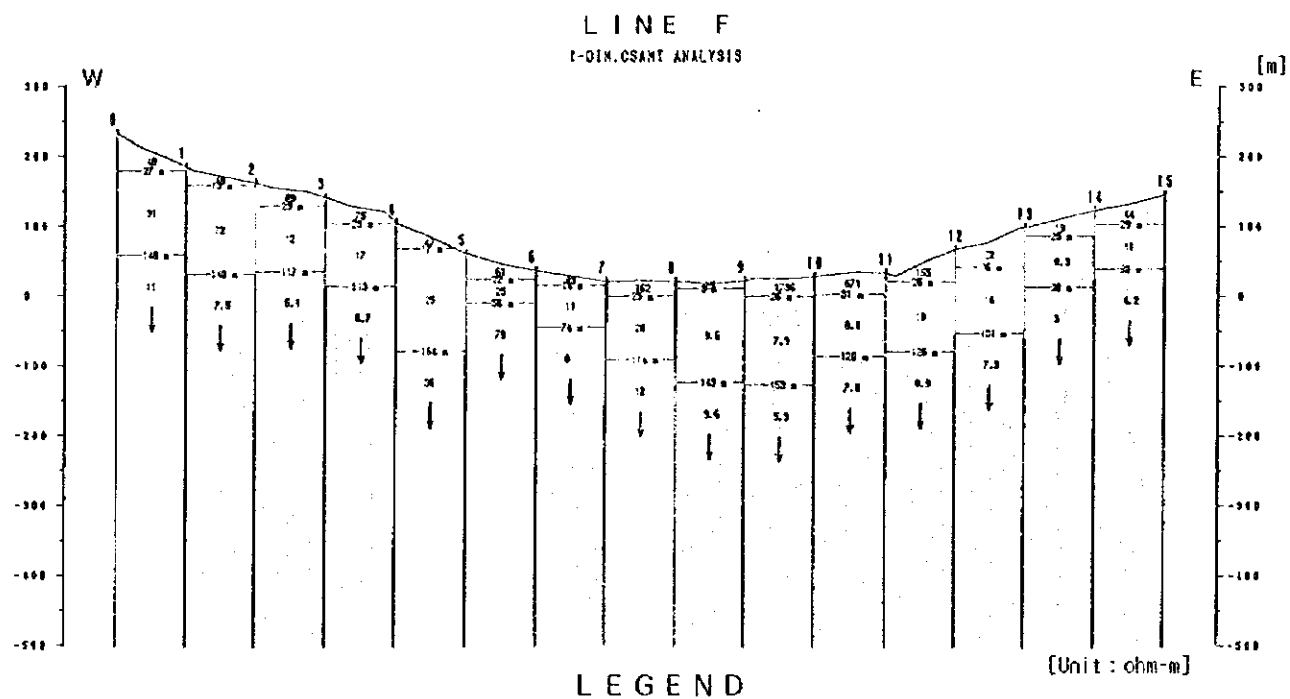
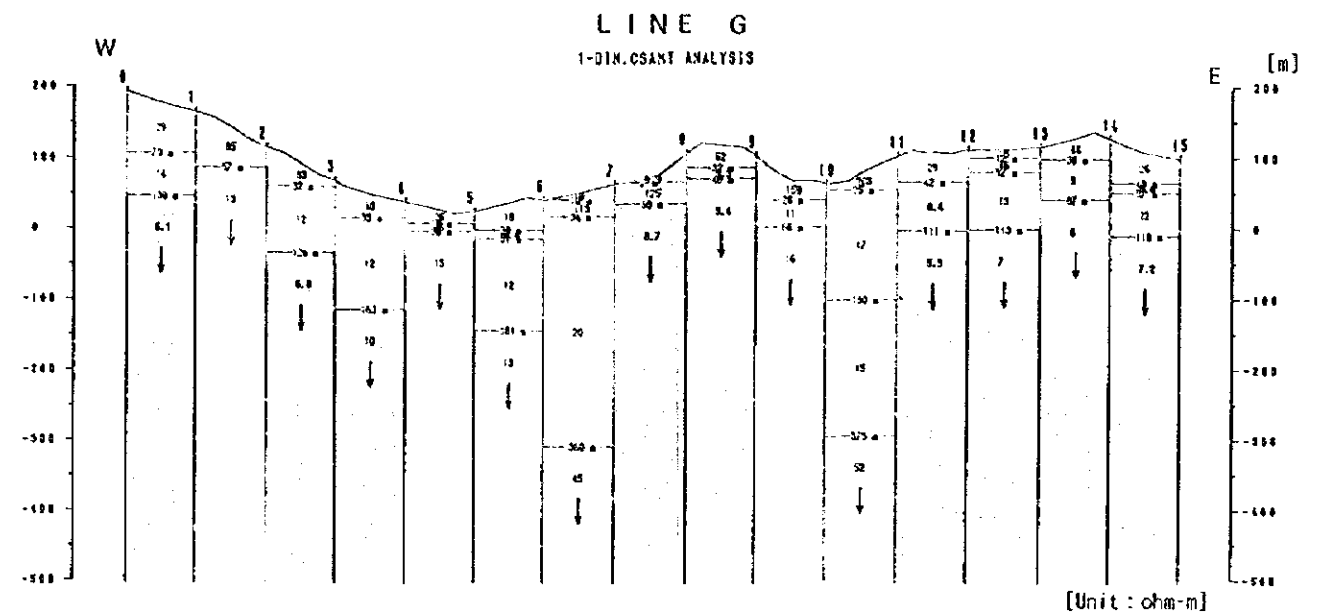
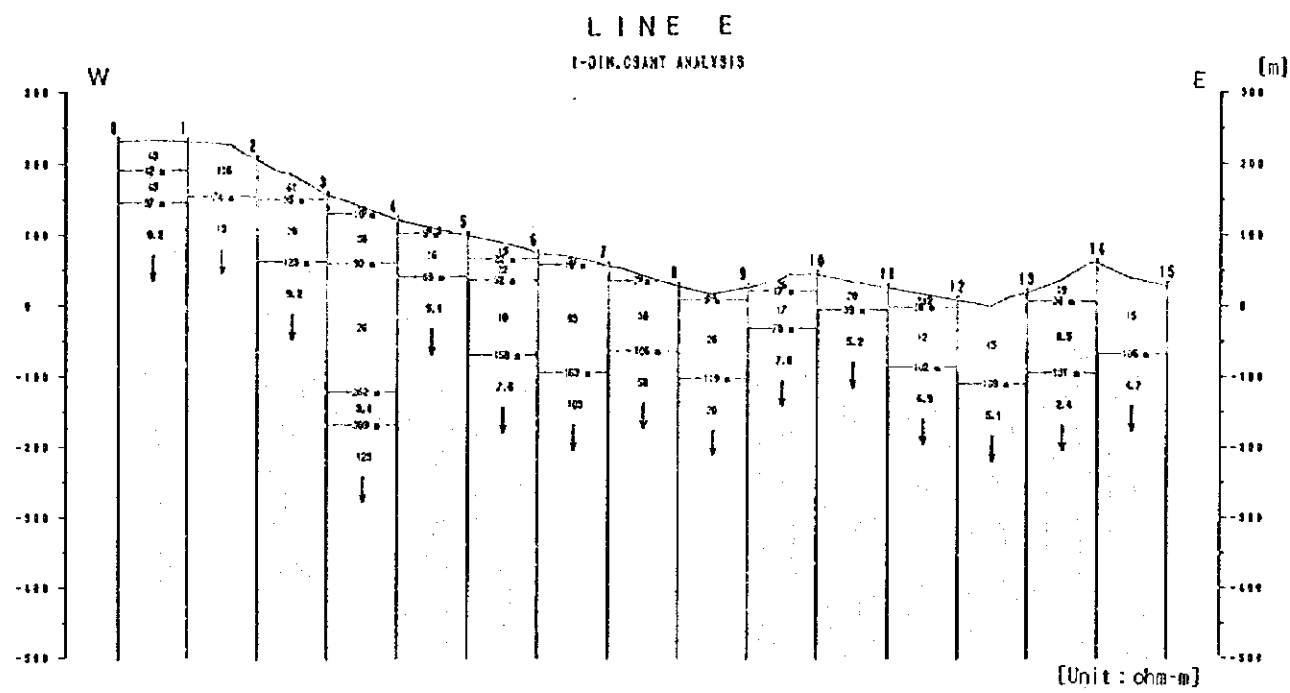


Fig. 2-5-8 (1) CSAMT Section of Resistivity Structure [Line A-D]



LEGEND

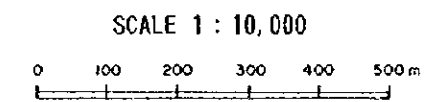
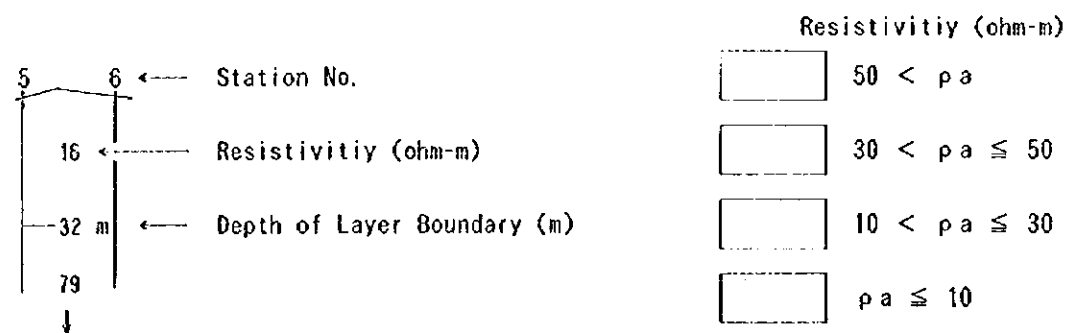
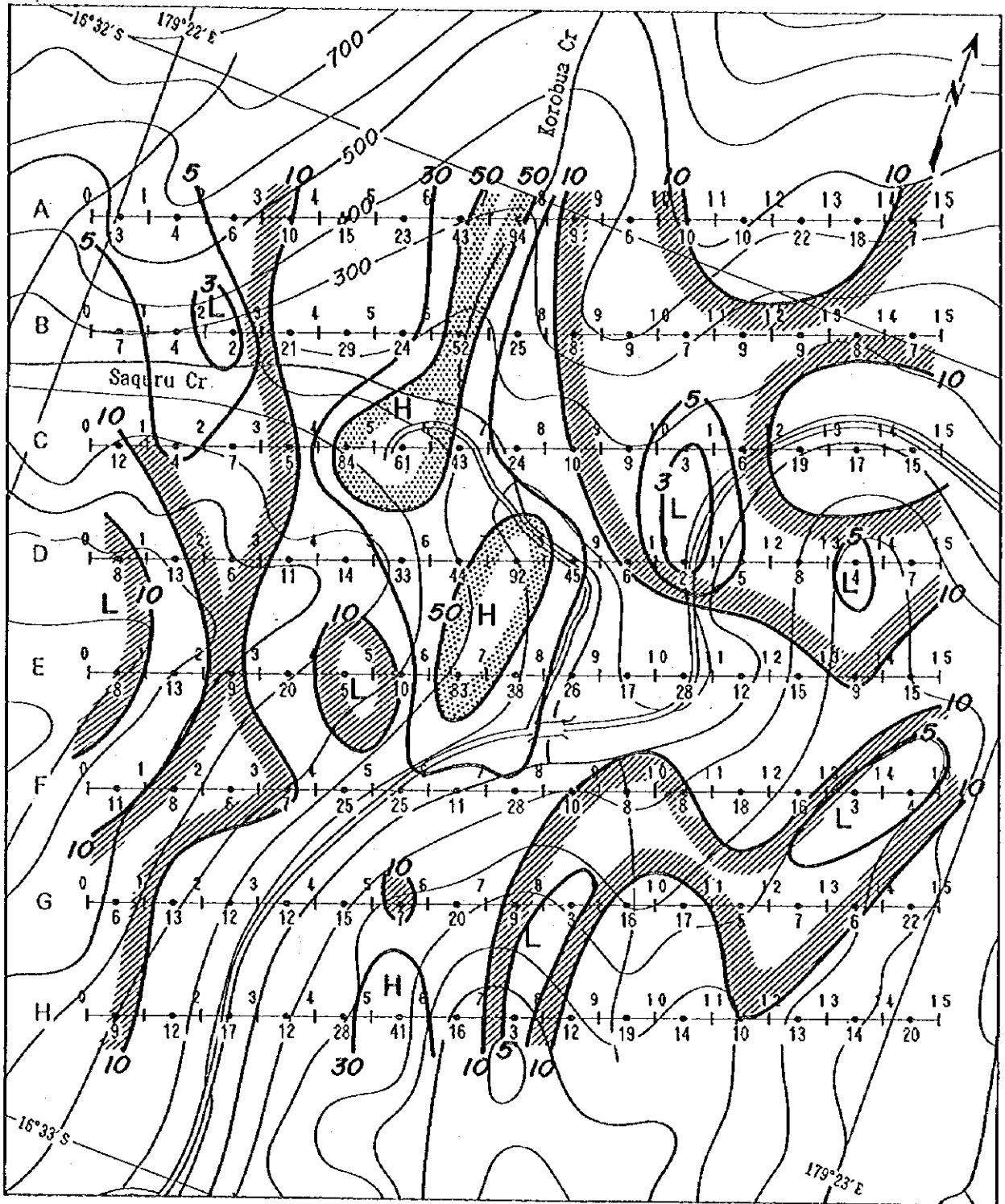
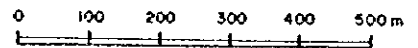


Fig. 2-5-8 (2) CSAMT Section of Resistivity Structure [Line E-H]



LEGEND

SCALE 1 : 10,000



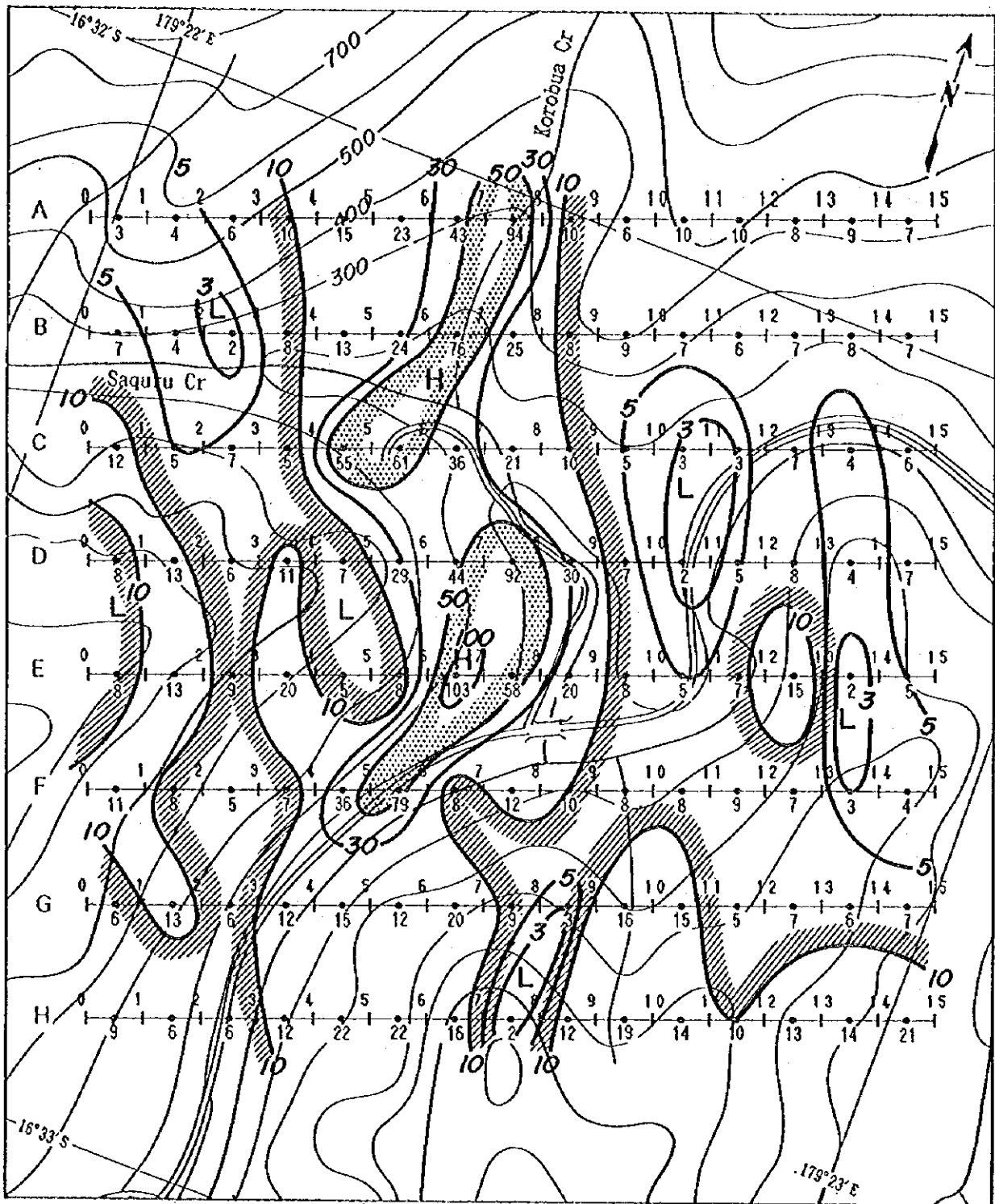
0 1 Line Name & Station No.
 A —●— Array CSAMT
 12 Resistivity (ohm-m)

H High Resistivity Zone
 L Low Resistivity Zone

30 Contour Line Value & Resistivity (ohm-m)

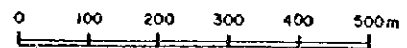
50 ≤ ρ_a
 ρ_a ≤ 10

Fig. 2-5-9 (1) CSAMT Plane Map of Resistivity Structure [0 ASL]



LEGEND

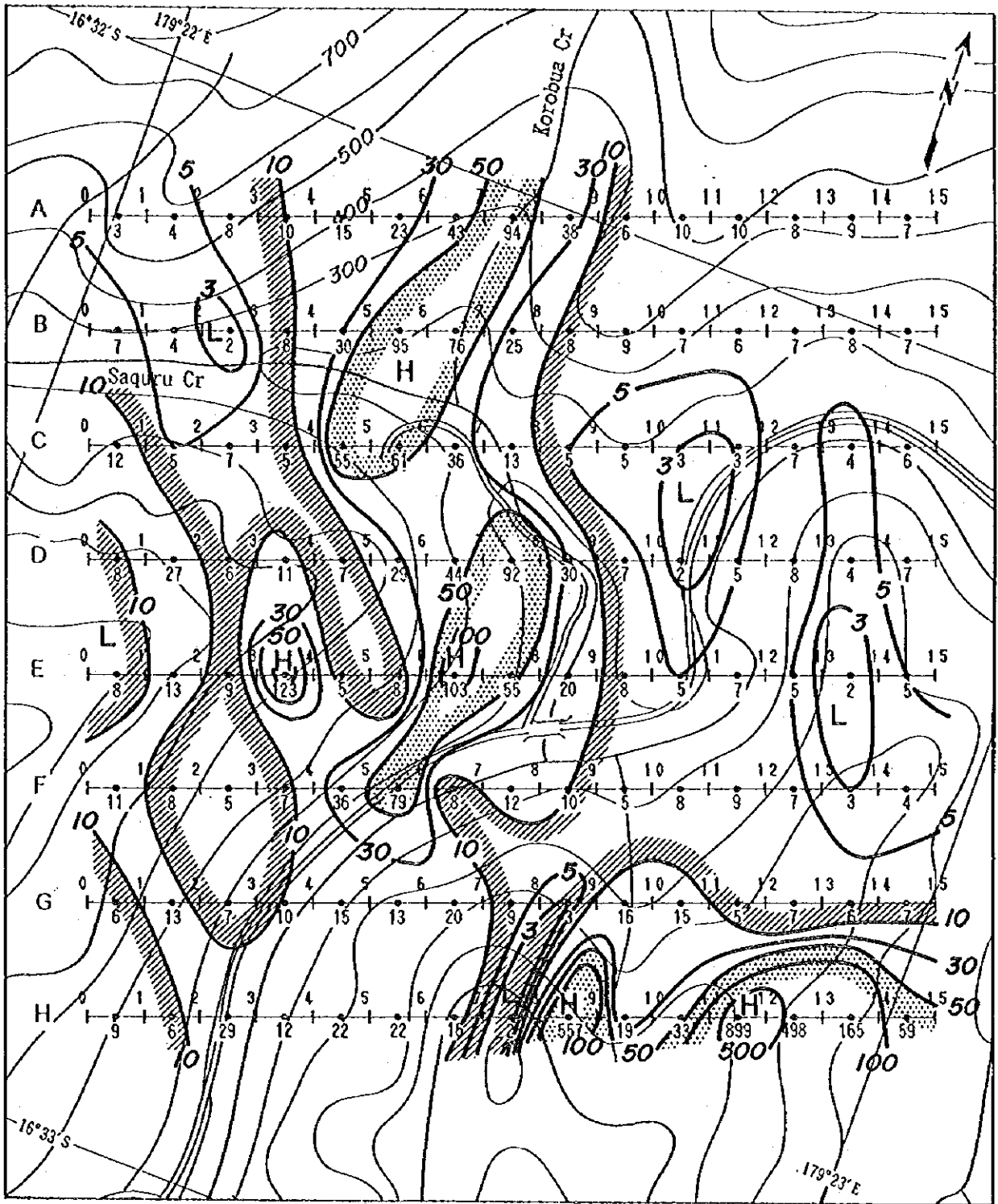
SCALE 1 : 10,000



- 0 1 Line Name & Station No.
- A | ● | + Array CSAMT
- 12 Resistivity (ohm-m)
- 50 Contour Line Value & Resistivity (ohm-m)

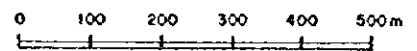
- H High Resistivity Zone
- L Low Resistivity Zone
- 50 ≤ ρa
- ρa ≤ 10

Fig. 2-5-9 (2) CSAMT Plane Map of Resistivity Structure [-100m ASL]



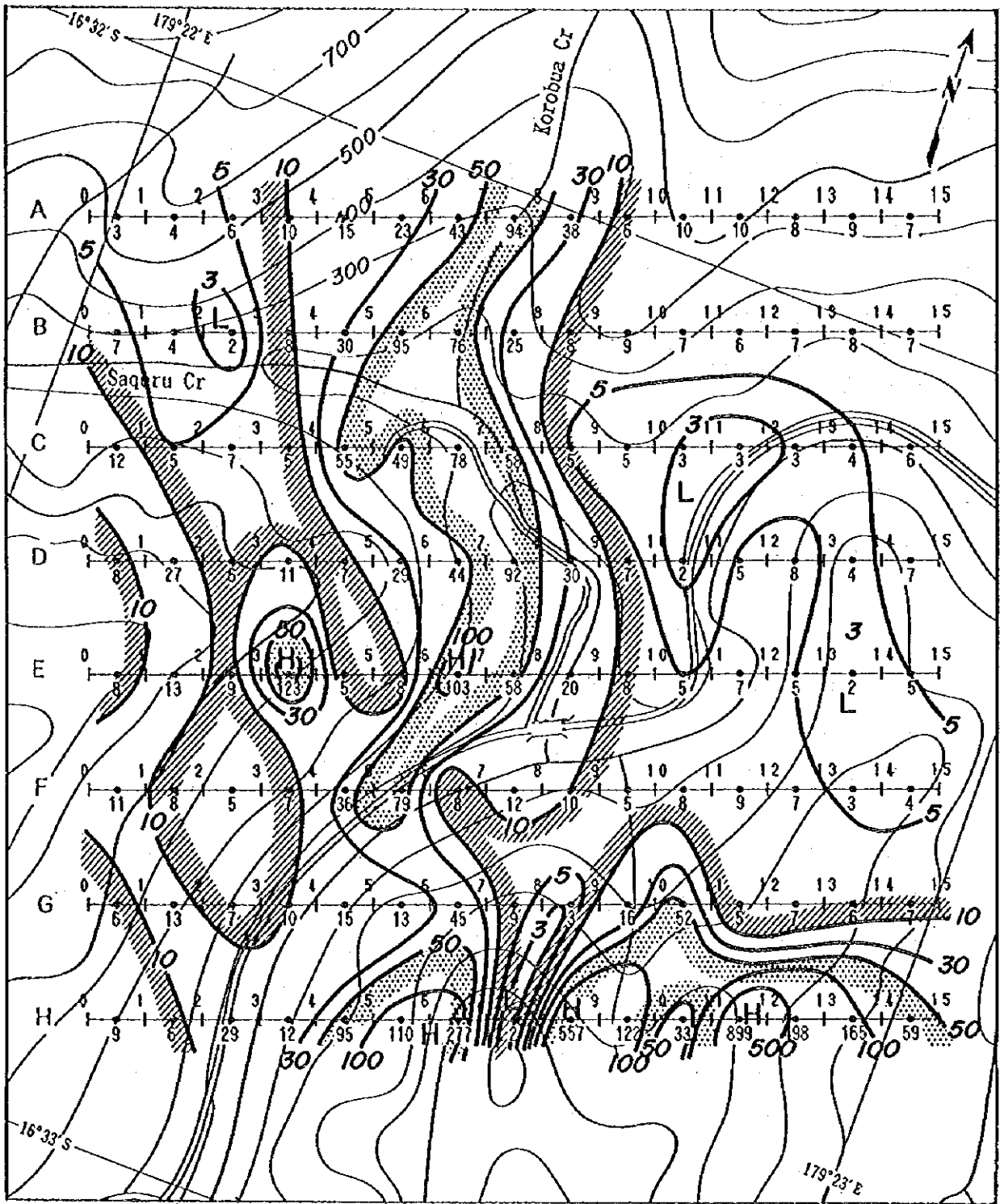
LEGEND

SCALE 1 : 10,000



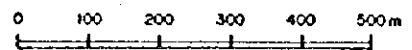
- | | | | | |
|----|---|--|---|-----------------------|
| 0 | 1 | Line Name & Station No. | H | High Resistivity Zone |
| A | ● | Array CSAMT | L | Low Resistivity Zone |
| 12 | — | Resistivity (ohm-m) | | |
| | ○ | Contour Line Value & Resistivity (ohm-m) | | |
| | | | | $50 \leq \rho_a$ |
| | | | | $\rho_a \leq 10$ |

Fig. 2-5-9 (3) CSAMT Plane Map of Resistivity Structure [-200m ASL]



LEGEND

SCALE 1 : 10,000



- | | | | |
|-------|--|---|-----------------------|
| 0 1 | Line Name & Station No. | H | High Resistivity Zone |
| A —●— | Array CSAMT | L | Low Resistivity Zone |
| 12 | Resistivity (ohm-m) | | |
| | Contour Line Value & Resistivity (ohm-m) | | $50 \leq \rho_a$ |
| | | | $\rho_a \leq 10$ |

Fig. 2-5-9 (4) CSAMT Plane Map of Resistivity Structure [-400m ASL]

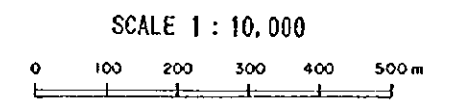
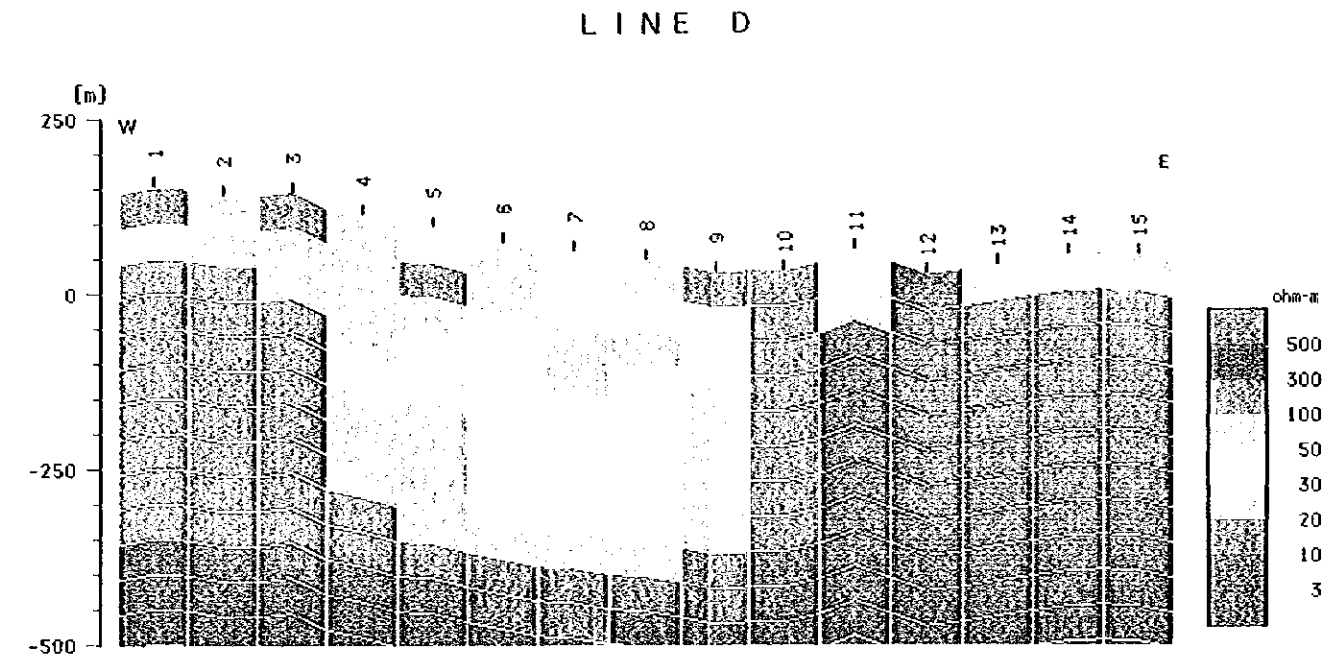
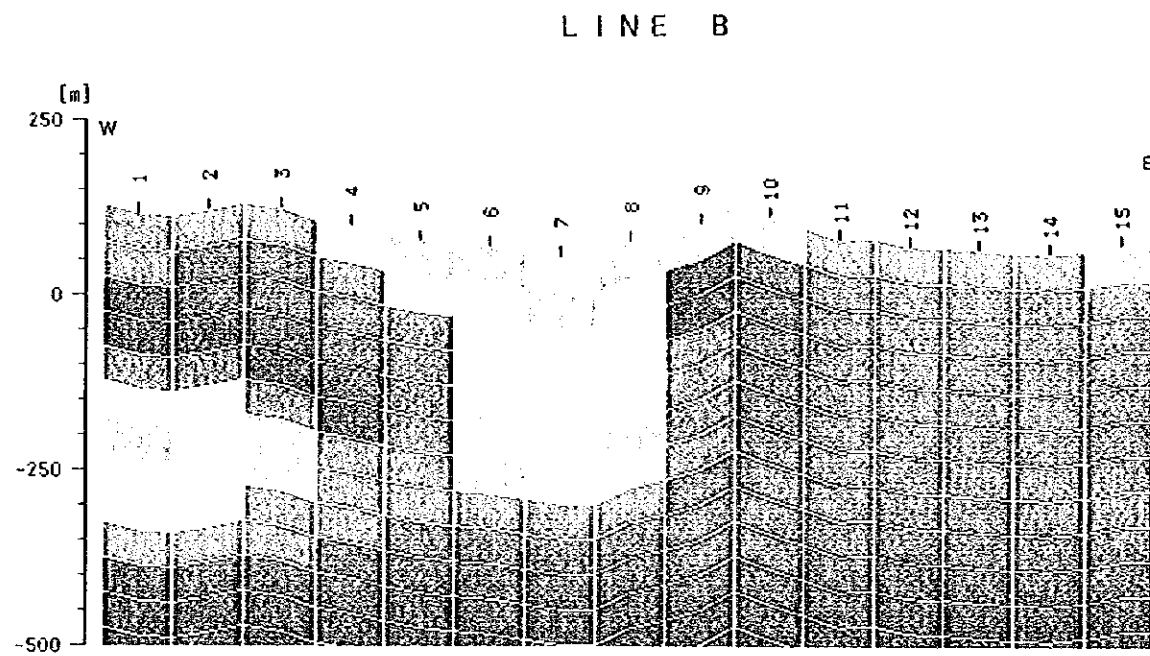
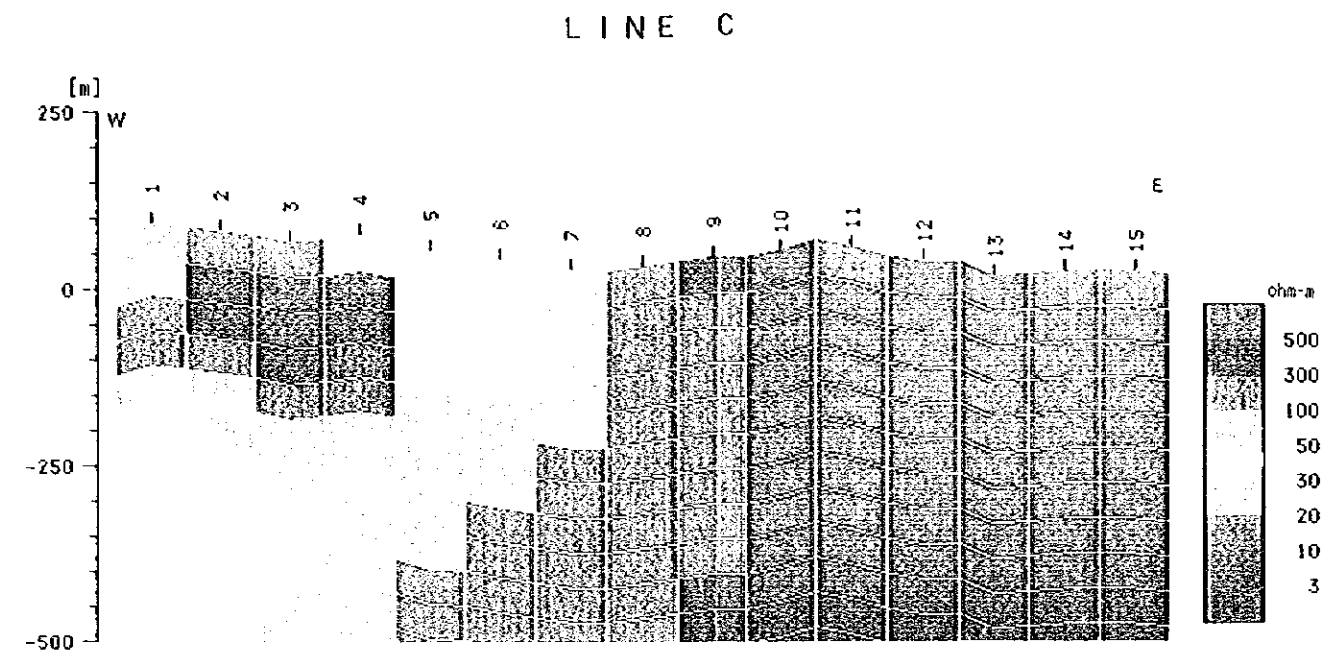
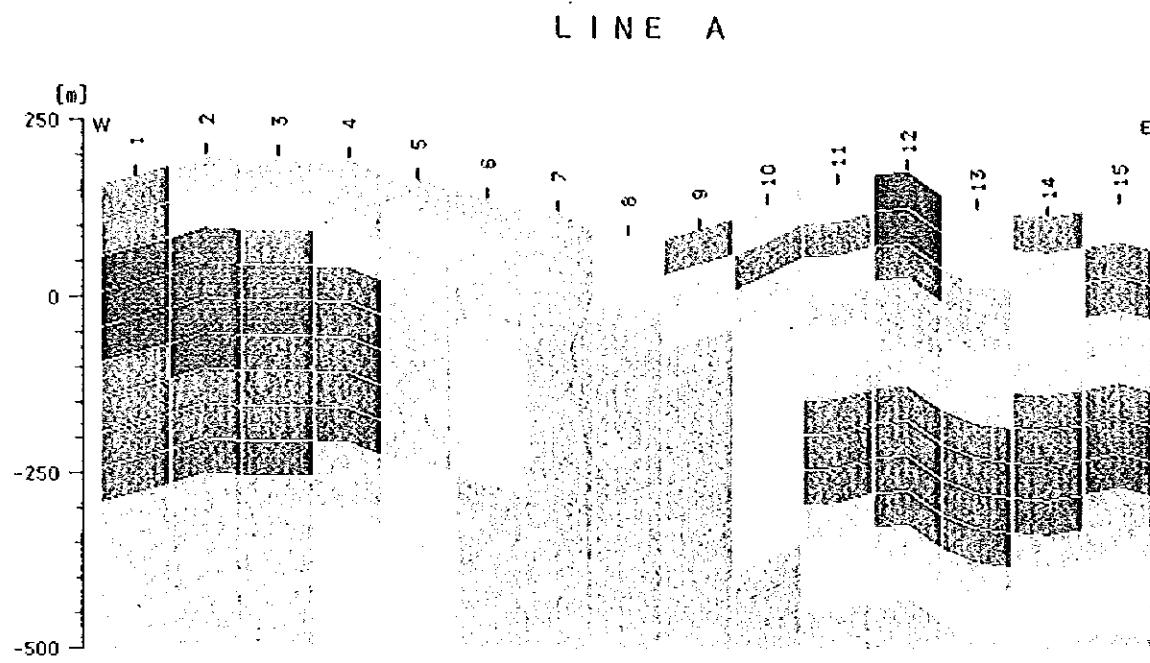


Fig. 2-5-10 (1) CSAMT 2-d. Simulation Analysis [Line A-D]

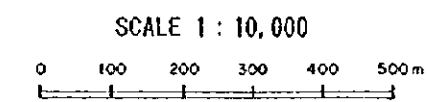
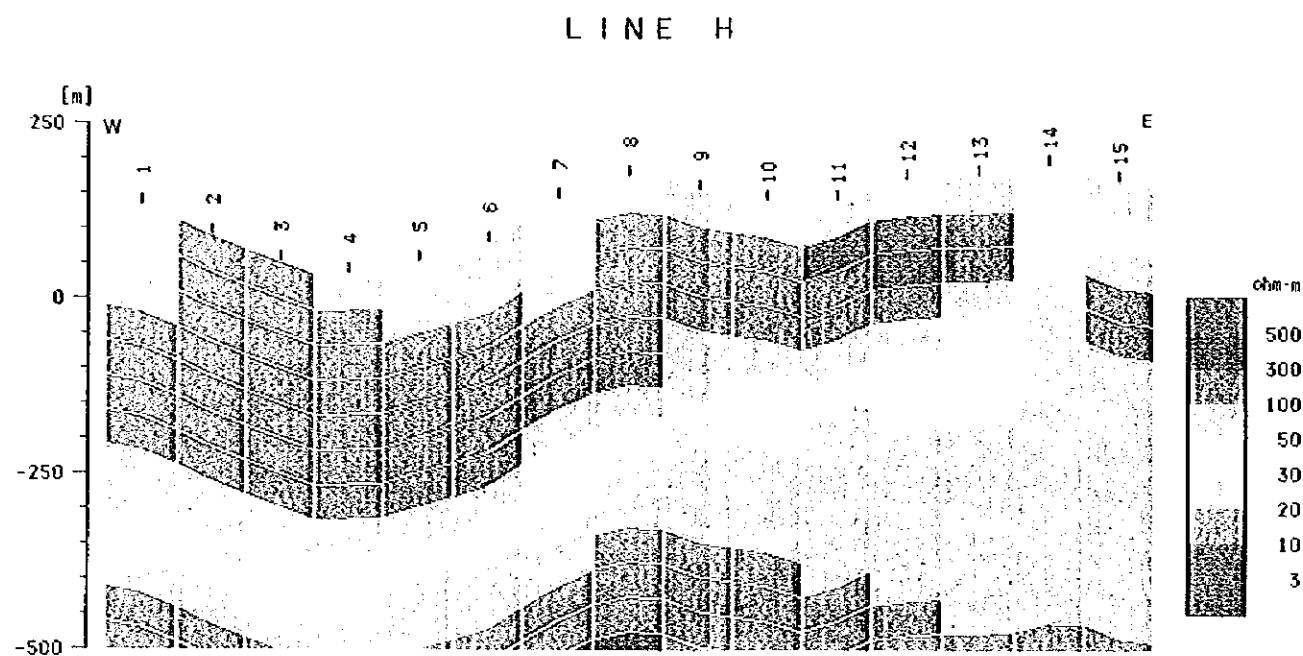
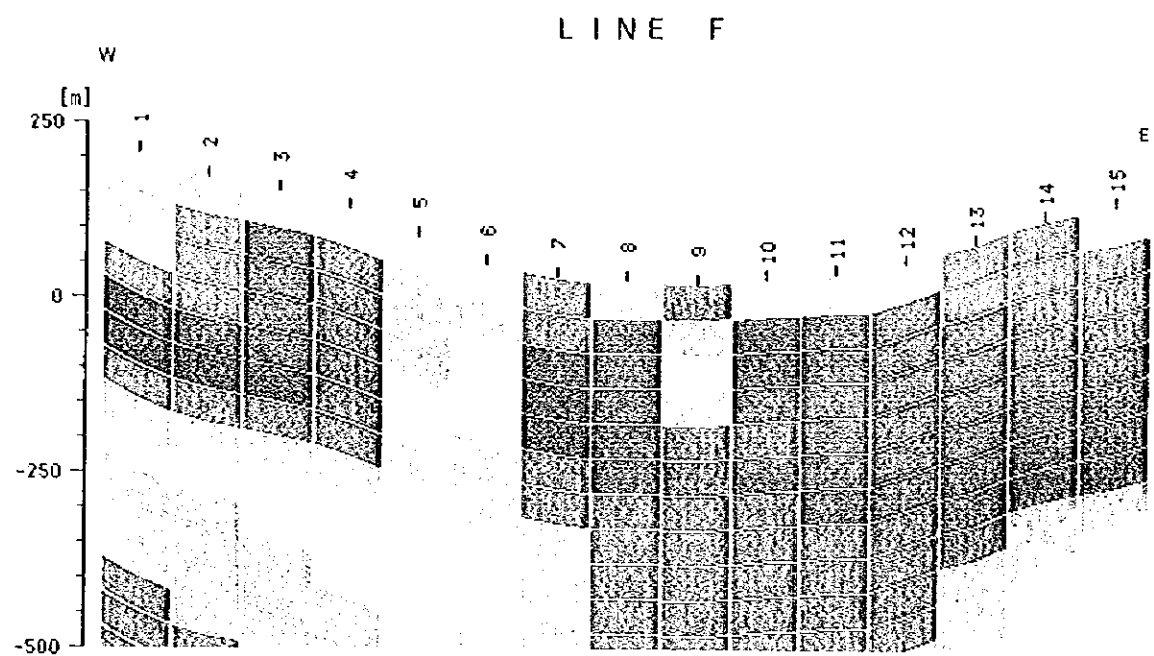
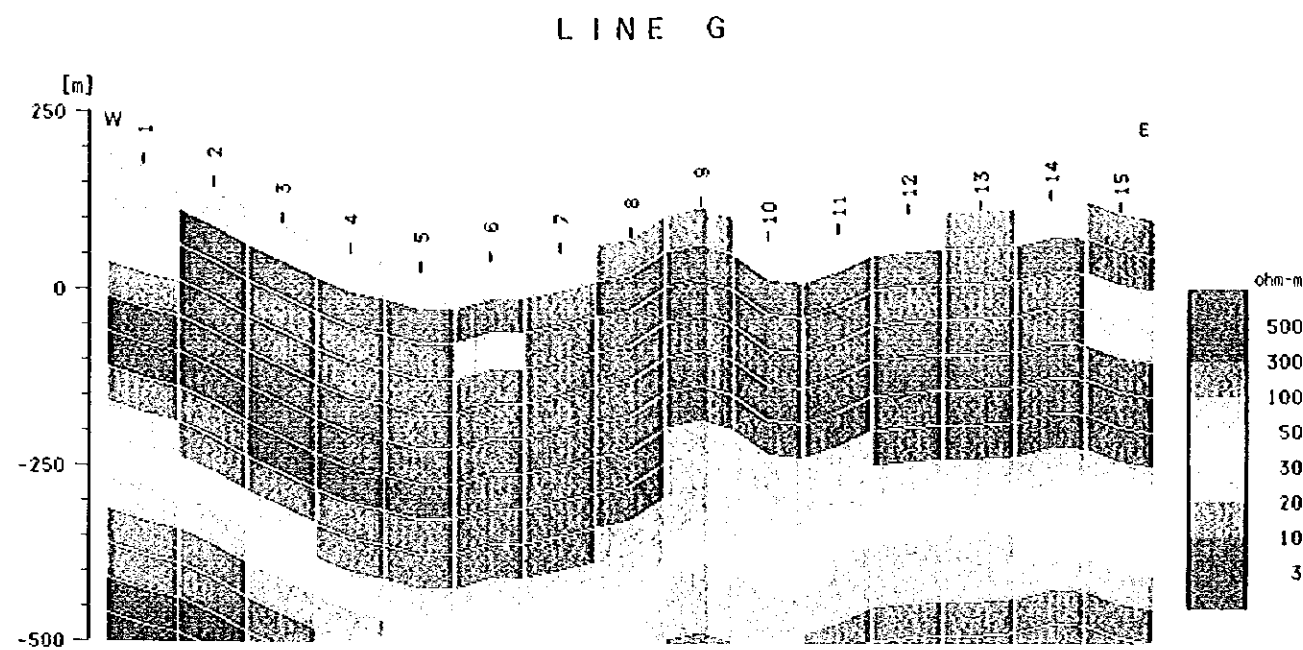
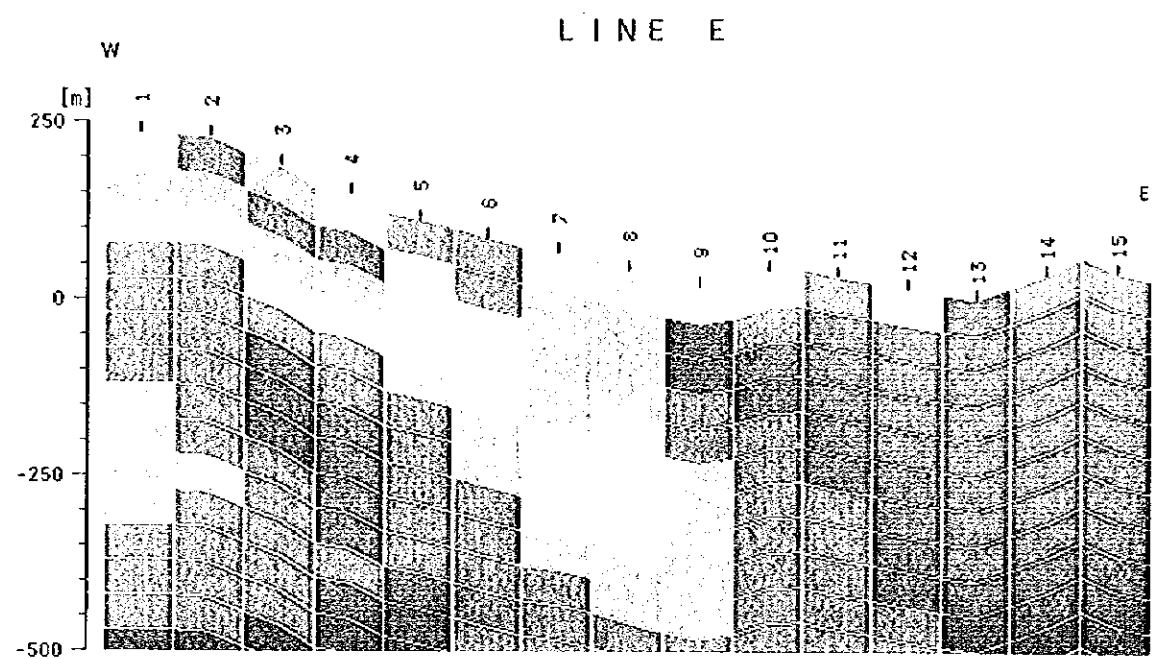
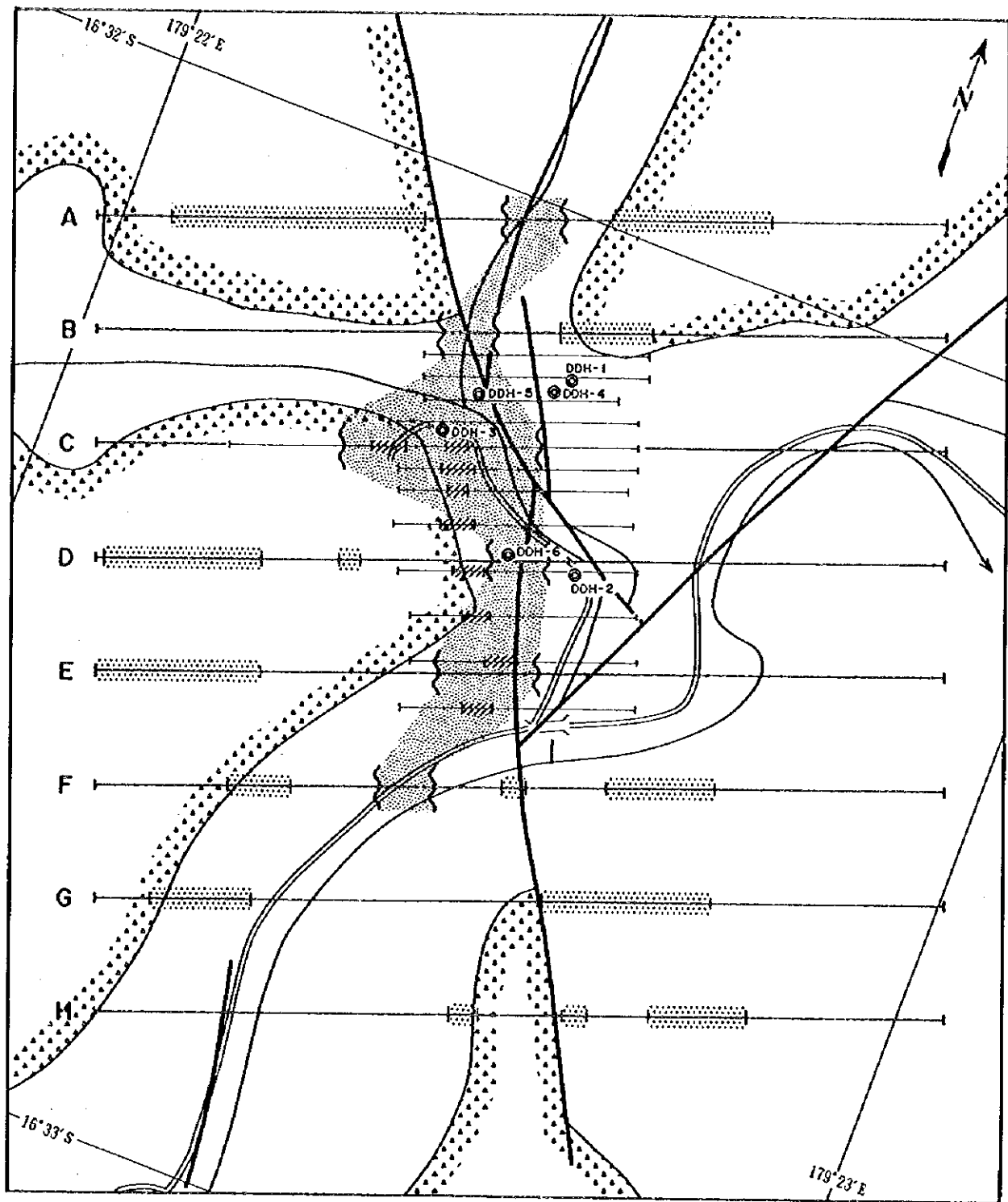
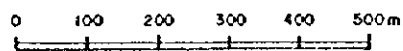


Fig. 2-5-10 (2) CSAMT 2-d. Simulation Analysis [Line E-H]



LEGEND

SCALE 1 : 10,000



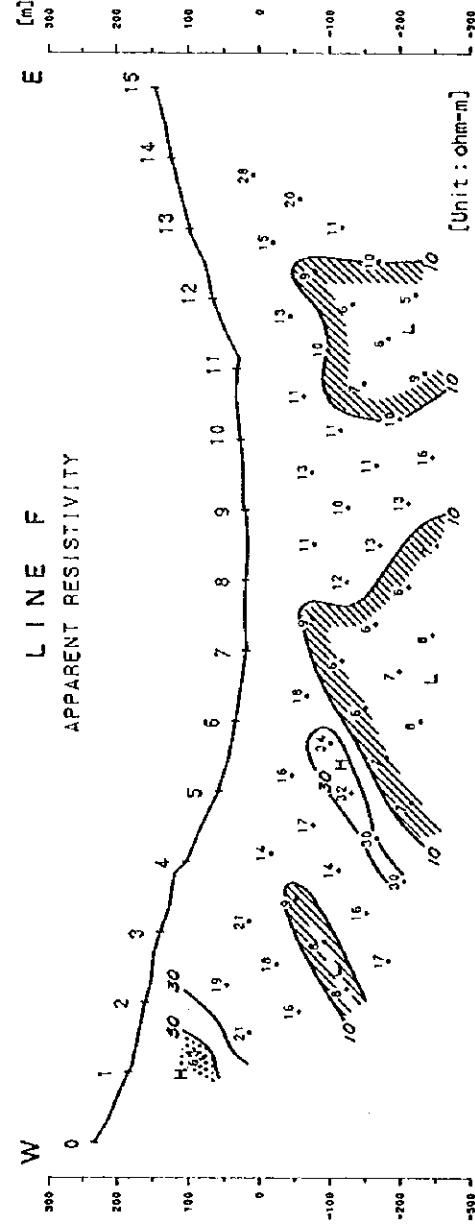
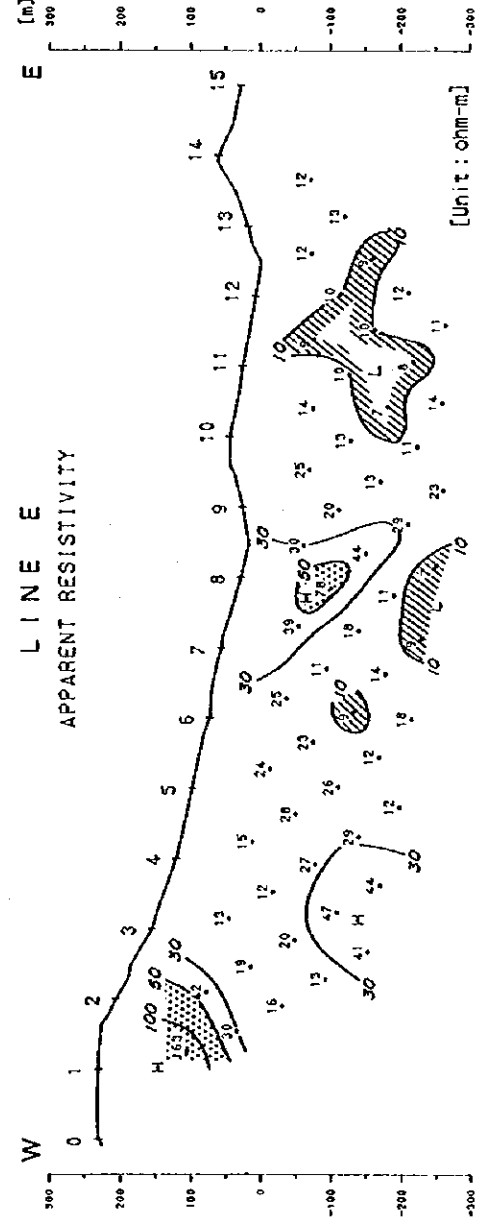
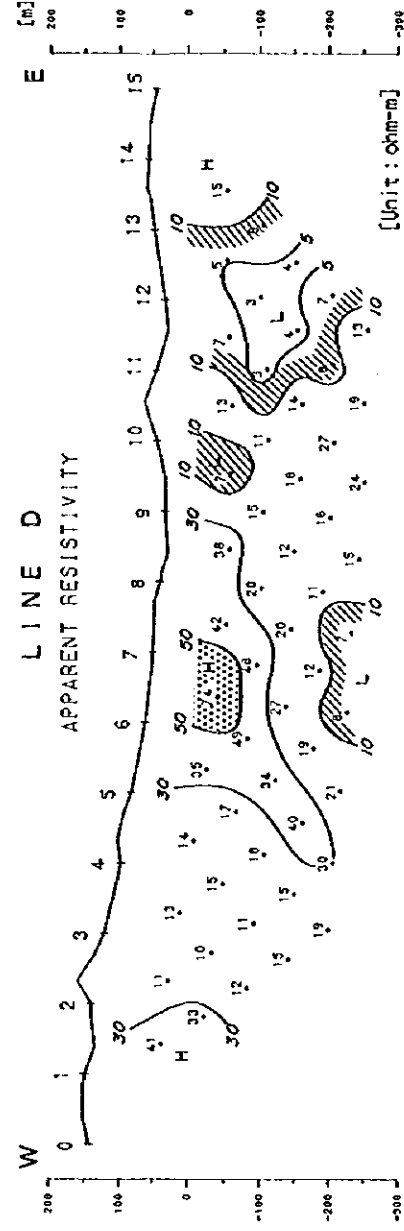
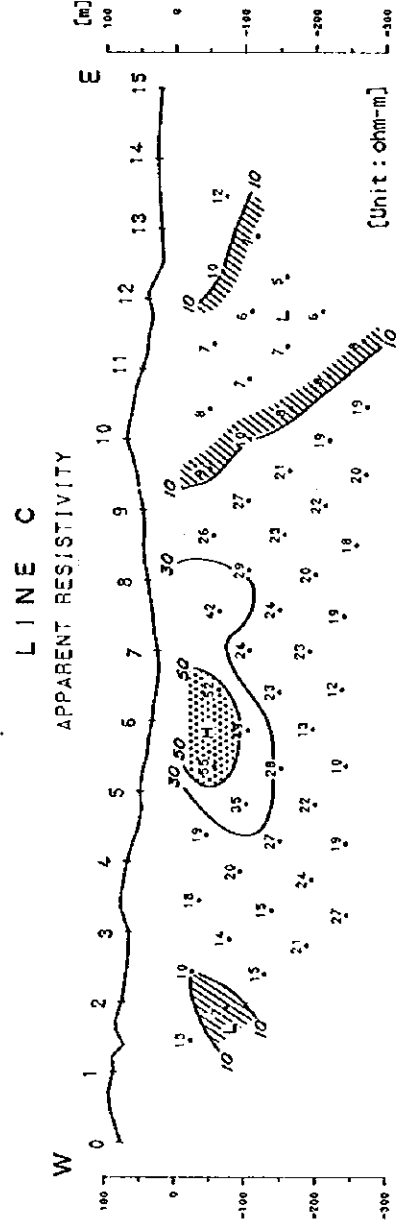
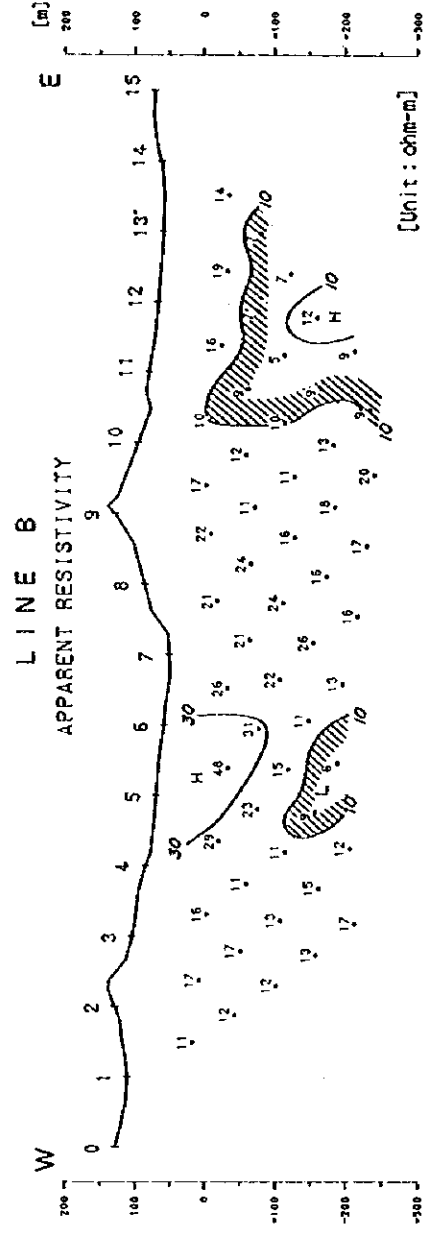
- Fault
- Andesitic volcanoclastic rocks
- Resistivity of discontinuity Line
- Soil geochemical anomalous zone
- High Resistivity zone (>50 ohm-m)
- IP anomaly (Geotrex, 1988)

Fig. 2-5-11 CSAMT Interpretation Map

0

0

0



LEGEND

- H High Resistivity Zone
- L Low Resistivity Zone
- $50 \leq \rho_a$
- $\rho_a \leq 10$

SCALE 1 : 10,000

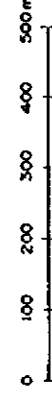
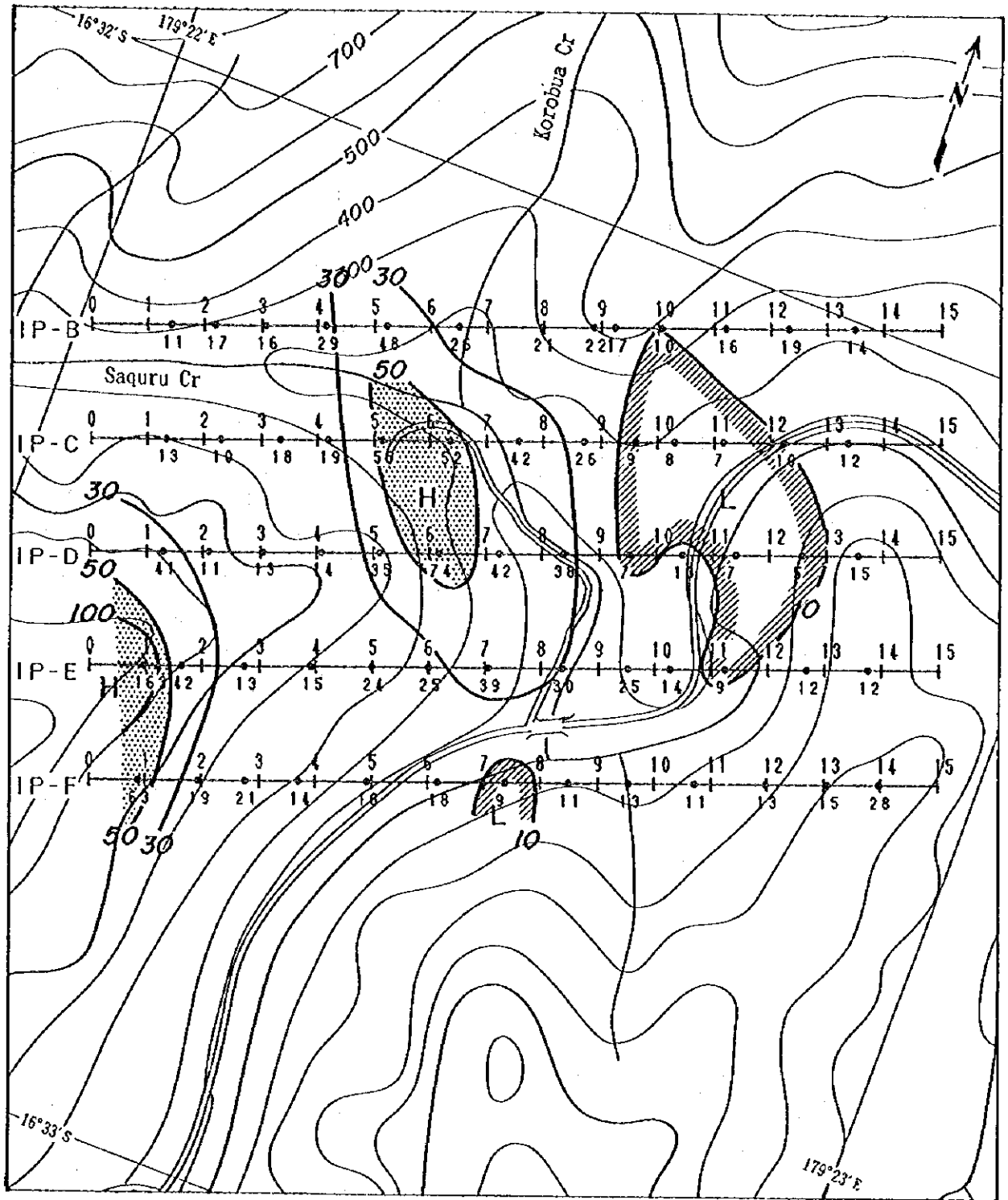
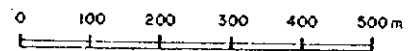


Fig. 2-5-12 TDIP Pseudosection of Apparent Resistivity [Line B-F]



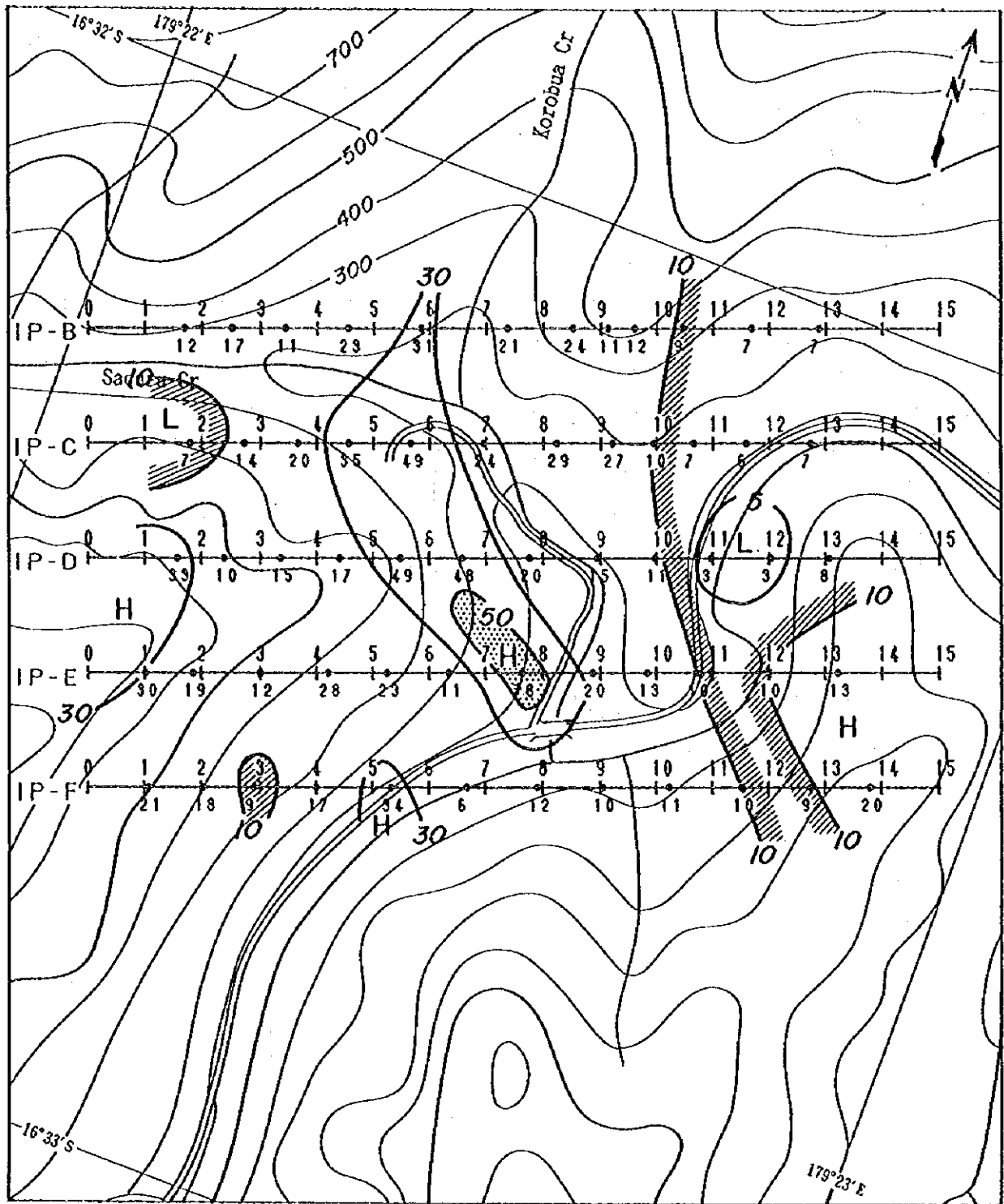
LEGEND

SCALE 1 : 10,000



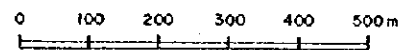
0 1	Line Name & Station No.	H	High Resistivity Zone
IP-B	Resistivity (ohm-m)	L	Low Resistivity Zone
12			
30	Contour Line Value & Resistivity (ohm-m)		$50 \leq \rho_a$
			$\rho_a \leq 10$

Fig. 2-5-13 (1) TDIP Plane Map of Apparent Resistivity [n=1]



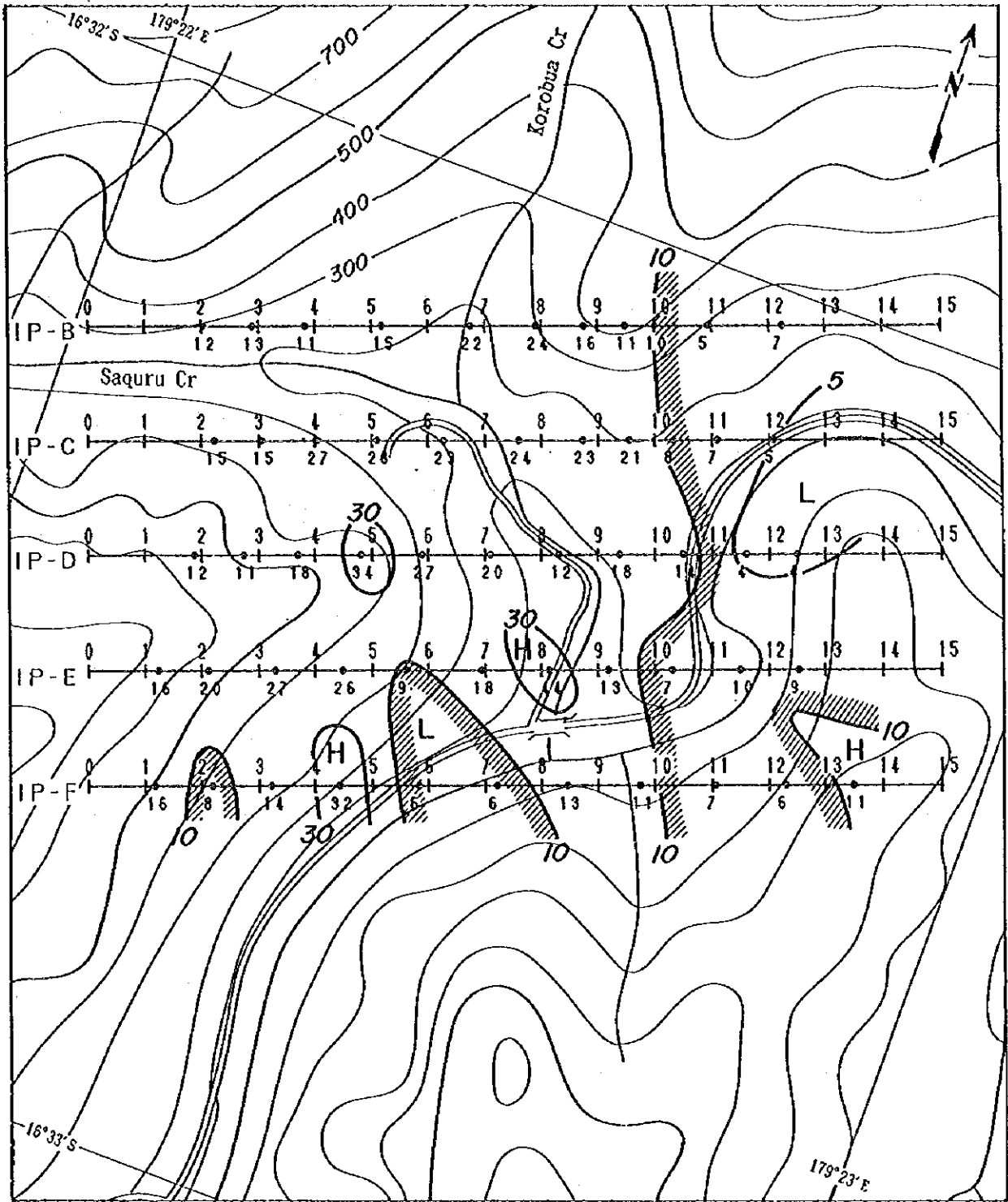
LEGEND

SCALE 1 : 10,000



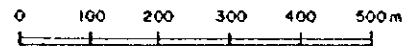
<p>0 1 IP-B —●—</p> <p>12 Resistivity (ohm-m)</p> <p>30 Contour Line Value & Resistivity (ohm-m)</p>	<p>Line Name & Station No.</p> <p>Resistivity (ohm-m)</p> <p>Contour Line Value & Resistivity (ohm-m)</p>	<p>H High Resistivity Zone</p> <p>L Low Resistivity Zone</p> <p> 50 ≤ pa</p> <p> pa ≤ 10</p>
--	---	--

Fig. 2-5-13 (2) TDIP Plane Map of Apparent Resistivity [n=2]



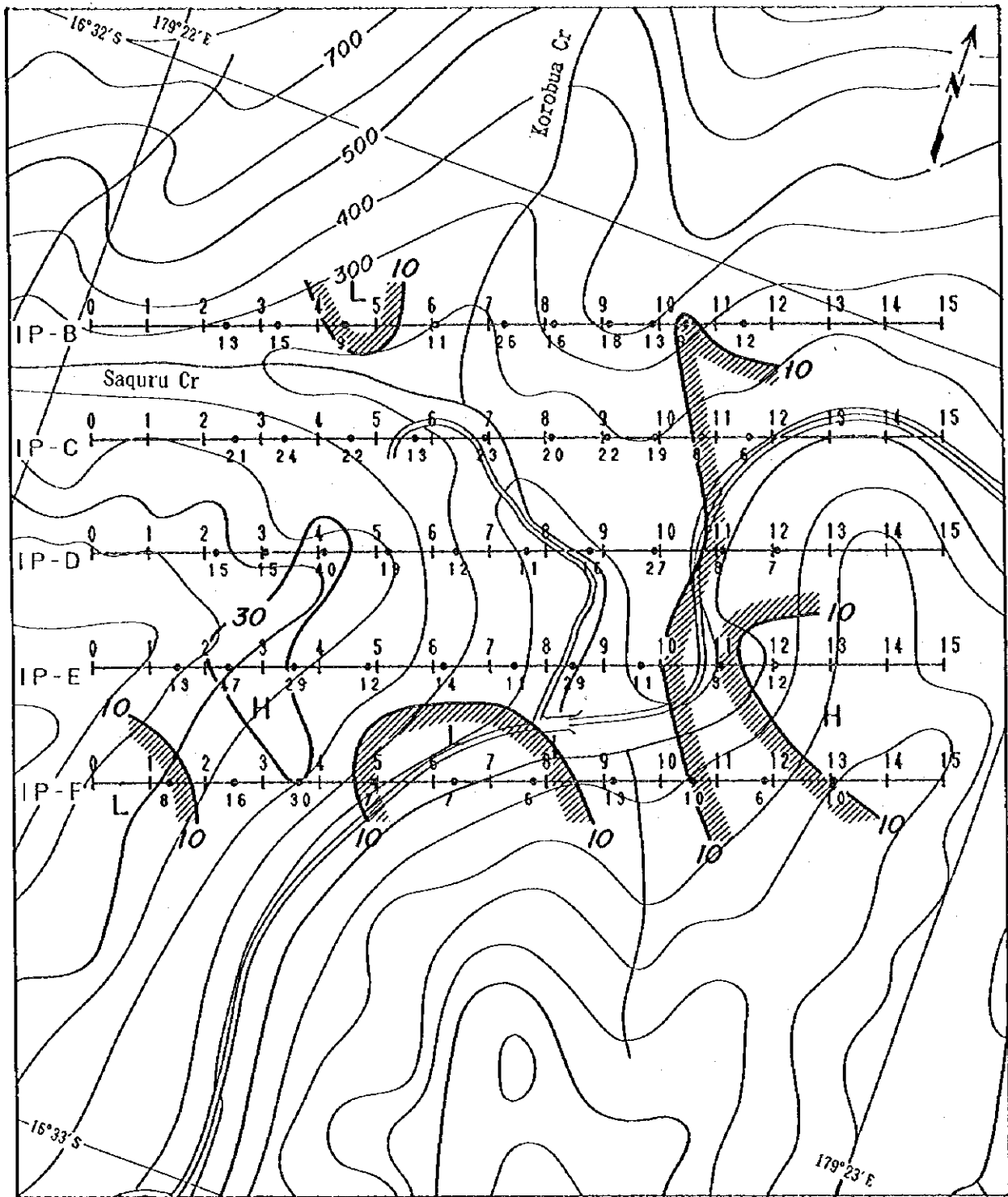
LEGEND

SCALE 1 : 10,000



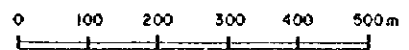
0 1	Line Name & Station No.	H	High Resistivity Zone
IP-B —●—	Resistivity (ohm-m)	L	Low Resistivity Zone
12			$50 \leq \rho_a$
	Contour Line Value & Resistivity (ohm-m)		$\rho_a \leq 10$

Fig. 2-5-13 (3) TDIP Plane Map of Apparent Resistivity [n=3]



LEGEND

SCALE 1 : 10,000




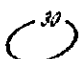

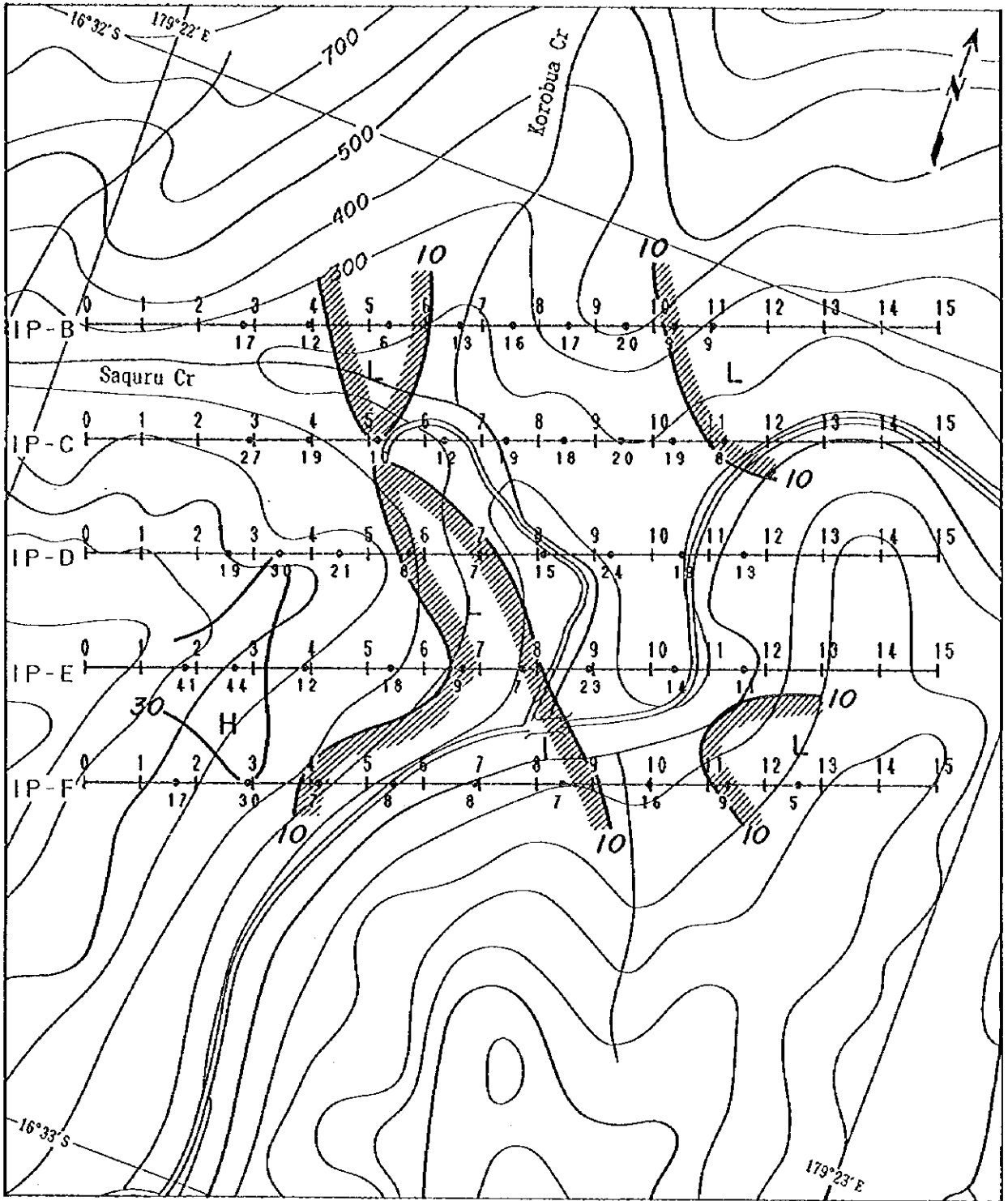
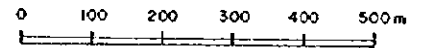
0 1	Line Name & Station No.	H	High Resistivity Zone
IP-B -----		L	Low Resistivity Zone
12	Resistivity (ohm-m)		$50 \leq \rho_a$
	Contour Line Value & Resistivity (ohm-m)		$\rho_a \leq 10$

Fig. 2-5-13 (4) TDIP Plane Map of Apparent Resistivity [n=4]



LEGEND

SCALE 1 : 10,000



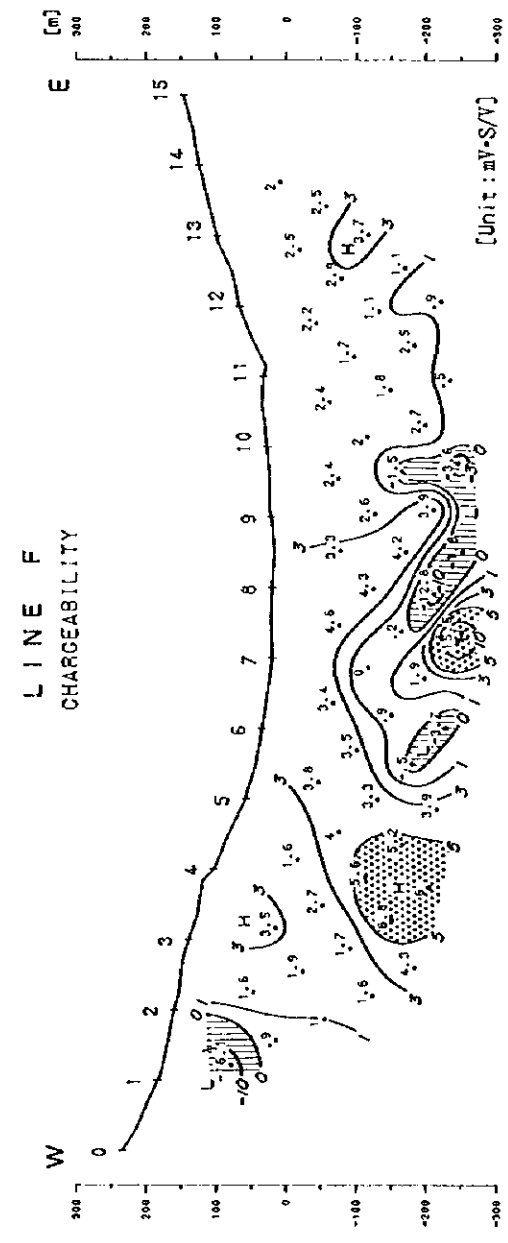
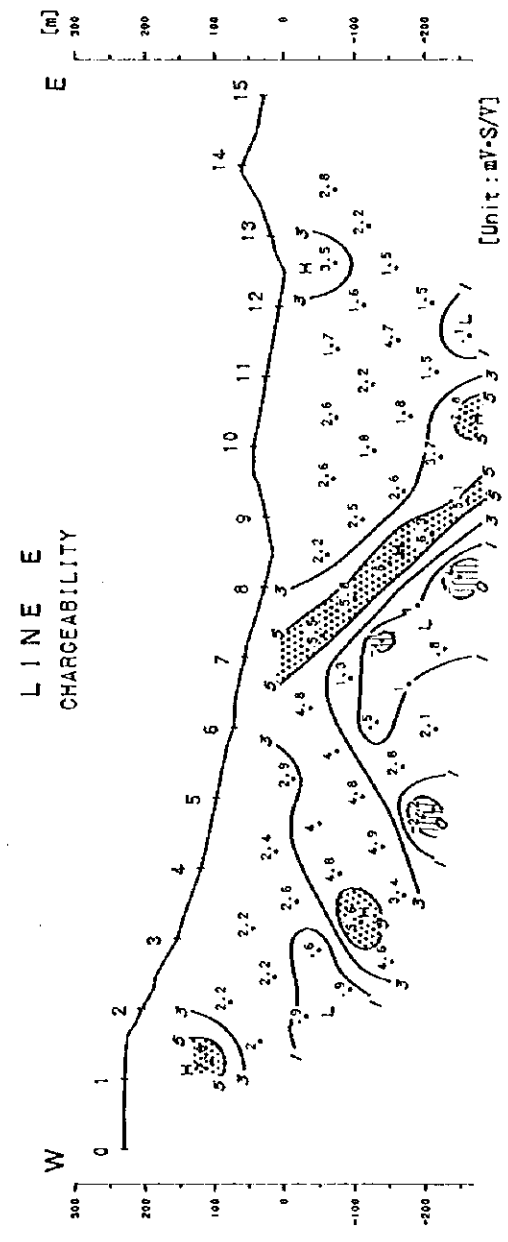
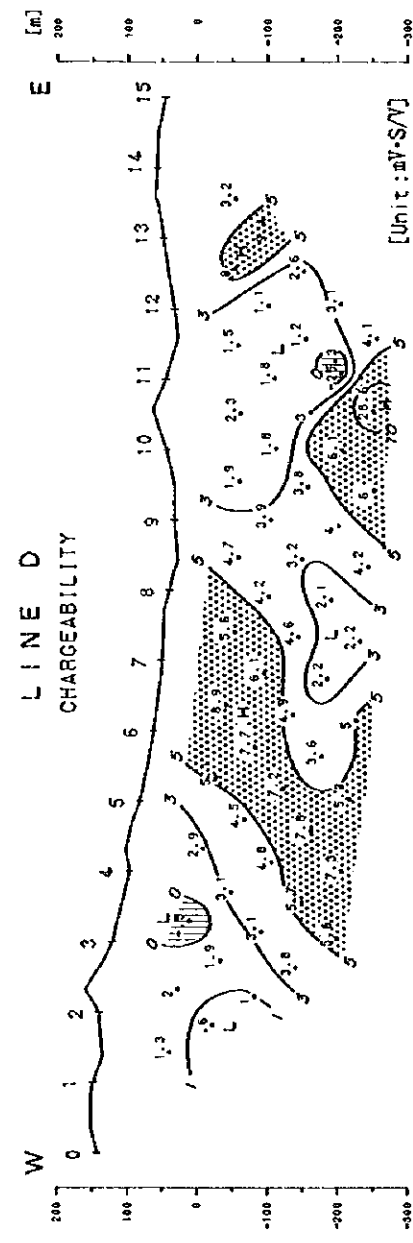
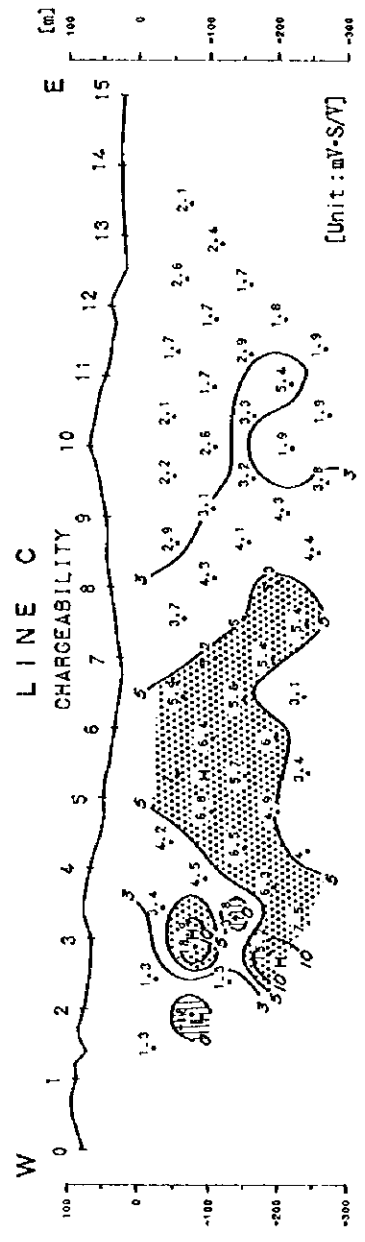
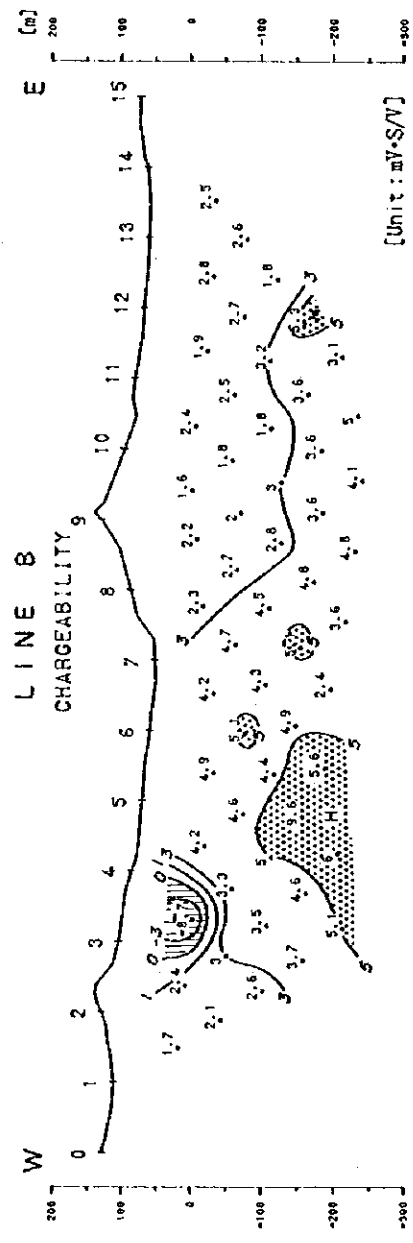
0	1	Line Name & Station No.	H	High Resistivity Zone
IP-B	12	Resistivity (ohm-m)	L	Low Resistivity Zone
30		Contour Line Value & Resistivity (ohm-m)		$50 \leq \rho_a$
				$\rho_a \leq 10$

Fig. 2-5-13 (5) TDIP Plane Map of Apparent Resistivity [n=5]

0

0

0



LEGEND

- H High Chargeability Zone
- L Low Chargeability Zone
- 5 ≤ M
- M ≤ 0

SCALE 1 : 10,000

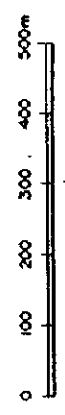
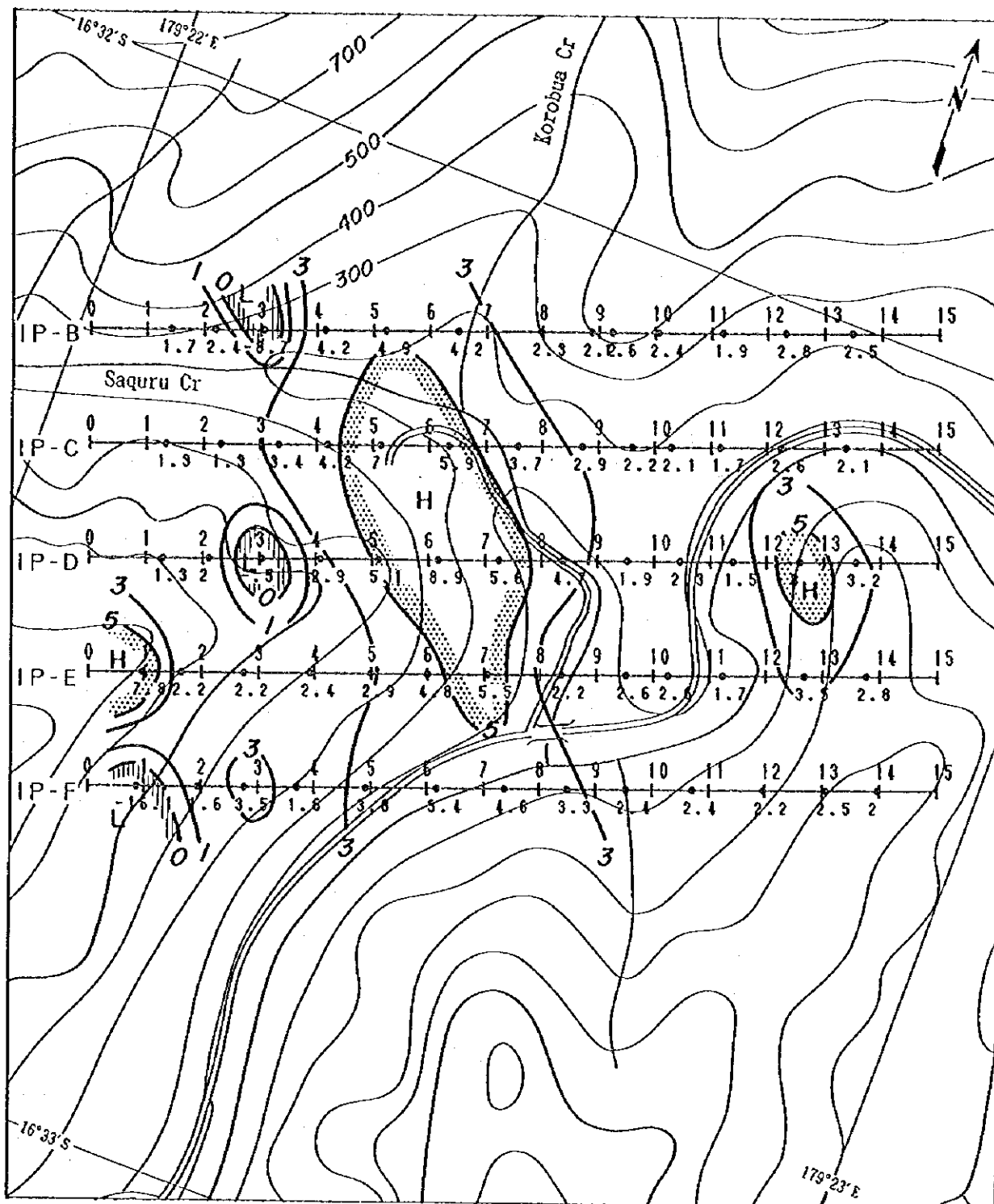
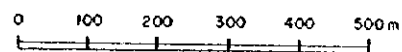


Fig. 2-5-14 TDIP Pseudosection of Chargeability [Line B-F]



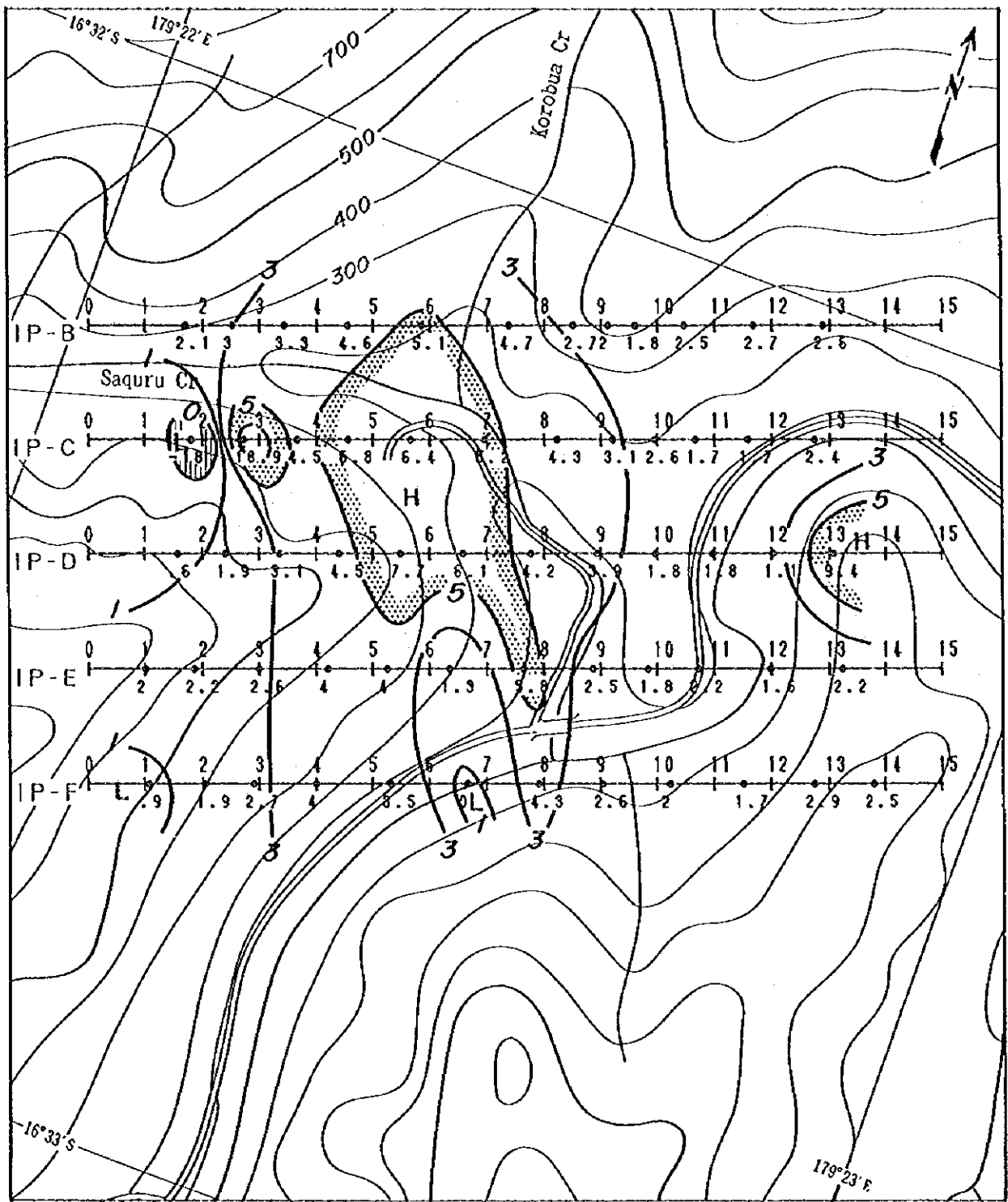
LEGEND

SCALE 1 : 10,000



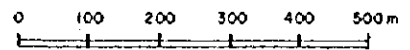
<p>0 1 IP-B ----- 2.3</p> <p>3 ○</p>	<p>Line Name & Station No.</p> <p>Chargeability ($\epsilon V \cdot S / V$)</p> <p>Contour Line Value & Chargeability ($\epsilon V \cdot S / V$)</p>	<p>H High Chargeability Zone</p> <p>L Low Chargeability Zone</p> <p> $5 \leq M$</p> <p> $M \leq 0$</p>
--	---	--

Fig. 2-5-15 (1) TDIP Plane Map of Chargeability [n=1]



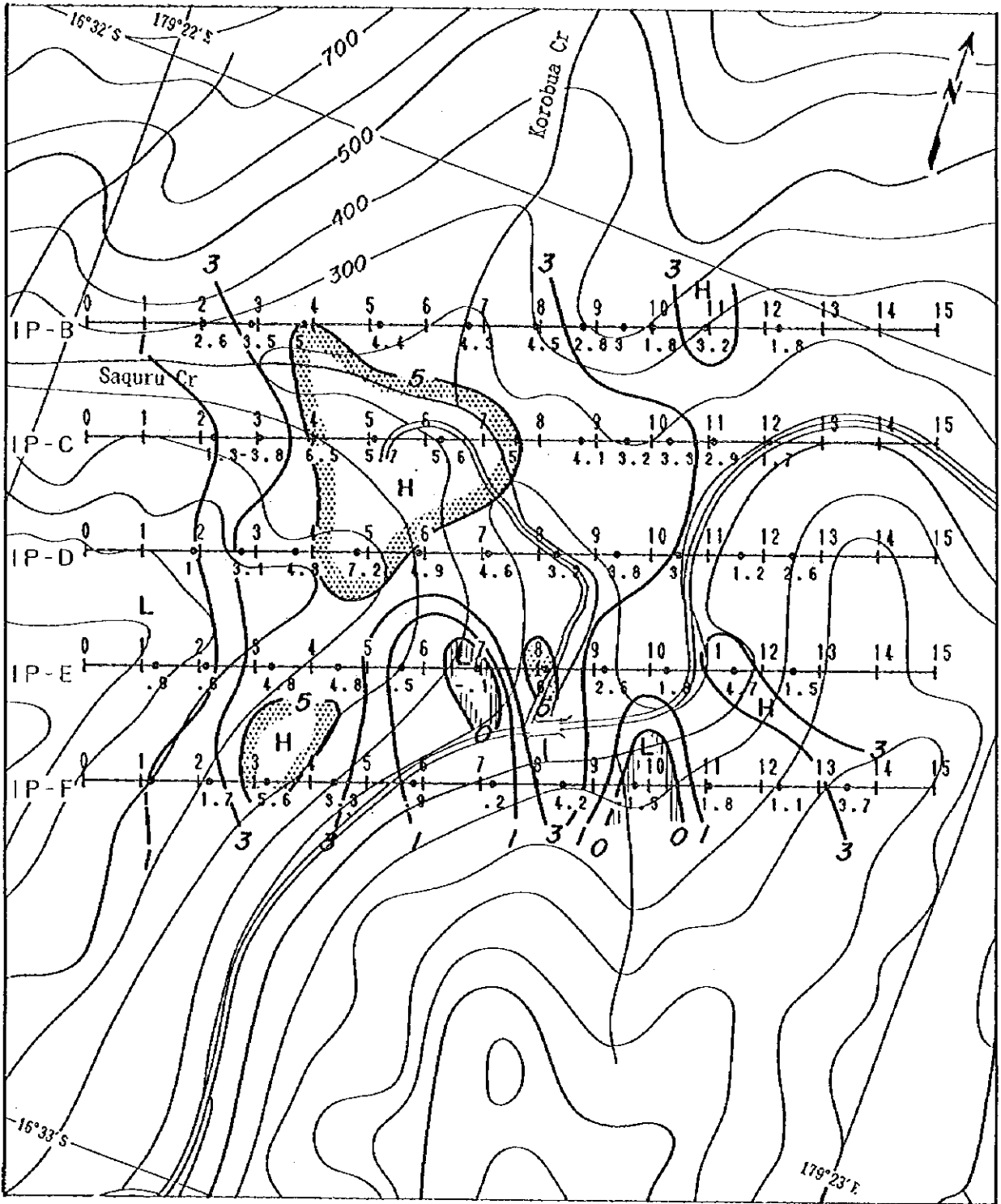
LEGEND

SCALE 1 : 10,000



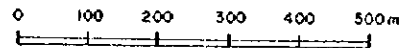
<p>0 1 IP-B ----- 2.3</p> <p>3</p>	<p>Line Name & Station No.</p> <p>Chargeability (αV·S/V)</p> <p>Contour Line Value & Chargeability (αV·S/V)</p>	<p>H High Chargeability Zone</p> <p>L Low Chargeability Zone</p> <p> 5 ≤ M</p> <p> M ≤ 0</p>
--	---	--

Fig. 2-5-15 (2) TDIP Plane Map of Chargeability [n=2]



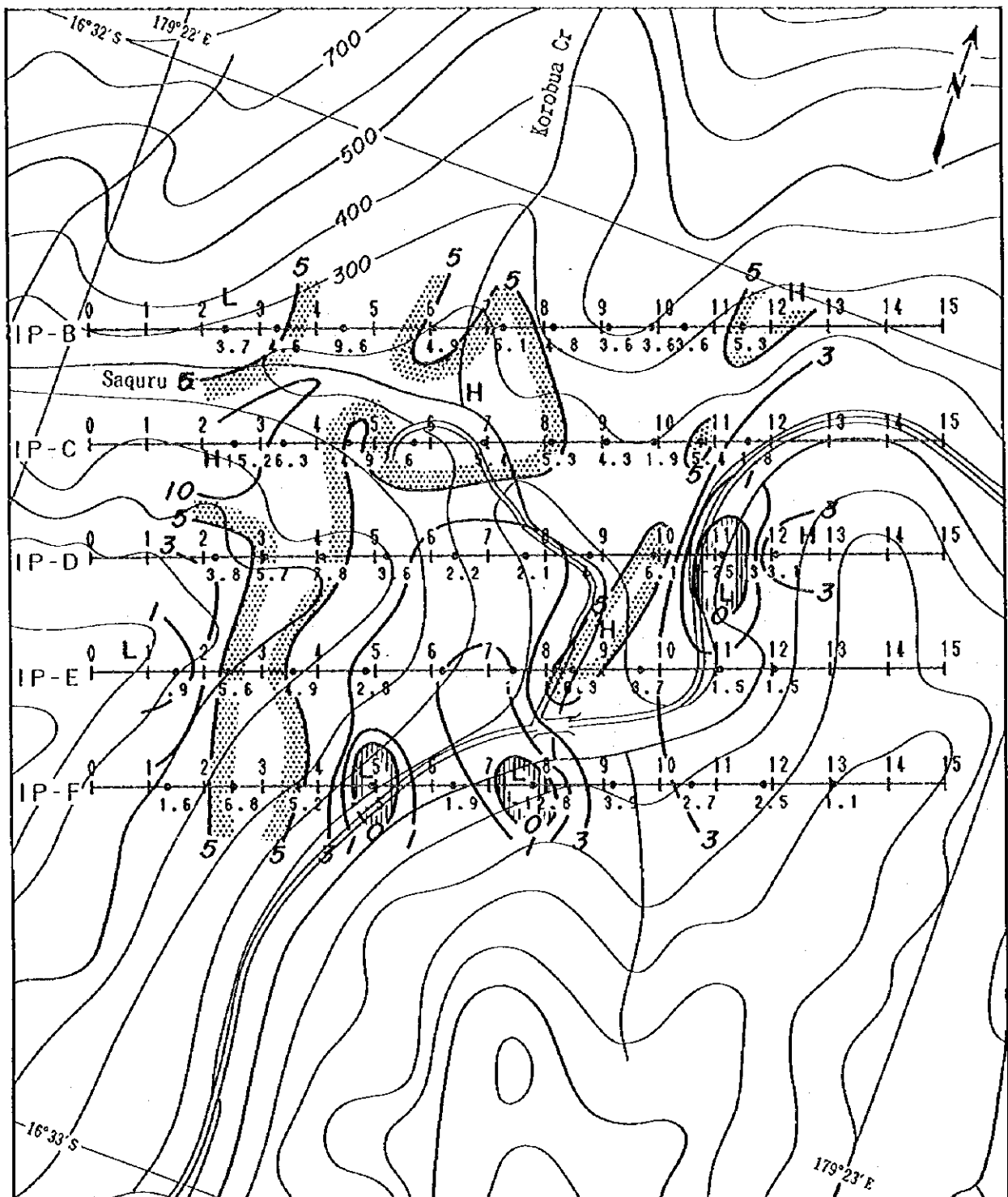
LEGEND

SCALE 1 : 10,000



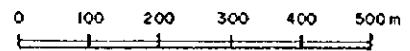
<p>0 1 IP-B —●— </p> <p>2.3</p> <p>3</p>	<p>Line Name & Station No.</p> <p>Chargeability ($\mu\text{V-S/V}$)</p> <p>Contour Line Value & Chargeability ($\mu\text{V-S/V}$)</p>	<p>H</p> <p>L</p> <p></p> <p></p>	<p>High Chargeability Zone</p> <p>Low Chargeability Zone</p> <p>$5 \leq M$</p> <p>$M \leq 0$</p>
---	---	-----------------------------------	--

Fig. 2-5-15 (3) TDIP Plane Map of Chargeability [n=3]



LEGEND

SCALE 1 : 10,000

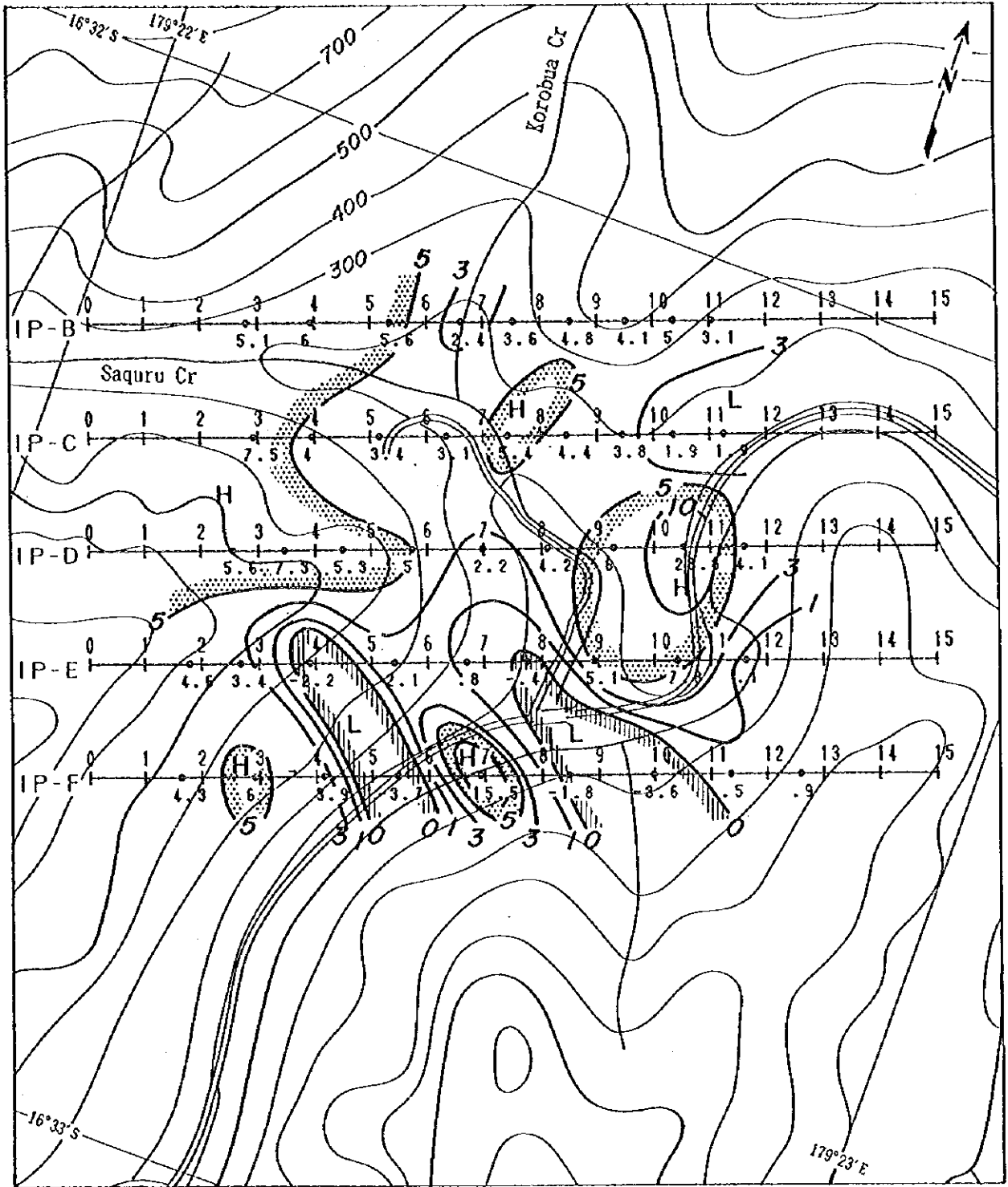


- 0 1 Line Name & Station No.
- IP-B |-----| Chargeability (mV-S/Y)
- 2.3
- Contour Line Value & Chargeability (mV-S/Y)

- H High Chargeability Zone
- L Low Chargeability Zone

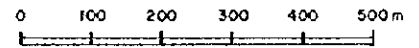
- 5 ≤ M
- M ≤ 0

Fig. 2-5-15 (4) TDIP Plane Map of Chargeability (n=4)



LEGEND

SCALE 1 : 10,000



0 1	Line Name & Station No.	H	High Chargeability Zone
IP-B —●—	Chargeability (αV·S/V)	L	Low Chargeability Zone
2.3			$5 \leq M$
	Contour Line Value & Chargeability (αV·S/V)		$M \leq 0$

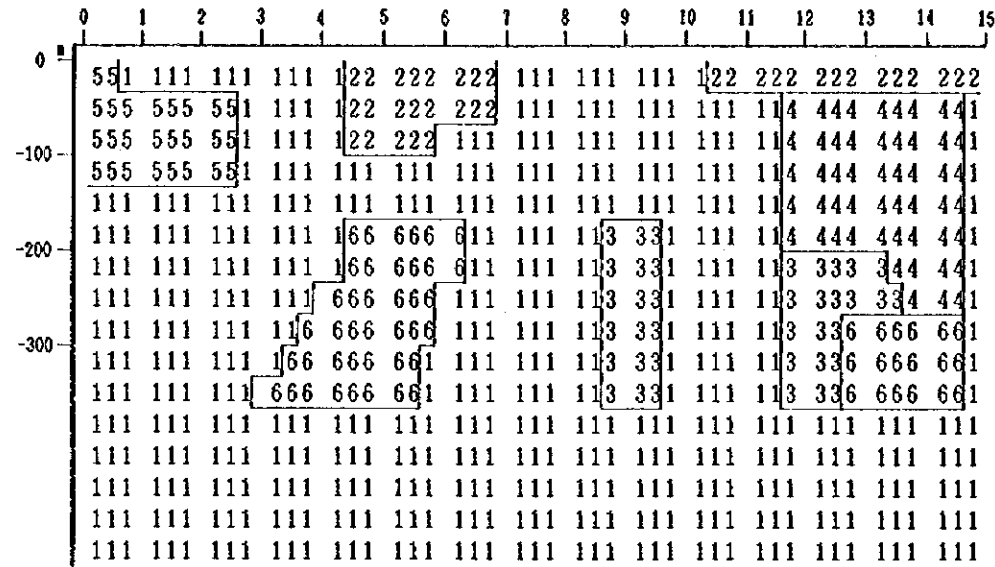
Fig. 2-5-15 (5) TDIP Plane Map of Chargeability [n=5]

0

0

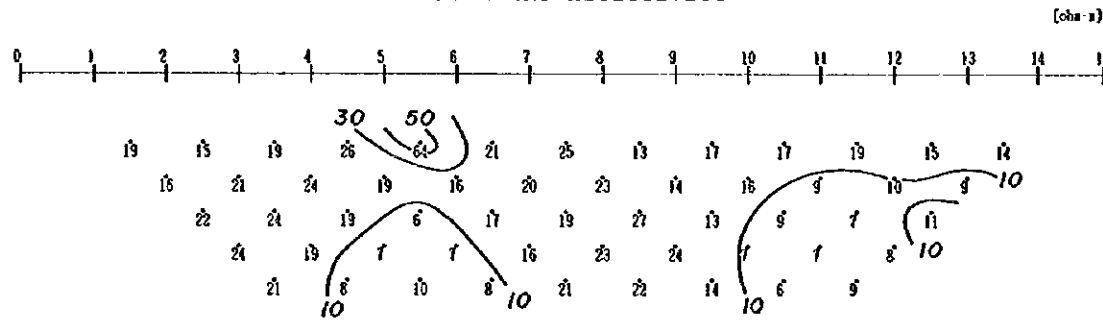
0

SIMULATION MODEL LINE B

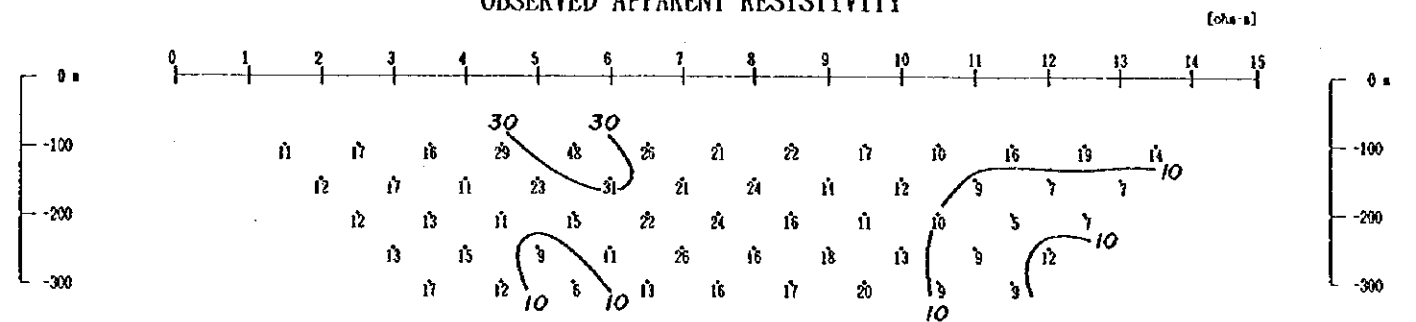


CODE	RESISTIVITY (ohm-m)	CHARGEABILITY (mV-S/V)
1	15	3.0
2	60	3.0
3	10	8.0
4	7	2.0
5	20	1.5
6	10	15.0

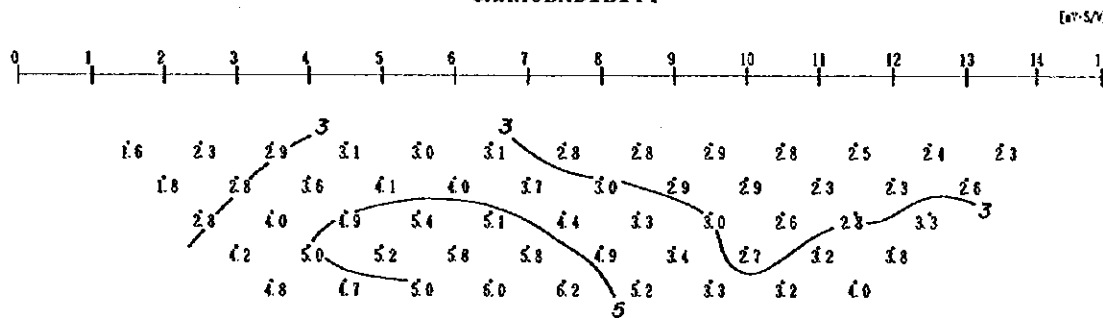
APPARENT RESISTIVITY



OBSERVED APPARENT RESISTIVITY



CHARGEABILITY



OBSERVED CHARGEABILITY

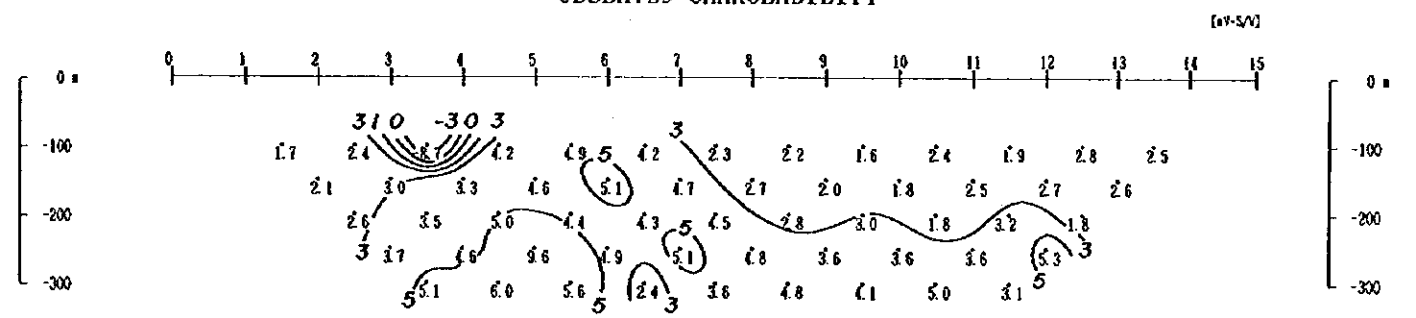
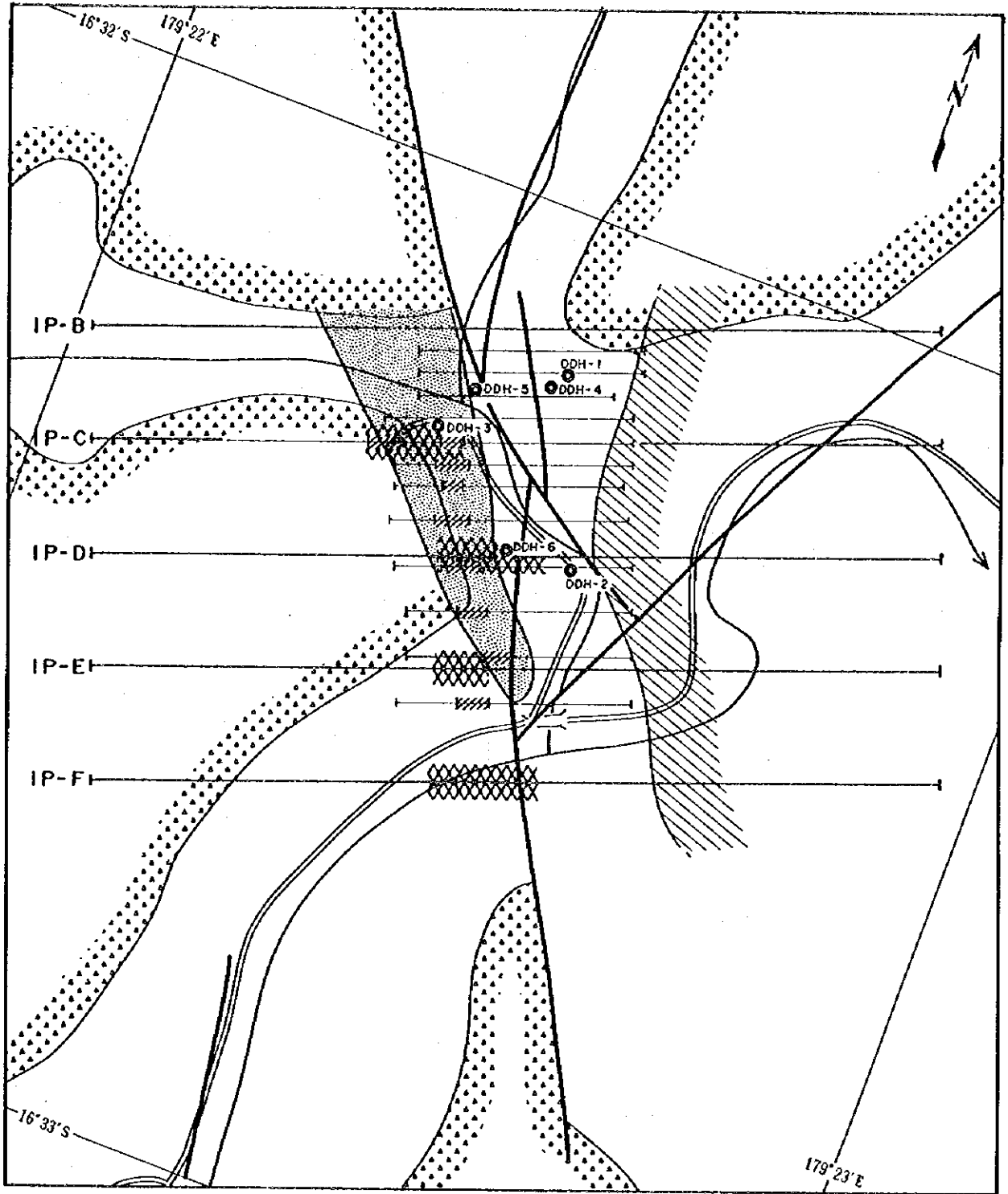
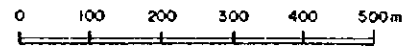


Fig. 2-5-16 (1) TDIP 2-d. Model Simulation Analysis [Line B]



LEGEND

SCALE 1 : 10,000








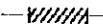
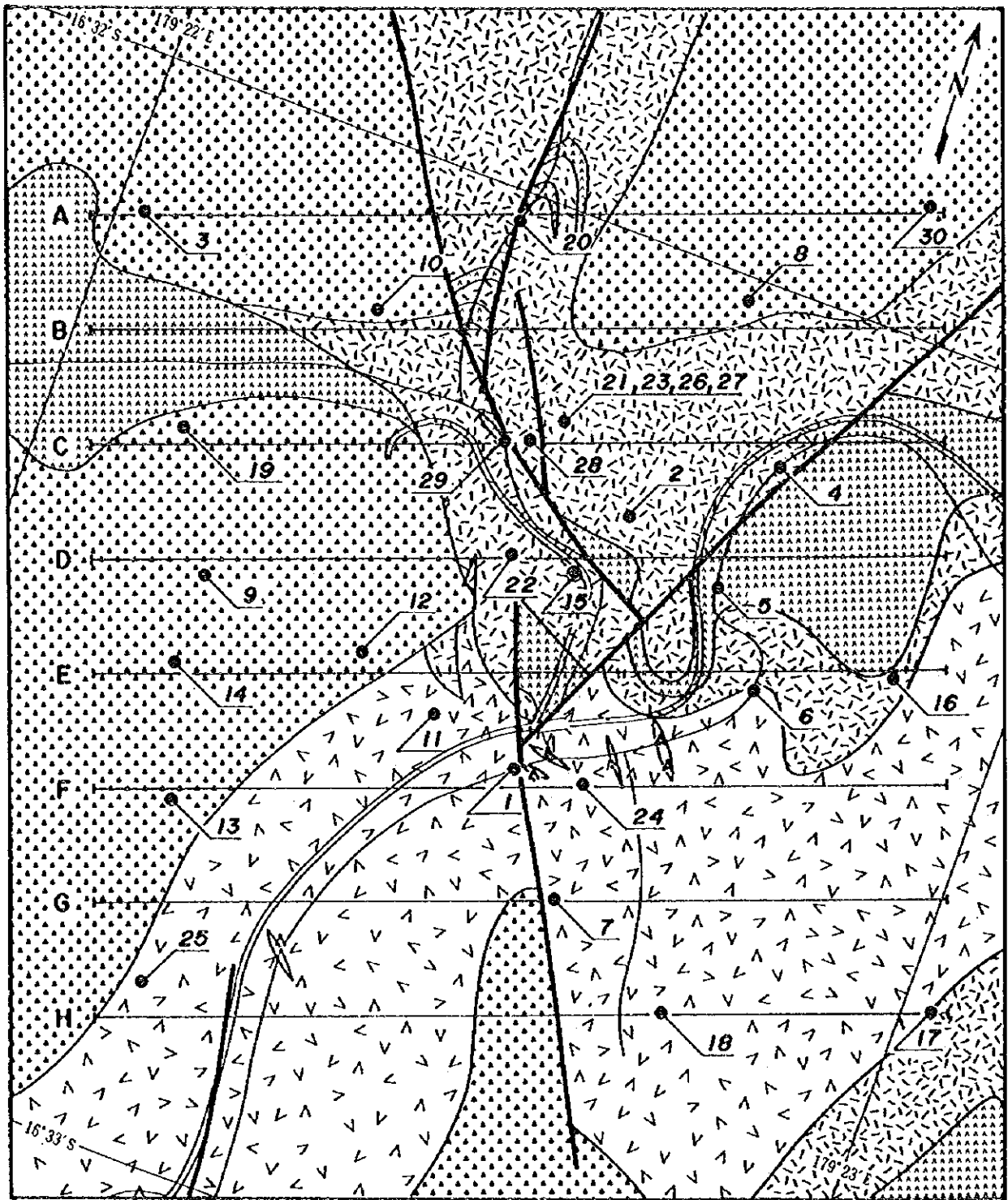
-  Fault
-  Andesitic volcanoclastic rocks
-  High Resistivity zone (>50 ohm-m)
-  Low Resistivity zone (<10 ohm-m)
-  Chargeability anomaly (>5 mV-S/V)
-  IP anomaly (Geotrex, 1988)

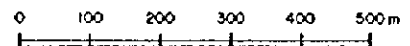
Fig. 2-5-17 TDIP Interpretation Map



LEGEND

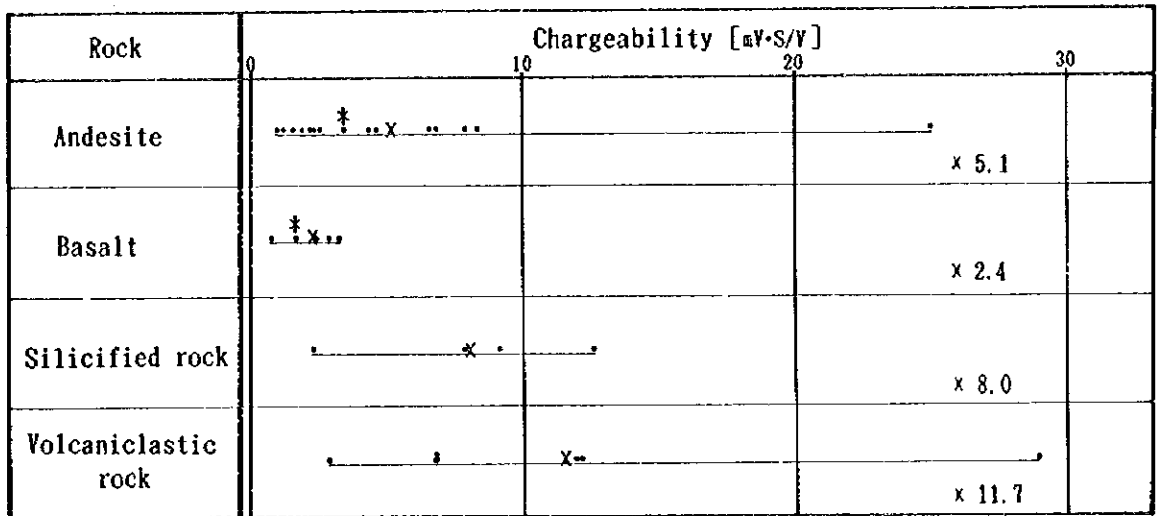
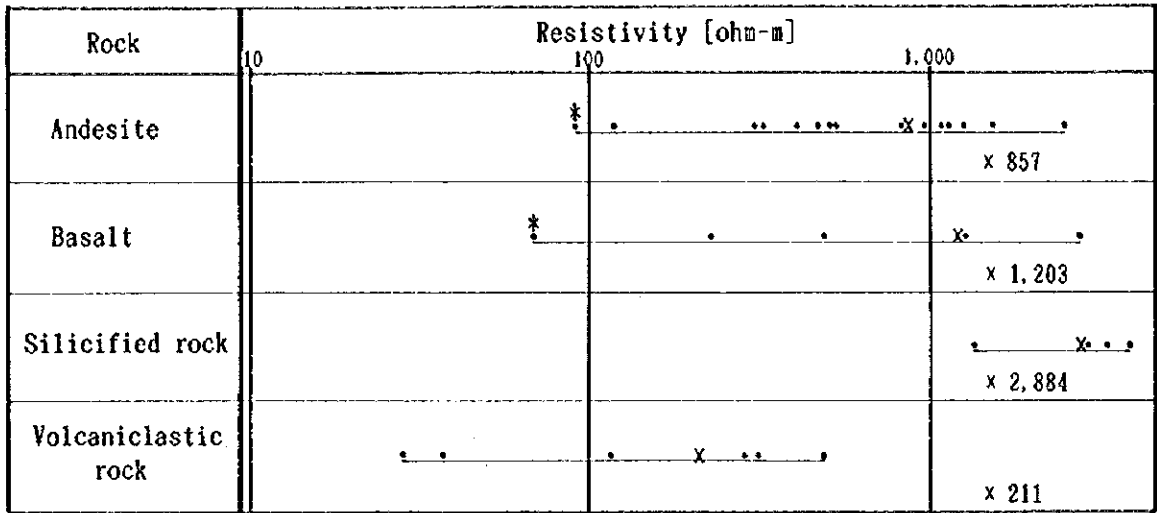
- Sueni Braccias
 - Andesitic volcaniclastic rocks
- Koroutari Andesites
 - volcaniclastic rocks
 - Andesite~basaltic andesite lavas
 - Basalt lavas
- Intrusive rock
 - Basalt
 - Fault

SCALE 1 : 10,000



- CSANT Survey Line
- Rock sample
- Core sample

Fig. 2-5-18 Location Map of Rock Samples



* omitted value for average calculation
x average value

Fig. 2-5-19 Distribution for Resistivity and Chargeability of Rock Samples

0

0

0

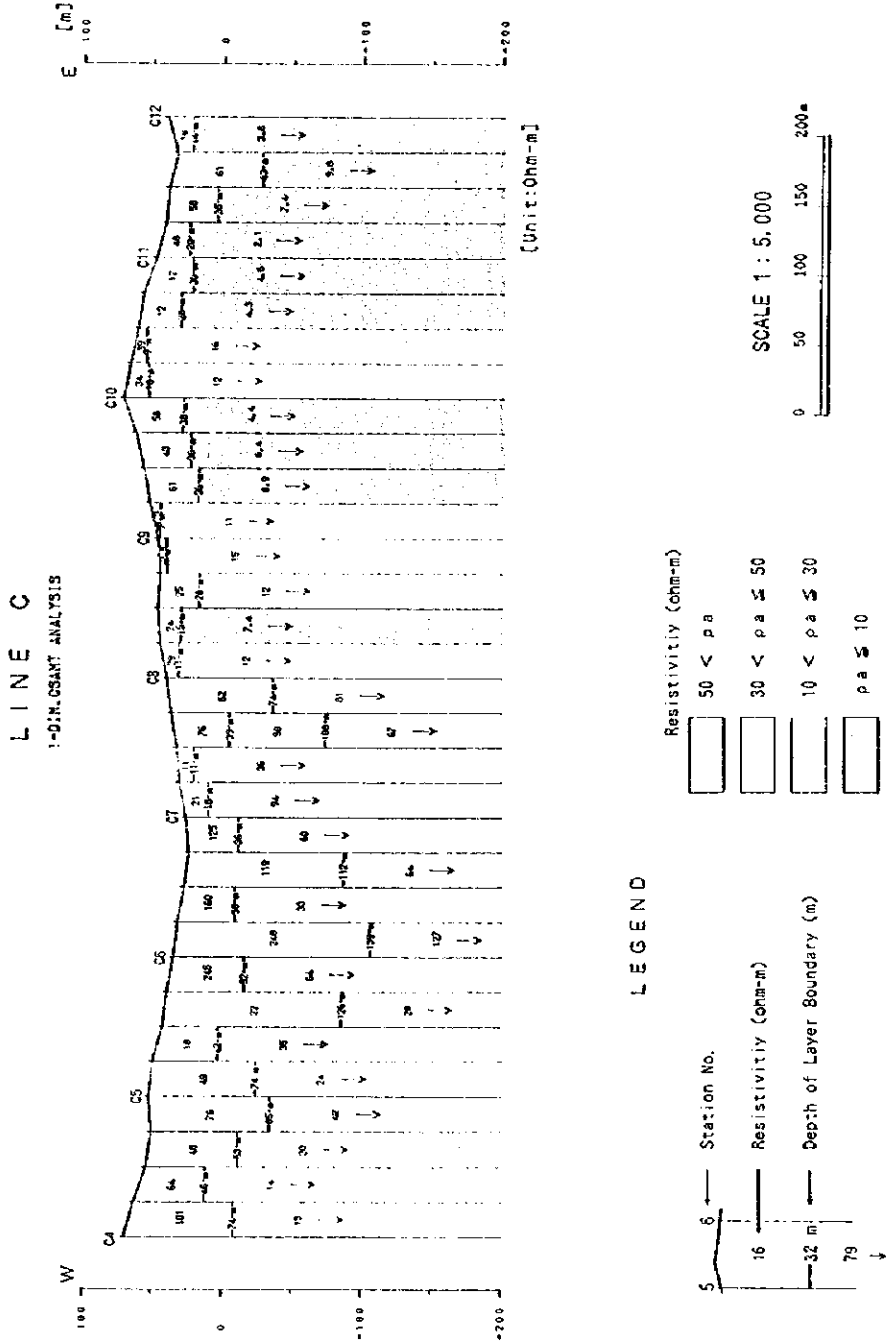
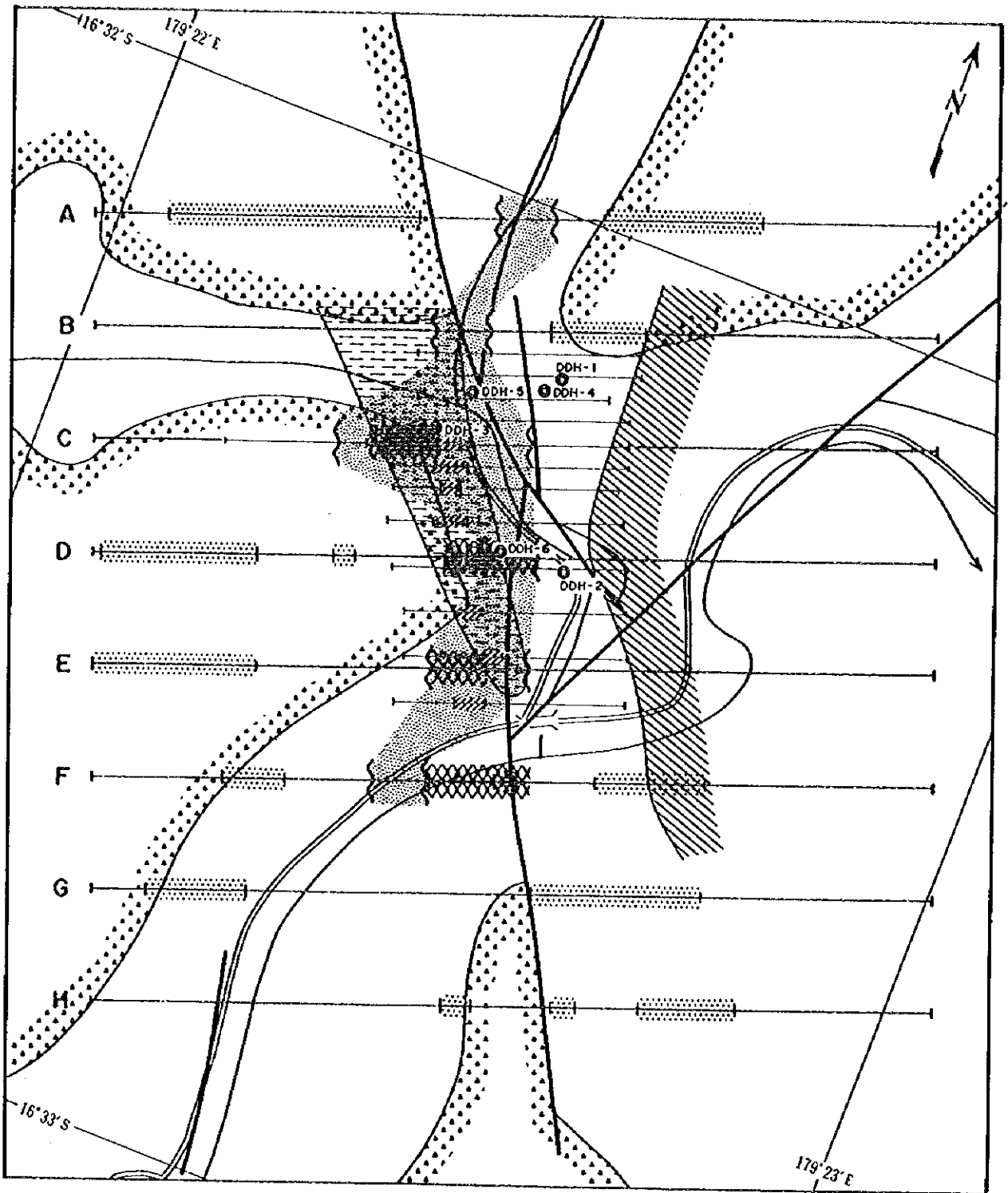


Fig. 2-5-20 CSAMT Line C Section of Resistivity Structure (a=25m)

0

0

0



LEGEND

SCALE 1 : 10,000

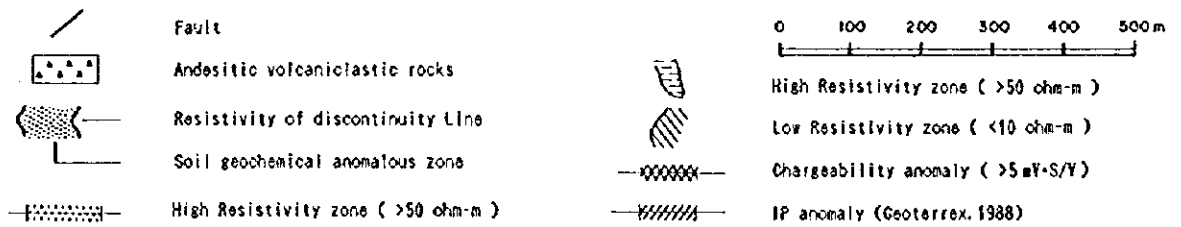


Fig. 2-5-21 Geophysical Interpretation Map

PART III CONCLUSIONS AND RECOMMENDATIONS

PART III CONCLUSIONS AND RECOMMENDATIONS

Chapter 1 Conclusions

(1) Nakoroutari Area

- a. This area comprises an areal extent of 36 km² and is located approximately 15 km south of Labasa. Geochemical, surface magnetic, and IP surveys have been conducted since 1988 in the Leli's Prospect. Also six holes with a total depth of 1,053m have been drilled in this prospect. The hole was aimed at a quartz breccia zone associated with the NNW-SSE fault system and encountered ores with a core thickness of 0.6 m and 11.6 g/t Au.
- b. The geology of this area is composed mainly of basalt-andesite lava and volcanics of the Koroutari Andesites, and andesitic volcanics of the Sueni Breccia. These units belong to Upper Miocene-Lower Pliocene Natewa Volcanic Group.
- c. Four zones were selected from the study of existing geological and resources data and information. They are; Leli's Prospect, a zone to the south of the same Prospect, Navakuru, and Mugsy's Prospect. Mineralization and alteration were found to occur in all five zones. The Leli's Prospect was concluded to be the most promising. It is noted that the altered zone to the south of Leli's show evidence of gold mineralization.
- d. The Leli's Prospect occurs within the quartz vein-breccia zone developed in the Koroutari Andesite lava-volcanics which belong to the Natewa Volcanic Group. There are two quartz vein-breccia zones, the eastern and western zones, part of the NNW-SSE system. A silicified tuff breccia sample with a grade of 12.9 g/t Au has been collected in the vicinity of the Leli's Prospect, and although in a limited area, high-grade zones have been confirmed.
- e. Geophysical survey by CSAMT array was carried out for 12 km and time domain IP for 7.5 km at the Leli's Prospect.
- f. The CSAMT array method identified intrusive-shaped high resistivity zones in the central parts of Line B-C and Line D-F. One-dimensional resistivity structure analysis showed the existence of two buried high-resistivity bodies which extend in the N-S direction between Lines A-C and D-F. These two bodies as a whole extend in the NW-SE direction and are interpreted to be areas of silicification.
- g. The apparent resistivity measured by the time domain IP method resulted in a distribution pattern harmonious with the results of the CSAMT array. The chargeability background is dominantly low. Chargeability anomalies exceeding 10 mS were detected at

three localities, but they are independent anomalies and their reliability is very low. Weak anomalies of over 5 mS occurred continuously in the central-western part of all traverse lines. These are inferred to be the anomalies detected by Geotrex (1988). A two-dimensional model simulation was made and it is inferred from the results that these IP anomalies are caused by bodies 100 m below the surface. Also the simulation results indicate that these bodies have chargeability in the general range of 5-7 mS and most probably formed by pyrite mineralization. These bodies and the two high-resistivity bodies detected by the CSAMT array between Lines B and F are located in approximately the same locality. Thus it is believed that pyritization and silicification are closely related in this area.

h. Resistivity and chargeability of 30 rock samples (including core samples) were measured in the laboratory. The resistivity of silicified rocks was the highest at 2,884 ohm-m, followed by basalt > andesite > volcanoclastic rocks. The chargeability of volcanoclastic rocks was the highest at 11.7 mS, followed by silicified rocks > andesite > basalt. It was shown from this work that identification of rock types from physical characteristics was difficult.

(2) Dakuniba Area

a. This area is located approximately 65 km east of Savusavu with an areal extent of 36 km². A zone comprising WNW-ESE striking quartz veins occurs 1 km north of the Dakuniba Village in the upper reaches of the Nagagani Creek. The zone was previously explored and is called the Dakunba Prospect. In the past, two holes with a total length of 176 m have been drilled, soil and rock geochemical survey, CSAMT geophysical survey, and trenching were carried out.

b. The geology of this area consists of basaltic lava and volcanoclastics of the Dakuniba Basalt belonging to the Upper Miocene - Lower Pliocene Natewa Volcanic Group.

c. Mineralization occurs in the quartz veins developed in the basaltic lava and volcanoclastics. The major veins are developed over 2 km in length and strike WNW-ESE and dip steeply. Alteration associated with mineralization is observed in the northeastern part of the area and they are; quartz-clay veins extending from the upper reaches of the Wailevu Creek to the Nagagani Creek, argillized and pyrite dissemination from the Nubuni Creek westward, and mineralization observed in the quartz veins of a tributary of the Waikava Creek.

d. The continuity of individual quartz veins exposed in the upper reaches of the Nagagani Creek has not been confirmed, but the grade of the quartz veins is high with a maximum of 16 g/t Au and 21 samples containing more than 1 g/t Au were collected from 1 km long outcrop. Thus, this zone is concluded to be promising.

(3) Waimotu Area

a. The Bill's Hill Prospect is located approximately 45 km northeast of Savusavu, and the Waimotu Lode and Nuku Prospect are 0.5 km and 2.5 km east-northeast from there.

b. A total of 18 holes have been drilled in the three prospects of this area. A total of 551 m adits was dug and seven holes with a total of 609 m length were drilled into the Waimotu Lodes, seven and four holes were drilled in the Bill's Hill Prospect and Nuku Prospect, respectively.

c. The geology of this area consists mainly of weakly propyritized andesite and basaltic lava and volcanoclastics of the Koroutari Andesite and Korotini Breccias. These units belong to the Natewa Volcanic Group.

d. The Waimotu Lodes are comprised of; Main Lode, East Lode, and West Lode. A length of about 70 m was confirmed for the Main Lode in outcrop, but both mineralization of the East and West Lodes were confirmed only at one outcrop and the entrance of the adit. All three veins have a N-S strike and with a dip of 75° - 90° east for the Main and East Lodes. The widths of the veins are, 1.2 m maximum for the Main Lode and 0.8 m was confirmed at an outcrop for the East Lode. The maximum grade is 24.2 g/t Au for the Main and 42.5 g/t Au for the East Lodes. The gold content of 42.5g/t was obtained in a sample collected from the East Lode (0.8 m wide), but a sample collected only 1 m south of this sample contained only 2.4 g/t Au, thus the fluctuation in the grade is strong. On the other hand, the average grade of four samples collected along the 70 m length of the Main Lode is 7.2 g/t Au and the gold content is constant. The grade of the West Lode is the lowest of the three at 0.92 g/t Au.

e. Silicified and argillized (kaolinized) zones are well developed in the Bill's Hill Prospect. Quartz and chalcedony stockwork is developed cutting through these zones, and its strike is N-S and the eastward dip is generally steep. Surface observation of the stockwork shows the occurrence of goethite as an opaque with very minor amount of chalcopyrite. The cores drilled in the past show strong dissemination of pyrite in the silicified zone. The maximum grade of individual veinlets of the stockwork is 0.21g/t Au.

f. At Nuku, a silicified zone comprising chalcedony-quartz veins extends in a N-S direction for approximately 150m and the average width of this zone is approximately 7m.

The direction of dip was seemingly east, but it is difficult to determine the dip on the surface and from the results of the past drilling, it is inferred to be westward dipping. The highest grade of the stockwork is 4.3 g/t Au (sampled width 2.5m) and the average of the total 150 m is 1.3 g/t Au (average sampled width 7 m). The past two holes encountered ores at approximately 50 m below the surface and the average grade over a 7 m width is 0.6 g/t Au.

g. The lower parts of the three prospects in this area have been drilled. All three have significant mineral potential and the zone extending from the lower part of the Waimotu Lode to the subsurface part of eastern Bill's Hill is concluded to be an interesting target for further exploration.

(4) Koroinasolo Area

The vicinity of the Koroinasolo Area in the western part of Vanua Levu was excluded from the present survey because private mining licenses had been issued when this survey began. At the time of preparing this report, however, these licenses have expired. In this area, caldera structures and a large number of NNW-SSE to NW-SE faults occur and altered zones are widely developed. It is known that there are many prospects and it is said that outcrops with gold content of over 1 g/t Au occur. Records of the details of the past surveys and exploration, however, could not be obtained and the nature of mineralization of this area is not clear.

Chapter 2 Recommendations for the Second Year

(1) Nakoroutari Area

In the Nakoroutari Area, the Leli's Prospect is the most promising for future work including drilling. The target for drilling should be the lower part of the high-grade veins of the quartz-breccia zone. This zone is accompanied by gold mineralization and was confirmed by the present survey. This location is near stations 7 and 8 of the electric survey Line C. Also, confirmation of the CSAMT and IP high-resistivity zones is strongly recommended and this target will be the lower part of the vicinity of stations 6 and 7 of Lines B and E.

(2) Dakuniba Area

The present survey confirmed the existence of gold-bearing quartz veins at the Dakuniba Prospect. The lower parts of the quartz veins of the Dakuniba Prospect are practically unexplored, and it is recommended that drilling be carried out during the 2nd Phase if this project. The high-grade zone in the upper reaches of the Nagagani Creek is considered to be a particularly promising target.

(3) Waimotu Area

In the past, geological survey and exploration were carried out covering limited parts of the Waimotu Lodes, Bill's Hill, and Nuku Prospects. This work, however, is not sufficient for

assessment of the resources in the area. Of these three zones, the Waimotu Lode has the highest assay results from outcrop and is therefore most interesting. Therefore, it is recommended that we first confirm the downward continuity and the distribution of the veins by electric survey, namely CSAMT and IP, then follow it up by drilling.

(4) Koronaisolo Area

It is recommended that as this area will be open for exploration next year, all available geological data regarding this area be studied and interpreted, and then if deemed warranted, implement geological and/or geophysical survey in the areas delineated as promising.

REFERENCES

REFERENCES

[Geology]

Mineral Resources Department(1992): Exploration and Mineral Digest.

Mineral Resources Department(1995): Exploration and Mineral Digest,Vol.11 No.2

Cox,M.E.(1980): Preliminary Geothermal Investigations in the Lambasa Area, Vanua Levu, Geothermal Report No.2, MRD.

Colley,H. and Greenbaum,D(1980): The Mineral Deposits and Metallogenesis of the Fiji Platform. Economic Geology vol.75,807-829.

Colley,B.(1976):Mineral Deposits of Fiji(Metallic Deposits),Memoir No.1

Colley,H. and Flint,D.J.(1985): Metallic Mineral Deposits. Memoir 4, 198pp,MRD.

Mallick,D.I.J.and Habgood,F.(1987): Interpretation of SLAR Imegery of the main islands of Fiji. British Geological Survey. 9 pp.

[Geophysics, General]

Cagniar, L. (1953) : Basic theory of the magnetotellurics method of Geophysicalprospecting, Geophysics, 37, pp605-635

Goldstein,M.A. and Strangway,D.W. (1975):Audio frequency magnetotellurics with a grounded electric dipole source, Geophysics, 40, pp669-683.

Kaufman,A.A.,and Keller,G.V. (1981):The Magmetotelluric Sounding method, Elsevier, p595.

Ogawa,Y. (1988):Fortan Program Codes for Two-Dimensional Magnetotelluric Forward and Inverse Analyses, Open File Report Geol. Surv. Japan No.59.

Strangway,D.W., Swift,C.M. and Holmer,R.C. (1973):The application of audio frequency magmetotellurics(AMT) to mineral exploration, Geophysics, 38, pp1159-1175

Yamashita, M. (1984): CSAMT Controlled Source Audio Magnetotellurics, PHOENIX Geophysics Limited.

Yamashita, M. and Hallof, P.G. (1985) : CSAMT case histories with a mult-channel CSAMT system and discussion of near-field data correction, The 55th SEG Annual Meeting, Washington, D.C.

Zonge engineering & research organization, INC. (1982): Interpretation Guide for CSAMT data.

[Geophysical prospecting (IP Method)]

Bertin, J. (1976): Experimental & Theoretical Aspect of IP. Vol. 1. Presentation and Application of the IP Method Case Histories. Gebruder Borntraeger, Berlin 1976, 250pp

Keller, G.V. and Frischknecht, F.C. (1966): Electrical Methods in Geophysical Prospecting. Pergamon Press, London, 517p

Madden, T.R., & T. Cantwell (1967): Induced Polarization. A Review, Mining Geophysics, 2, pp 373-400, S.E.G. Tulsa, Okla.

Parasnis, D.S. (1972): Principles of Applied Geophysics. Chapman & Hall, London.

Parasnis, D.S. (1973): Mining Geophysics. Elsevier, Amsterdam, p 395

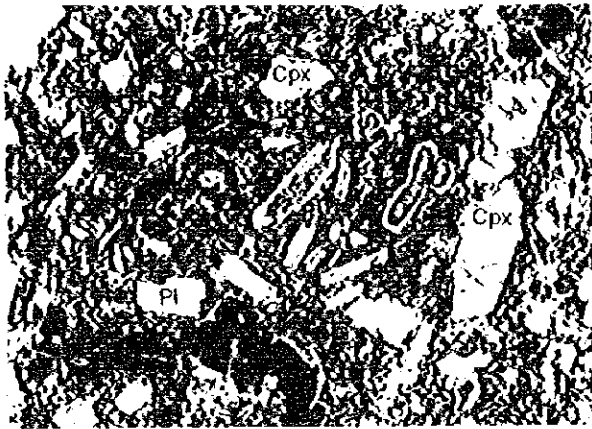
Sato, M. and Mooney, H.M. (1960): The Electrochemical Mechanism of Sulphide Self-potentials. Geophysics 25 No. 1, pp 226-249.

Seigel, H.O. (1959): Mathematical Formulation and Type Curves for Induced Polarization. Geophysics 24 pp 547-565.

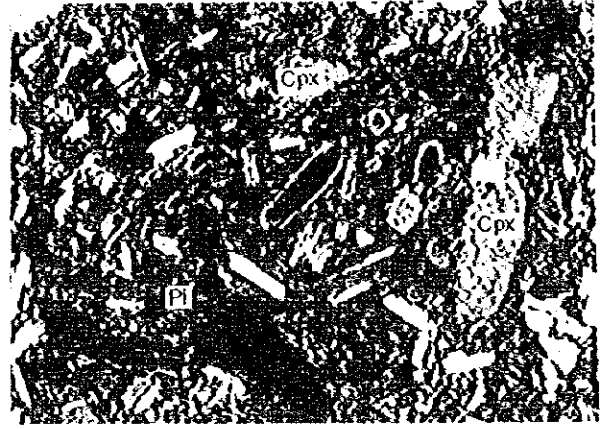
Seigel, H.O. (1967): The Induced Polarization Method. In L.W. Morley (Editor), Mining and Groundwater Geophysics. Geol. Rep., No. 26. Geol. Surv. Can. pp 123-137.

PHOTOGRAPHS

NS003 Basalt (Nakoroutari)



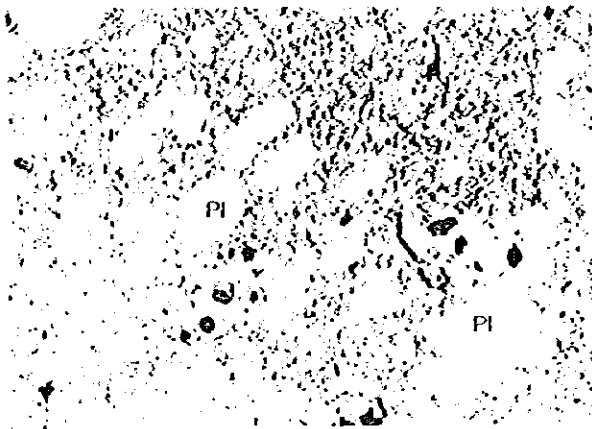
Open nicols



Closed nicols

0 0.5 mm

NK009 Andesite (Nakoroutari)



Open nicols



Closed nicols

0 0.5 mm

DM089 Picrite (Dakuniba)



Open nicols

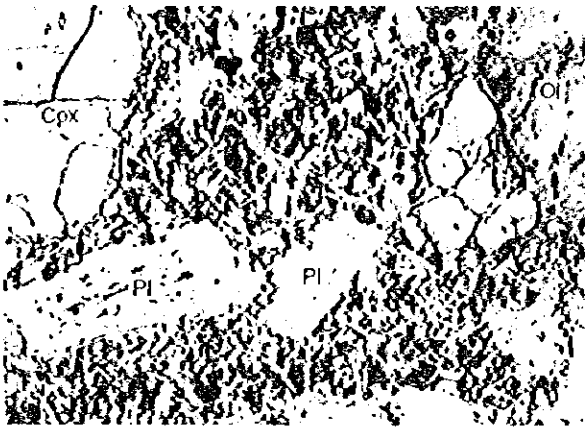


Closed nicols

0 0.5 mm

Photo. 1 Microscopic photograph (Thin section)

DB122 Basalt (Dakuniba)



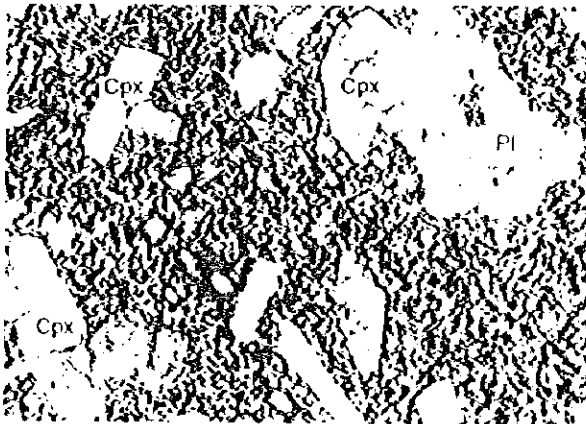
Open nicols



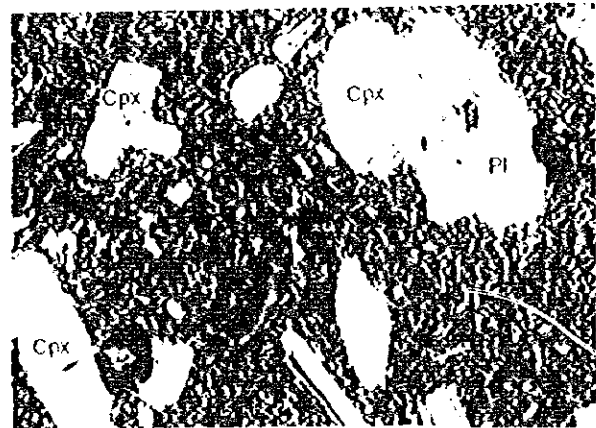
Closed nicols

0 0.5 mm

WB184 Basalt (Waimotu)



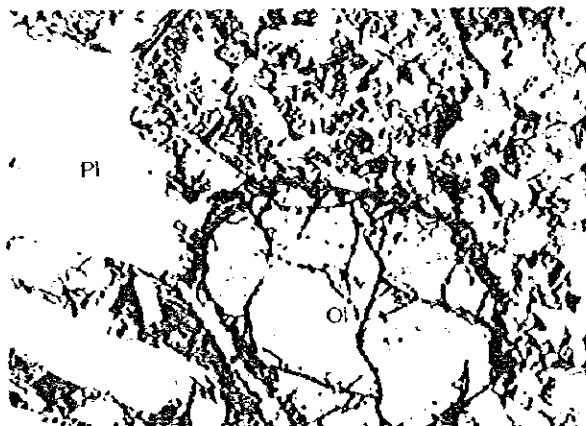
Open nicols



Closed nicols

0 0.5 mm

WB192 Basalt (Waimotu)



Open nicols



Closed nicols

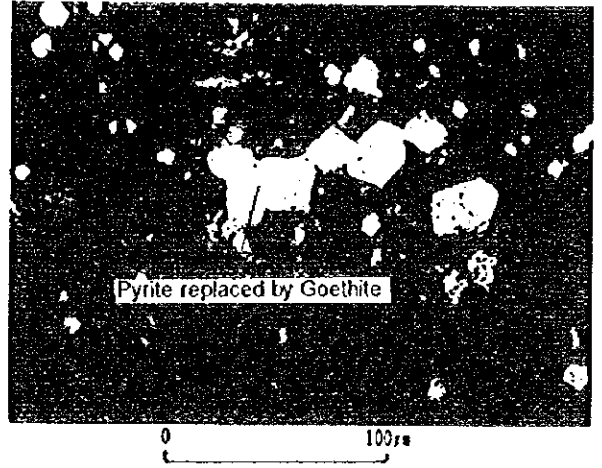
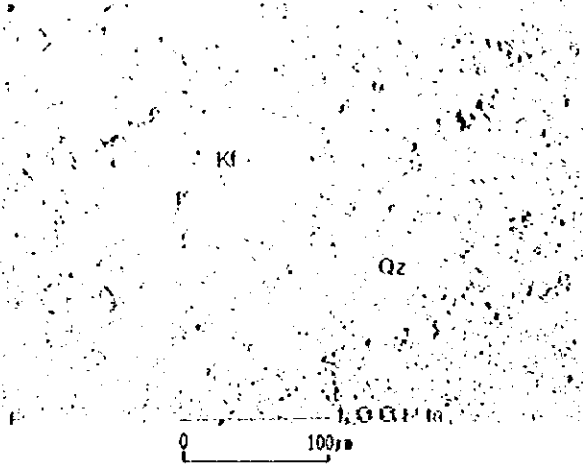
0 0.5 mm

LEGEND

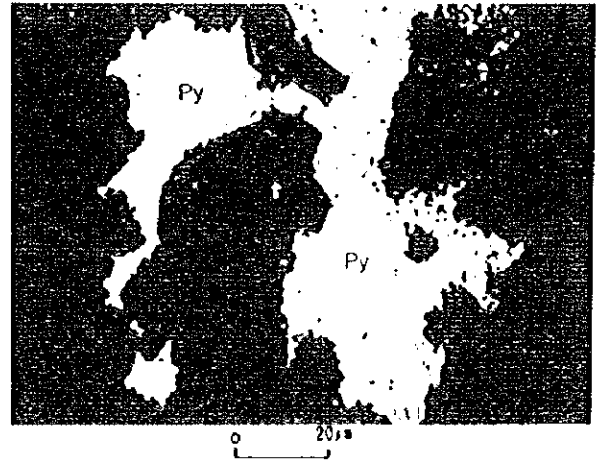
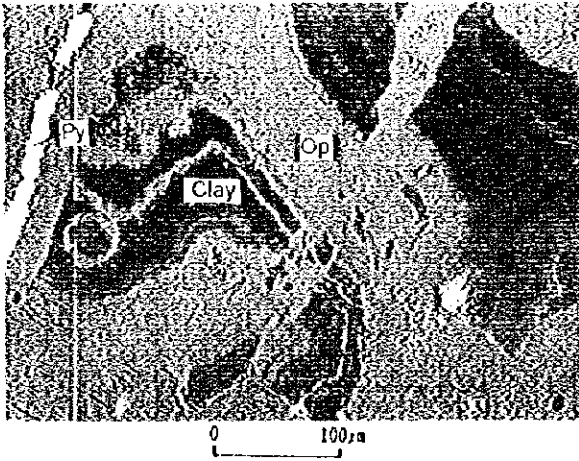
Pl Plagioclase Ol Olivine Cpx Clinopyroxene

Photo. 2 Microscopic photograph (Thin section)

WK214 (Waimotu Lodes Prospect)



WB231 (Nuku Prospect)



WM219 (Waimotu lodes Prospect)

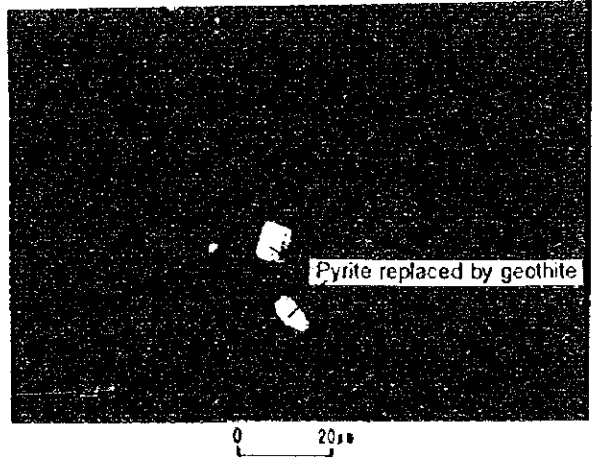
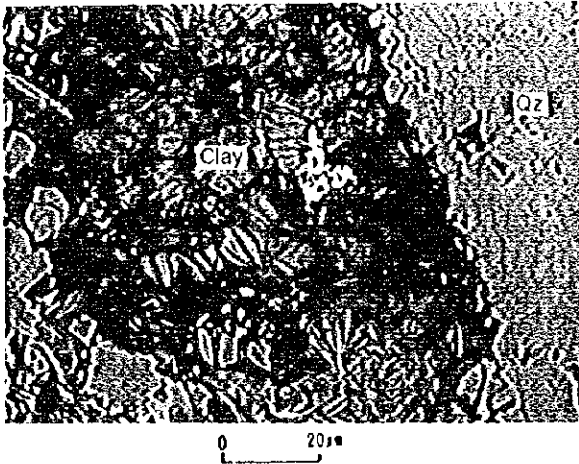
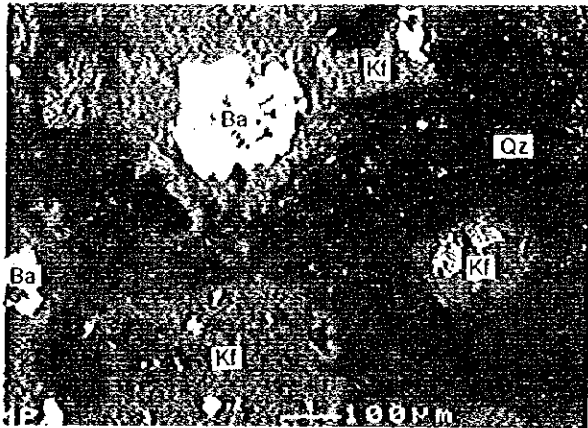
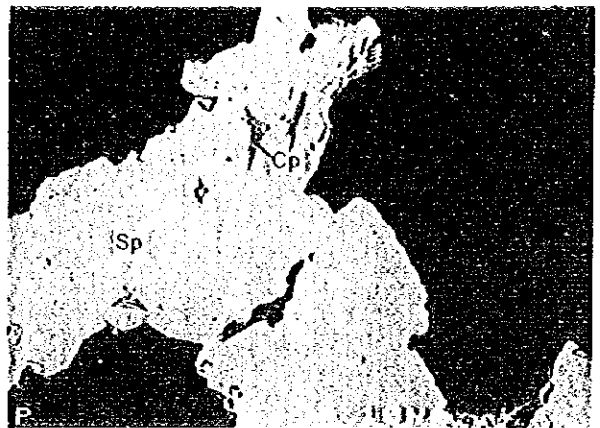


Photo. 3 Microscopic photograph (Polished section)

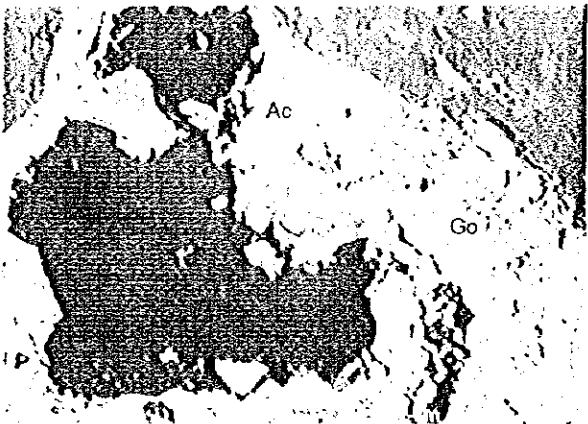
NM068 (Leli's Prospect)



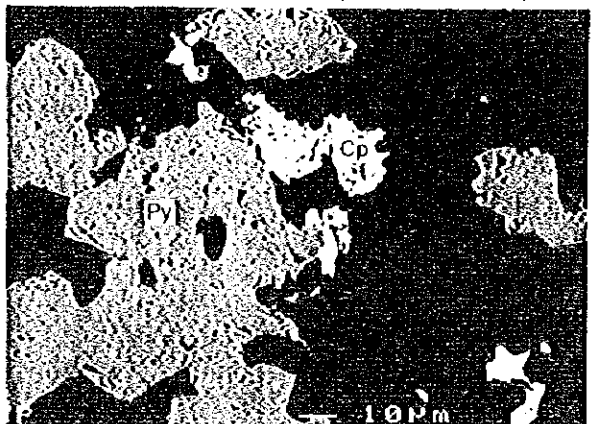
NK033 (Leli's Prospect)



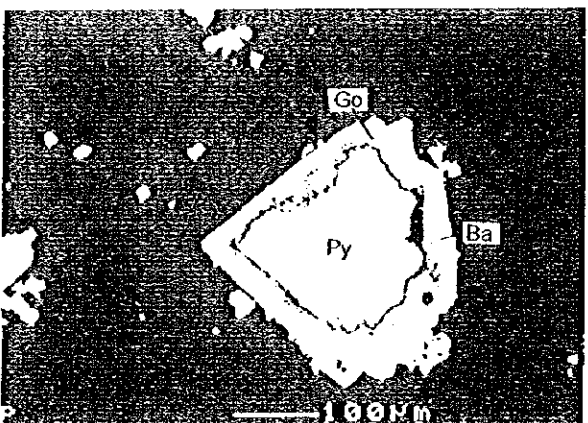
DB148 (Dakuniba Prospect, Trench-29)



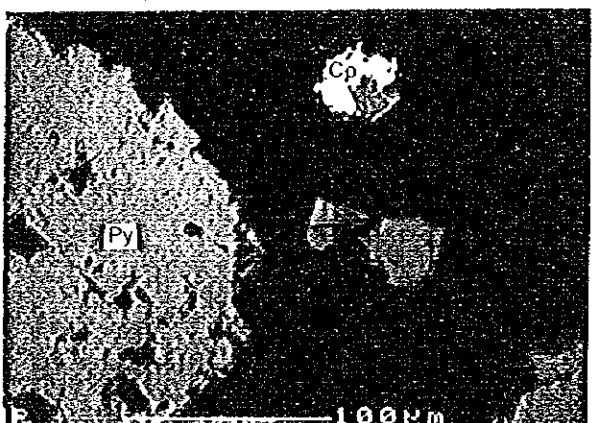
DB118 (Dakuniba Prospect, Trench-7)



DK117 (Dakuniba Prospect, Trench-1)



DK154 (Dakuniba)



LEGEND

Ac:Acanthite Cp:Chalcopyrite Py:Pyrite Go:Goethite Sp:Spalerite Ba:Barite Qz:Quartz
Op:Opal KfPotassium feldspar

Photo. 4 Microscopic photograph (Polished section)

